CALIBRATION OF A CLIMATOLOGICAL EVAPOTRANSPIRATION PREDICTION EQUATION USING EDDY CORRELATION METHODS

By

MICHAEL ANDREW KIZER

Bachelor of Science
Oregon State University
Corvallis, Oregon
1971

Master of Science
Oregon State University
Corvallis, Oregon
1976

Submitted to the Faculty of the
Graduate College of the
Oklahoma State University
in partial fulfillment of
the requirements for
the Degree of
DOCTOR OF PHILOSOPHY
May, 1987

CALIBRATION OF A CLIMATOLOGICAL EVAPOTRANSPIRATION PREDICTION EQUATION USING EDDY CORRELATION METHODS

Thesis Approved:

Ronald L. Elliott
Thesis Adviser

Bruce Wilson

[illegible]

[illegible]

Norman N. Durham
Dean of the Graduate College

PREFACE

This study is concerned with developing an integrated system of equations to predict the rate of water use for crops in Caddo County, Oklahoma Eddy correlation methods were used to measure evapotranspiration (ET) over alfalfa to calibrate the modified Penman equation. A crop coefficient function was determined for Florunner peanuts. Relationships for determining net radiation and soil heat flux from more easily measured meteorological parameters were determined.

I wish to thank Dr Ronald L. Elliott, my adviser, for his input and guidance during this research, and for his valued friendship Thanks to Dr. John F. Stone for his insight and instruction in the area of micrometeorology, and his service on my committee. Thanks also go to Dr. C. T. Haan, Prof. A D Barefoot, and Dr. Bruce N Wilson for their service on my committee and their input and guidance in preparing this document.

Special thanks are due to Wayne Spies, David Farmer, Jerry King, and Glen Millwee for their patience and cooperation in allowing me to clutter their fields with various pieces of equipment Thanks to Lonnie Sellers, formerly Caddo County Extension Director, for his recruitment of these cooperating farmers

My thanks to the faculty and staff of the Agricultural Engineering Department for their academic, technical and clerical support during my graduate program Special thanks to my fellow graduate students in the department Their support, friendship and humor helped me to keep everything in proper perspective.

Last but not least, thanks to my family. To my parents, Willie and Nicky, no thanks are enough for their love and encouragement. To my sons, Matt and Eric, for their love and their acceptance of all the games of T-Ball and catch I had to miss these last three years, I give my love and thanks. To my wife, Sheryl, go my love and my thanks for her support, encouragement and love Her belief in me, and her willingness to go anywhere and do anything have sustained me in all we have done together

TABLE OF CONTENTS

LIST OF TABLES

LIST OF FIGURES

CHAPTER I

INTRODUCTION

General

Farmers must be efficient in order to survive in today's troubled economic times. With the constant escalation of production costs and the stagnation of commodity prices, an operator can ill afford the inefficient use of any production input. In Oklahoma, as well as much of the rest of the western United States, irrigation water is a major production input for many important crops. To improve the profitability of irrigated agriculture, the irrigator must manage the application of water so that the maximum production increase is attained with each unit depth of water applied. To assure the optimal use of irrigation water, the irrigator must be aware of the status of the available soil water in the root zone of his crop at any given time. This will prevent him from wasting water through over-irrigation, or from unduly stressing his crop through under-irrigation.

The development of a reliable irrigation scheduling method is of the utmost importance in the efficient management of irrigated agriculture. To accurately schedule irrigations it is necessary to determine the rate of evapotranspiration (ET) of the field crop rapidly and

inexpensively. None of the methods currently available to the average irrigator in Oklahoma meet these criteria. Gravimetric soil moisture sampling is a slow and labor intensive operation. Tensiometers function over only a limited range of conditions and require frequent service. Neutron probe soil moisture meters are expensive, labor intensive to use, and require federal licensing and special safety considerations. Electrical resistance blocks are of questionable accuracy. All of the aforesaid methods take point measurements that should be replicated at several sites to obtain average values that are representative of an entire field. This integration of point source data to represent a larger area requires careful selection of measurement sites.

One way to avoid the problems associated with using point source data to reflect conditions for an entire field is to maintain a water budget. Periodic adjustments to the budget are made dependent upon rainfall, irrigation, and predicted ET. The use of meteorological data to predict the rate of water use by a crop has been practiced for many years. There are many equations that have been used, some purely empirical and some with a sound theoretical base. Virtually all of the equations used require local calibration of one or more terms to obtain accurate results in any specific location. Local calibration involves the simultaneous measurement of crop evapotranspiration and the meteorological factors required for the application of the

equation. The device most commonly used to measure evapotranspiration in calibration processes in the past has been the weighing lysimeter. Weighing lysimeters can give an accurate accounting of crop water use even for very short periods. However, lysimeters have limitations as calibration tools because of their expense, the time required to establish crops in them, the difficulty in maintaining them so that they accurately measure conditions as they exist in the surrounding field, and their non-portability.

The measurement of evapotranspiration by eddy correlation methods offers a viable alternative to lysimeters as a calibration tool. Micrometeorologists have long held that eddy correlation techniques offer the most promise for providing accurate measurements of evaporative flux with a sound theoretical basis (Kaimal, 1975). The method can measure the rate of water use by a crop through measurements made in the air above the crop surface. The major problems associated with the eddy correlation method center on the limitations of the instrumentation available to make the required measurements rapidly enough. Developments in electronics in recent years have resulted in new sensors capable of measuring the required atmospheric entities with sufficient speed and accuracy to render the method practical at this time.

Objectives

The overall project objective is to develop an integrated system of functions to predict the consumptive use race of crops in Caddo County, Oklahoma from basic meteorological parameters. The specific supporting objectives included in the overall objective are:

1. Verification that the eddy correlation system can accurately evaluate the energy fluxes necessary to balance a surface energy budget;
2. Calibration of the wind function of the modified Penman evapotranspiration prediction equation for local conditions;
3. Development of prediction functions that will permit the estimation of net radiation and soil heat flux inputs to the modified Penman equation from other, more easily measured meteorological parameters.
4. Development of a relationship for the crop coefficient for Florunner peanuts as a function of stage of growth.

CHAPTER II

BACKGROUND THEORY

Energy Balance Equation

The law of conservation of energy dictates that energy in a system can neither be created nor destroyed. For the canopy of a growing crop in a field, the energy from the sun is the driving force for all activities that occur. The net radiation from the sun either goes into vaporizing water (latent heat flux), heating the air (sensible heat flux), heating the ground (soil heat flux), driving plant processes (photosynthesis), or miscellaneous energy uses (heat storage in the biomass, etc.). A summary of the utilization of the energy available at the crop canopy is found in the energy balance equation:

$$R_n + H + G + LE + P + M = 0 \qquad (2.1)$$

where

R_n = Net radiation

H = Sensible heat flux

G = Soil heat flux

LE = Latent heat flux

P = Photosynthetic energy exchange

M = Miscellaneous energy exchange.

The contributions of photosynthesis and miscellaneous energy exchanges in field crop situations are insignificant

in comparison to other components of the energy balance. Therefore, it is normally simplified to:

$$R_n + H + G + LE = 0 \ . \qquad (2.2)$$

A sign convention of positive for energy flow toward the crop canopy, and negative for flow away from it is normally assumed. During the daylight hours, net radiation is the major positive energy flow, while latent heat is the major negative energy flow.

Eddy Correlation

Theory Development

The instantaneous flux of a transportable entity in a body of fluid in fully turbulent flow is given by:

$$F = pvc \qquad (2.3)$$

where

F = Flux of the entity (g/m^2s)

p = Fluid density (g/m^3)

v = Fluid velocity in the given direction (m/s)

c = Concentration of the entity in the fluid (g/g).

To apply this theory in a more specific situation, consider the vertical flux of water vapor in the earth's atmosphere. In this case:

$$E = pwq \qquad (2.4)$$

where

E = Vertical flux of water vapor (g/m^2s)

p = Air density (g/m^3)

w = Vertical wind velocity (m/s)

q = Specific humidity (g/g).

Each of the constituents of the equation can have its instantaneous value expressed as:

$$p = \bar{p} + p' \tag{2.5}$$

$$w = \bar{w} + w' \tag{2.6}$$

$$q = \bar{q} + q' \ . \tag{2.7}$$

The overbar denotes the mean value during an averaging period, and the prime denotes the instantaneous deviation from the mean. For limited elevations, within 30 m of the ground surface, and for relatively short averaging periods, it is not unreasonable to assume that air density is constant. Therefore, it can be assumed that $p'=0$, and that $p=\bar{p}$. Using this simplifying assumption, and equations 2.6 and 2.7, equation 2.4 can be expanded to:

$$E = p\overline{wq} + p\bar{w}q' + pw'\bar{q} + pw'q' \ . \tag{2.8}$$

By careful selection of the measurement site, components of the equation containing the mean vertical wind velocity term can be eliminated. Logic shows that for any averaging period longer than a few seconds, there can be no long-term net wind velocity upward or downward above a level, uniform surface. Eddy correlation measurements by Dyer (1961) confirmed that the mean vertical wind velocity was essentially zero over a level crop canopy for periods ranging from half a minute up to several hours. Applying this assumption, equation 2.8 becomes:

$$E = pw'\bar{q} + pw'q' \ . \tag{2.9}$$

Considering an averaging period of some length, the

average flux is expressed as:

$$\bar{E} = p\bar{w}'\bar{q} + p\overline{w'q'} \quad . \tag{2.10}$$

By definition, the average value of the deviations of a quantity from its mean value is zero. Therefore, $\bar{w}'=0$. Removing the term with this expression reduces equation 2.10 to:

$$\bar{E} = p\overline{w'q'} \tag{2.11}$$

where

$\overline{w'q'}$ = Covariance of vertical wind and specific humidity, (g-m/g-s).

Thus, over a level, uniform surface the vertical flux of water vapor is entirely due to eddy transport, with no contribution from mean vertical flow.

The eddy correlation method can be applied to the vertical fluxes of other atmospheric entities as well. To complete the crop canopy energy budget, the sensible heat flux must be evaluated also. Following the same procedure as for evaporative flux, but using the covariance of vertical wind and air temperature, the sensible heat flux is found to be:

$$\bar{H} = pC_p\overline{w'T'} \tag{2.12}$$

where

$\bar{H}$ = Mean sensible heat flux, (W/m^2)

p = Air density, (g/m^3)

C_p = Specific heat of air, (J/g-C)

$\overline{w'T'}$= Covariance of vertical wind and temperature, (m-C/s).

Frequency Requirements

The frequencies of the eddies involved in turbulent exchange above crop canopies are known to be dependent upon horizontal wind velocity and height above the canopy. A normalized frequency that is independent of these factors has been defined as follows:

$$f = nz/\bar{u} \qquad (2.13)$$

where

f = Normalized frequency, unitless

n = Cyclical frequency, (Hz)

z = Height of measurement, (m)

$\bar{u}$ = Mean horizontal wind velocity (m/s).

Using the approach to sampling frequency outlined by Kaimal (1975), a system must sample at a rate three times the Nyquist frequency, or six times the highest frequency of physical significance, in order to keep aliasing effects from becoming significant. Therefore, a system operating at a frequency of 10 Hz can adequately sample frequencies of 1.67 Hz or lower. If eddy sensors are located at a height of 1.8 m, and winds as fast as 9 m/s will be tolerated during measuring periods, equation 2.13 shows that fluxes from normalized frequencies of 0.33 and lower can be adequately measured by the system. The eddies associated with the vertical transport of water vapor and specific heat have been shown to have normalized frequencies in the range of 2 to 0.001, with frequencies of the order of 0.1 being most important (Kanemasu et al.,

1979). According to McBean (1972) a measurement system functioning at 10 Hz at a height of 1.8 m in a 9 m/s horizontal wind will suffer approximately a 5% error in flux measurement due to frequency response in neutral or unstable atmospheric conditions.

In regard to atmospheric stability, conditions are neutral when a parcel of air raised adiabatically an infinitesimal amount has the same density as the surrounding air. If the parcel of air is less dense, conditions are said to be unstable. Stable or inversion conditions exist if the parcel of air is more dense than the surrounding air. The effects of bouyancy enhance turbulence in an unstable atmosphere, and suppress turbulence in a stable atmosphere.

Height Requirements

Eddies of many sizes are responsible for the vertical transport of water vapor and other atmospheric entities. The size of the eddies involved in transport processes generally increases with increasing height. Even though the size of the eddies increases and their frequency decreases with height, it has long been assumed that the vertical fluxes of atmospheric entities are constant with height. Between elevations of 6 m and 22 m, Kaimal (1969) found the fluxes of sensible heat and momentum to vary by $\pm$20% or less. Dyer and Hicks (1972) found the variation in sensible heat and momentum flux between 4 m and 14 m to be

on the order of 10% or less. Thus, raising the height of measurement reduces the need for speed in the measurement process, but still measures virtually the same flux given off by the canopy.

The height at which sensors are operated is dictated to some degree by their spatial resolution. This factor is especially important in the measurement of vertical wind fluctuations because of the variation in eddy size with height. A sonic anemometer with a 10 cm path length could conceivably measure the average velocity of two or more small eddies within its sensors, giving an erroneous output. To avoid this, the instrument should be operated at a height where the number and importance of eddies smaller than its spatial resolution is not significant. Kaimal (1975) gives the relationship for unstable air:

$$z_{min} = 6 \pi d \qquad (2.14)$$

where

z_{min} = Minimum operating height (m)

d = Spatial resolution of the instrument (m).

A sonic anemometer with a 10 cm path length should be limited to heights of approximately 1.9 m and above to avoid the effects of spatial averaging.

Sensor Separation

Ideally, all of the eddy correlation sensors should occupy the same physical location, taking measurements at the same point. Any separation of sensors will necessarily

lead to inaccuracies because the atmospheric properties measured may come from different eddies. Since eddy size is a function of height above the ground surface, the degree of error introduced due to a given separation of sensors will also be a function of height.

The criterion for the separation of paired sensors is the same for individual sensors. Therefore, an absorption hygrometer and a sonic anemometer physically separated by 10 cm should not operate below a height of approximately 1.9 m. Dyer et al. (1983) graphically expressed a relationship between physical separation of instruments and measurement errors. A transverse separation of 10 cm results in approximately a 5% reduction in correlation of vertical wind sensors at a height of 4 m in a 9 m/s horizontal wind. The reduction in correlation will be greater at lower heights.

Koprov and Sokolov (1973) developed an empirical relationship for the reduction in correlation of the covariance of vertical wind speed and temperature due to transverse sensor separation. Their relationship is:

$$r_{wT} = 0.93 \exp(-y/z_0) \qquad (2.15)$$

where

r_{wT} = Normalized correlation function, R_{wTy} / R_{wT0}

(R_{wTy}= Correlation function at separation=y)

(R_{wT0}= Correlation function at separation=y_0)

y = Transverse separation, (m)

z_0 = Instrument height, (m).

The correlation function, as defined by the authors, is:

$$R_{wTy} = w(0,0,0,z_0)\ T(0,y,0,z_0) \qquad (2.16)$$

where

$w(0,0,0,z_0)$ = Vertical wind speed at height=z_0

$T(0,y,0,z_0)$ = Temperature at height=z_0, y meters away in the transverse direction.

Partitioning the variables, and making the same assumptions as in the original development of the eddy-correlation theory, the correlation function equates to the covariance of the two measured variables. One covariance is determined with the sensors a distance, y, apart, and the other with the sensors at the baseline separation, y_0.

The instruments used in determining this relationship suffered from interference when spaced closer than 10 cm. As a result, the relationship is based on R_{wT0} at a baseline separation of y_0=10 cm rather than at y_0=0. While the authors do not recommend the use of the relationship at y/z_0 ratios of less than 0.2, extrapolation of the exponential function to y=10 cm yields the intercept value of 0.93. This indicates a reduction in $\overline{w'T'}$ of 7% at a 10 cm separation. Errors in the covariance, $\overline{w'q'}$, would be approximately the same.

Averaging Period

One complication associated with increasing instrument height relates to the length of averaging period required to account for low frequency eddies. Kanemasu et al.

(1979) suggest the relationship:

$$T > 100\ z/u \qquad (2.17)$$

where

T = Averaging time (T)

z = Measurement height (L)

u = Average horizontal wind velocity (LT^{-1}).

This will account for eddies with normalized frequencies as low as 0.001, which have been shown to have significant contributions to vertical fluxes. The longer averaging period at greater heights is necessary to ensure that mean vertical wind velocity is zero. The greater contribution of low frequency eddies is the cause for this requirement.

Fetch Distances

The greater the height of eddy correlation instruments, the greater the fetch distance required for accurate measurements. This is because the turbulent boundary layer of the air mass must adjust to the changed conditions over which it is flowing. Fetch refers to the distance downwind from a change in surface conditions to the point of measurement. The height to which the fully adjusted boundary layer is developed over a new surface can be estimated from surface conditions and the distance from the point of change. Munro and Oke (1975) estimate the relationship to be:

$$d(x) = 0.1\ x^{.8}\ z_0^{.2} \qquad (2.18)$$

where

$d(x)$ = Height of the boundary layer at point x, (m)

x = Fetch distance, (m)

z_0 = Roughness length, (m).

The roughness length is an aerodynamic parameter that quantifies the drag characteristics of a vegetated surface. It can be determined by measuring the horizontal wind velocity profile above the surface and determining the height at which velocity is effectively zero. Szeicz et al. (1969) developed an empirical relationship for the roughness length of agricultural crops as:

$$\log_{10} z_0 = 0.997 \log_{10} h - 0.883 \qquad (2.19)$$

where

z_0 = Roughness length, (m)

h = Crop height, (m).

Using this approach, a 20 cm tall reference crop has an estimated roughness length of 0.0263 m. A fetch distance of 92 m downwind from the leading edge of the field is required for the full adjusted boundary layer to reach instruments located at a 1.8 m height. However, Kanemasu et al. (1979) and Rosenberg et al. (1983) both suggest that a fetch-to-height ratio of 100:1 is more appropriate for agricultural fields than the approximately 50:1 ratio derived from the equation.

CHAPTER III

REVIEW OF LITERATURE

Penman Equation

General

The use of meteorological data to predict the rate of a crop's evapotranspiration (ET) is an exercise that has been practiced for many years. There are at least 16 different equations that have enjoyed some degree of popularity in predicting reference crop ET over the years (Jensen,1973). Some of these equations are purely empirical, while others have a sound theoretical basis. Penman (1948) was one of the first investigators to develop a combination equation to predict ET. Combination equations consider both the energy required to vaporize liquid water within the crop canopy and soil surface, and the aerodynamic factors involved in transporting the water vapor away from the evaporation surface and into the atmosphere. Penman's approach is not a purely theoretical equation, because it contains an empirical factor in the aerodynamic portion of the equation. Nearly forty years after its initial development the Penman equation is still one of the most popular ET prediction equations worldwide.

The equation for evaporation from open water as originally put forth by Penman (1948) is:

$$ET_o = [d/(d+g)]\ (R_n+G) + [g/(d+g)]\ 15.36\ W_f\ (e_s-e) \quad (3.1)$$

where

ET_0 = Open water evapotranspiration, (cal/cm^2-day)

d = Slope of the vapor pressure-temperature curve, (mb/C)

g = Psychrometric constant, (mb/C)

R_n = Net radiation, (cal/cm^2-day)

G = Soil heat flux, (cal/cm^2-day)

15.36 = Constant of proportionality, (cal/cm^2-mb-day)

W_f = Empirical wind function

e_s = Saturation vapor pressure of air, (mb)

e = Ambient vapor pressure of air, (mb).

The value of the wind function, W_f, is given by:

$$W_f = a + bU_2 \quad (3.2)$$

where

U_2 = Horizontal wind run at 2 m elevation, (km/day)

a,b = Linear regression coefficients.

Several other investigators have since developed variations or improvements on the combination approach of Penman. Monteith (1963,1964) modified the original Penman equation, incorporating aerodynamic resistance and bulk stomatal resistance terms into the aerodynamic portion of the equation. Inclusion of these terms eliminates all empiricism from the equation. The terms are not easily measured or predicted, however. van Bavel (1966) developed a variation on Penman's equation which also contains no empirical terms. His equation includes an aerodynamic

parameter related to surface roughness. The predicted ET of the equation is very sensitive to this parameter, which is constantly changing and difficult to quantify. Slatyer and McIlroy (1961) developed a combination equation similar to the Penman equation as modified by Monteith. Their version uses wet bulb depression instead of saturation deficit in the aerodynamic term.

Net Radiation

Net radiation is the major input factor controlling the magnitude of the predicted Penman ET. Net radiation is a meteorological parameter that is not always measured, even at agricultural research installations. This is due, to some extent, to the fragility of the more common designs of net radiometers. In order to protect the collection surface and still permit the measurement of all wavelengths of radiation that support the evaporation of water, they are covered by light-weight domes of polyethylene.

Numerous methods have been devised to predict net radiation from other radiation measurements. One rather involved procedure is outlined by Jensen (1973), in which it is predicted from solar radiation, air temperature and saturation deficit. This method requires empirical coefficients which are site specific, to some degree.

Several experimenters have developed simple linear regression models which estimate net radiation from solar radiation alone. This method is especially useful in light

of the development of automated weather stations that use silicon pyranometers and electronic integrators. These devices measure solar radiation reliably with very little maintenance. Fritschen (1967) found that daytime hourly net radiation over alfalfa could be predicted by:

$$R_n = 0.75\ R_s - 6.6 \qquad (3.3)$$

where

R_n = Net radiation, (cal/cm^2-hr)

R_s = Solar radiation, (cal/cm^2-hr).

The correlation coefficient for this relationship was approximately 0.995.

Soil Heat Flux

Soil heat flux is the flow of thermal radiation into and out of the ground. It is a function of the soil thermal conductivity and the temperature gradient in the soil. The determination of soil heat flux requires knowledge of the temperature gradient across a region of known conductivity. Since this is a measurement that is not easily made in the field, some investigators have made efforts to determine a functional relationship between soil heat flux and more easily measured parameters.

Moore (1976) did energy balance evaluations of a forested site in which soil heat flux was determined to be approximately 3% of the net radiation during daylight hours. Lloyd et al. (1984) found the soil heat flux under a stand of pine trees to be approximately 2% of net

radiation.

Kincaid and Heermann (1974) predicted daily soil heat flux for irrigated crops from mean daily air temperatures. Their relationship is:

$$G = 5\ (T_a-(T_1+T_2+T_3)/3). \qquad (3.4)$$

where

G = Soil heat flux, (cal/cm^2-day)

T_a = Mean daily air temperature, (F)

T_1, T_2, T_3 = Mean daily air temperatures of the three previous days, (F).

Wind Function

The original form of Penman's equation predicted the rate of evaporative loss from a free water surface. An adjustment was then made by use of a coefficient to apply the result to grass and bare soil. Penman (1963) later changed the empirical factors in the wind function term to a=1.0 and b=0.00621. This allowed the direct prediction of the ET of a short grass reference crop without the need of the conversion coefficient. Wright and Jensen (1972) subsequently developed coefficients of a=0.75 and b=0.0115 to apply to well watered alfalfa in Idaho. Doorenbos and Pruitt (1977) developed coefficients for the aerodynamic term at a variety of sites in an effort to obtain a single function that was applicable in a wide range of conditions. Considerable variability was evident from site to site, however. A slightly different approach was described by Burman et al. (1980) in which the factors are described by

polynomials which are a function of the number of days of the growing season which have elapsed.

Saturation Deficit

One important consideration in the application of the Penman equation is the manner in which the saturation deficit is computed. Pruitt and Doorenbos (1977), and Cuenca and Nicholson (1982), among others, have emphasized the importance of using the same method of computing the saturation deficit when predicting ET as was used when the equation was calibrated. All investigators agree that the most accurate of the popular methods of determining mean daily saturation deficit is to average hourly values. The accuracy of the method used to compute the saturation deficit is not the critical factor, but rather consistency between calibration and application.

Crop Coefficients

The ratio of a given crop ET to the reference crop ET is called the crop coefficient (Jensen,1968). Experimentally developed crop coefficients are necessary to apply an ET prediction equation to a wide range of crops. Crop coefficients are functions of crop physiology, degree of cover, planting date, length of growing season, and climatic conditions as well as the type of reference crop used.

Wright (1979) has developed a series of basal crop

coefficients that relate the ET of several crops grown at Kimberly, Idaho to alfalfa reference crop ET under well-watered conditions with a dry soil surface. Empirical relationships have been developed to modify basal crop coefficients, making them applicable in a variety of field conditions. Jensen et al. (1971) developed coefficients that modify the basal crop coefficient to account for reduced soil water availability, and also for wet soil surface conditions. Wright (1981) has further developed mean daily crop coefficients that can be applied without precise knowledge of exact soil water conditions. They can be applied to predict ET for a general area with a variety of soil water conditions, rather than for accurate prediction of water use in a specific field.

Eddy Correlation

Swinbank (1951) was the first to propose the application of fluctuation theory to the measurement of evaporative flux. At that time little was known of the frequencies of importance in the vertical transport of atmospheric entities close to the ground surface. Swinbank theorized that the eddies of importance in water vapor transport had periods on the order of a few seconds. His instrumentation consisted of a hot-wire anemometer, and fine-wire wet and dry thermocouples, placed 4.5 ft above the ground surface. He felt that his instrumentation could satisfactorily record fluctuations of wind speed and humidity with a

frequency of 1 Hz or lower.

Later work by Dyer (1961) used a device called an Evapotron, which was a unit that utilized a hot-wire anemometer and fine-wire wet and dry thermocouples. Initial testing at a height of 1.5 m above the ground showed that the unit had too slow a response time to accurately record the fluctuations of vertical wind speed and humidity so close to the evaporation surface. Upon raising the instrumentation to a height of 4 m, the sum of the measured latent and sensible heat fluxes accounted for an average of 99 per cent of the net radiation and soil heat flux. There was, however, considerable variability between individual trials.

The elevation of instrumentation to heights of 4 m above the ground surface presents problems in terms of adequacy of fetch distances at many agricultural installations. It is difficult to position instrumentation at a height of several meters in any but the largest experimental plots with sufficient distance from the boundaries to ensure development of the fully adjusted turbulent boundary layer. Adequate fetch is also necessary to ensure horizontal equilibrium of the vertical flux being measured. Consequently, readings taken with inadequate fetch may not necesarily reflect conditions in the field directly under the instrument. Work done by Dyer and Pruitt (1962) reflected these very problems with fetch distances of up to 190 m for instruments at a height of 4 m.

Due to problems in obtaining instruments capable of measuring humidity fluctuations with sufficiently rapid response times, little work of consequence was done using eddy correlation to measure evaporative flux until recently. During the last thirty-five years the method has been used in many studies of other types of vertical fluxes for which more satisfactory instrumentation was available. Dyer et al. (1967) used a device called a Fluxatron to measure vertical sensible heat flux at a height of 4 m. The Fluxatron used a propeller anemometer and resistance thermometers to make the eddy measurements. Wesley et al. (1970) used a pressure sphere anemometer and resistance thermometry to satisfactorily measure sensible heat flux to within 1 m of the ground surface. Hicks (1973) used a propeller anemometer, fast response thermisters, and conventional cup anemometers to measure sensible heat and momentum fluxes. Bottemanne (1979) tested eddy correlation instrumentation that measured sensible heat and momentum fluxes. Wesley et al. (1981) used the method to measure the flux of nitrogen oxides over soybean fields.

Relatively recent instrumentation and data processing advances have rekindled interest in the application of eddy correlation methods to the measurement of evaporative flux. Kaimal and Businger (1963) reported on an early device that used sonic transmissions to measure wind speed. Campbell and Unsworth (1979) reported on the development of an inexpensive sonic anemometer with frequency response

capabilities that reportedly permit measurement of vertical wind fluctuations at heights as low as 50 cm above the ground.

The rapid measurement of absolute humidity has been the greatest challenge to eddy correlation measurement of water vapor flux. Studies of the absorption of radiation by water vapor led to the development of humidity measuring devices with extremely rapid response times. Absorption hygrometers use a source of radiation that is highly susceptible to absorption by hydrogen. The degree of extinction of the emitted radiation before it strikes a sensing device located across an air gap is an indication of the hydrogen content of the air in the gap. Staats et al. (1965) described an absorption hygrometer that utilized infrared radiation. Randall et al. (1965) reported on a humidiometer that used another type of radiation, the Lyman-alpha line. Miyake and McBean (1970) compared a Lyman-alpha humidiometer to a dew-point hygrometer and found it to be capable of responding to a broader range of frequencies than the hygrometer. Humidity fluctuations for the eddy correlation method can now be measured accurately with a rapid response Lyman-alpha hygrometer developed by Buck (1976). The reported response time for this instrument is 12 milliseconds. Redford et al. (1980) compared humidity fluctuation measurements made over a vegetated surface with a Lyman-alpha hygrometer and a fine-wire thermocouple psychrometer. Their conclusion

was that the Lyman-alpha hygrometer was superior in response to the high frequency eddies responsible for water vapor transport at lower heights.

Campbell and Tanner (1985) have reported the development of an ultraviolet absorption hygrometer using a krypton filled glow tube as the radiation source. The extinction coefficients for the krypton line of radiation are not as favorable for atmospheric measurements as for the Lyman-alpha radiation line. The krypton radiation is absorbed to a greater degree by atmospheric oxygen, and to a lesser degree by hydrogen. The device will still permit accurate and rapid measurements of absolute humidity, however. It has the advantage of a more stable calibration, and a longer radiation tube life than the Lyman-alpha hygrometer. One complication with the instrument is the build up of an unidentified deposit on the windows of the source and sensor tubes that attenuates the signal. The deposit appears to be due to some reaction of the air with the radiation, and is easily removed by wiping the windows with damp cotton.

Several investigators have used eddy correlation systems incorporating these rapid response instruments to measure evaporative flux with a fair degree of success. Hicks et al. (1975) used light-weight cup anemometers, a propellor anemometer, a micro-bead thermister and an infrared hygrometer to measure the eddy fluxes of momentum, sensible heat and latent heat over a pine forest. The instruments

were placed 2.9 m, 3.85 m, and 4.5 m above the forest canopy for each of three sets of measurements. The response speed of the anemometers was deemed to be too slow at the lower heights. At 4.5 m above the canopy, the energy balance was satisfactory, provided an empirical canopy heat storage term was included.

Moore (1976) used a Gill propellor anemometer, a micro-bead thermister and an infrared hygrometer to measure the eddy fluxes of sensible and latent heat over a pine forest. Soil heat flux was estimated, from a previously determined experiment, to be 3% of the net radiation. During periods for which the horizontal wind speed was in excess of 2 m/s, the energy budget balanced to within 20%. In lighter winds the fluxes of sensible and latent heat were severely underestimated.

Spittlehouse and Black (1979) used an energy balance/ eddy-correlation technique to measure evapotranspiration over a Douglas fir forest. Sensible heat flux was measured with a fast response thermister and Gill propellor anemometers. Net radiation and soil heat flux were measured directly, and canopy heat storage was estimated. Latent heat flux was estimated as the residual left when sensible heat flux, soil heat flux and canopy heat storage were subtracted from net radiation. The authors experienced difficulties with their propellor anemometers, finding that they stalled at low wind speeds. Their eddy-correlation system was found to underestimate latent heat

flux relative to a Bowen ratio system operating at the same site.

Anderson et al. (1984) used a rapid response CO_2 sensor, a drag anemometer, a Lyman-alpha hygrometer, and a fine-wire thermocouple to measure CO_2 flux and to balance a surface energy budget over a soybean crop. The results of balancing the energy budget were presented graphically by the authors, and the closure error appears to be on the order of $\pm$30%.

Lloyd et al. (1984) described a microprocessor controlled eddy correlation system that measured the eddy fluxes of sensible heat, latent heat, and momentum. The system used a vertical sonic anemometer, an infrared hygrometer, fast response thermocouples, and propellor anemometers. The system instrumentation was placed at a height of 3.5 m, and scanned at a rate of 10 Hz. The eddy correlation system showed a shortfall in balancing the energy budget on all days of operation. On one day the fluxes of sensible and latent heat fell 13% short of measured net radiation. The next best closure reported was a 16% shortfall. Soil heat flux was not measured directly in this experiment, but was estimated as a percentage of measured net radiation based on a previously determined relationship.

Neumann and den Hartog (1985) measured atmospheric fluxes of momentum, sensible heat, water vapor, ozone, and sulphur with an eddy correlation apparatus. They used a

triple axis sonic anemometer to measure wind speed and air temperature, and a Lyman-alpha humidiometer to measure humidity. Their instrumentation was placed at a height of 4 m, and scanned at a rate of 20 Hz. The measurement of water vapor and sensible heat fluxes was of secondary interest in this study on pollutant deposition. Consequently, the authors did not report their success in measuring these fluxes.

Tanner (1984) described a portable eddy correlation system, utilizing a sonic anemometer, Lyman-alpha hygrometer, and fine-wire thermocouple, that is capable of closing a surface energy budget over vegetated surfaces. The system was tested near the precision weighing lysimeters at Kimberly, Idaho. The values of the latent flux measured by two systems evaluated there accounted for 75% and 81%, respectively, of the energy required to balance the energy budget at the test site. The failure to more closely balance the energy budget was felt to be largely due to underestimation of latent heat flux. The author suggested, as one problem, poor response by the hygrometer due to mechanical constriction of air flow between the source and sensor tubes. Another possible difficulty given was the 20 cm physical separation between the hygrometer and the sonic anemometer, which has been shown to cause underestimation of latent heat flux.

Tanner et al. (1985) reported on a comparison of six portable eddy correlation systems. The systems all used

single axis sonic anemometers to measure vertical wind fluctuations. Two of the systems used Lyman-alpha hygrometers, while the others used krypton ultraviolet hygrometers. Measurements of latent and sensible heat fluxes made by the systems ranged from 0.69 to 1.02 times the energy needed to balance the measured net radiation and soil heat flux at the test site. The six systems measured an average of 0.89 of the sensible and latent heat fluxes required to balance the energy budget on all days of observation.

Verma et al. (1986) used a Lyman-alpha hygrometer, rapid response CO_2 sensor, sonic anemometer, and a fine-wire thermocouple to measure the vertical fluxes of CO_2, latent heat and sensible heat over a deciduous forest. The sum of latent and sensible heat fluxes measured by eddy correlation methods was compared to the sum of measured net radiation and soil heat flux, plus a computed canopy heat storage term. The measured eddy fluxes varied within $\pm$30% of the values required to balance the other energy terms. The authors state that an error of $\pm$20% should be expected due to variability in the measurement of all energy fluxes. The remaining 10% error was felt to be due to uncertainty in the computation of the stored energy in the forest canopy mass.

CHAPTER IV

PROCEDURE

Eddy Correlation Sensors

General

Both the calibration of the ET prediction equation and the development of crop coefficients depend upon the accurate measurement of evapotranspiration concurrent with measurement of the necessary weather parameters. The eddy correlation apparatus is capable of measuring the evapotranspiration directly in the air above the crop canopy. The major components of the eddy correlation apparatus are rapid response instruments that measure the fluctuations of vertical wind speed, air temperature and absolute humidity.

Sonic Anemometer

The vertical wind speed fluctuations are measured by a single axis Campbell Scientific CA-27 sonic anemometer (Figure 1). The device uses a pair of sonic transducers to alternately send and receive sound signals in opposite directions along a 10 cm long vertical path. Differences in vertical wind speed are detected by variations in signal phase shift between the upward and downward signals in a given measurement interval. The device has a stable

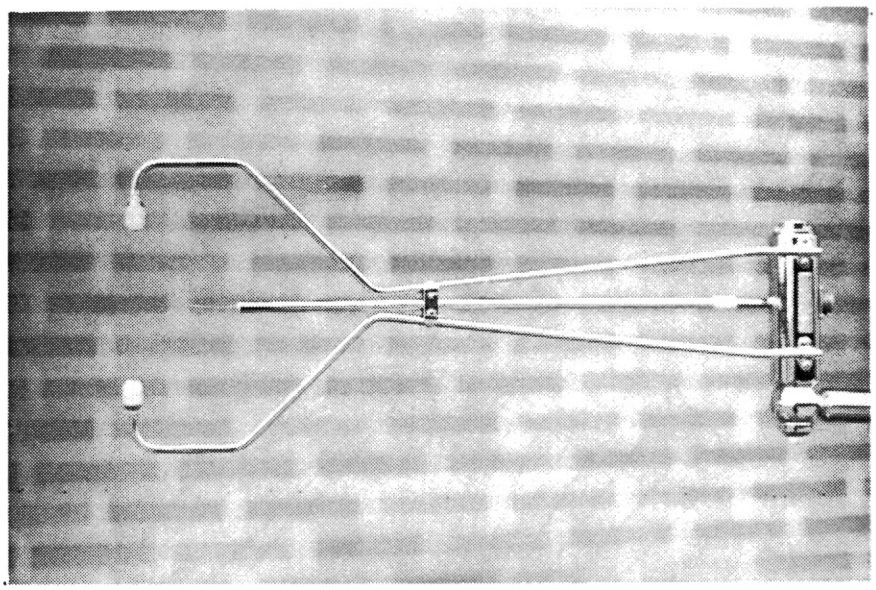

Figure 1. The CA-27 Sonic Anemometer

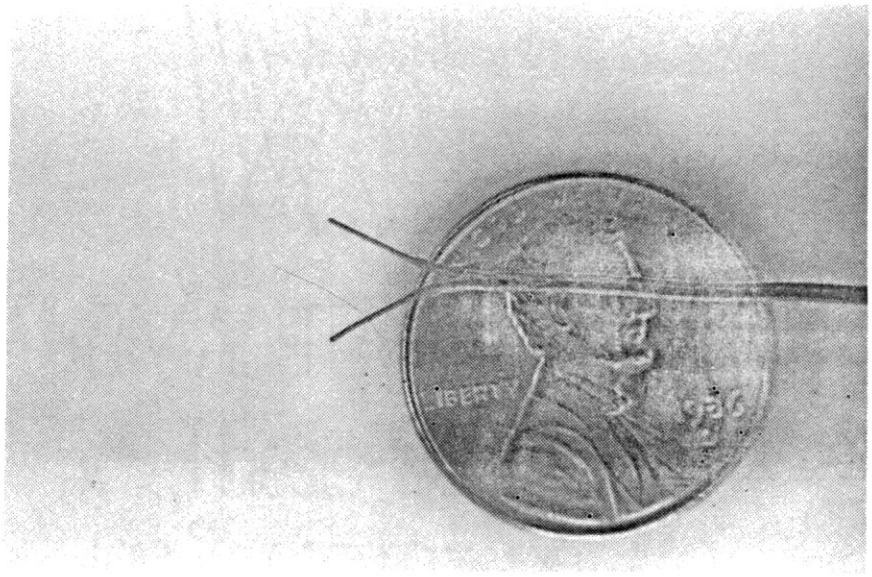

Figure 2. The 13 Micron Fine Wire Thermocouple for the CA-27 Sonic Anemometer

calibration slope, but the intercept tends to shift with variations in temperature. This renders it impractical for measurements of absolute wind speed. However, the eddy correlation method requires only the relative fluctuations in vertical wind speed, which the anemometer effectively measures. The circuitry of the anemometer is capable of responding at frequencies of greater than 40 Hz. The magnitude of vertical wind speeds that the anemometer can measure range from +4 m/s to -4 m/s.

An integral part of the sonic anemometer is a fine-wire thermocouple located midway between the transducers, and approximately 2 cm from the sonic signal path (Figure 2). The thermocouple is made from 13 micron diameter chromel-constantan wire, capable of responding to air temperature fluctuations at frequencies greater than 30 Hz. The thermocouple reference junction is a thermister embedded in the solid stainless steel base of the anemometer, which has sufficient mass to have a thermal time constant of 20 minutes. The fine-wire thermocouple registers the fluctuations in air temperature relative to the temperature of the anemometer base. Thus, the thermocouple cannot directly measure absolute air temperature. However, the eddy correlation method of measuring sensible heat flux requires only the relative temperature fluctuations over the measurement interval.

Krypton Hygrometer

Absolute humidity is measured by the Campbell Scientific KH-20 krypton hygrometer (Figure 3). The device measures the water vapor content of the air by means of the absorption of a certain wavelength of radiation between a source and a sensor. The source of radiation is an ultraviolet glow tube filled with krypton gas. The radiation line emitted by the source tube is strongly absorbed by hydrogen. The emitted signal is detected by the sensor located opposite the source tube with an air gap of known length between. The reduction of the signal strength between source and sensor is a function of the hydrogen content of the air in the gap. The only major source of hydrogen in normal air is water vapor.

The hygrometer is calibrated at the factory by measuring the voltage output of the sensor in air samples with known water vapor contents. The device has a log-linear calibration function which gives it a distinct advantage over the Lyman-alpha hygrometer, which has a non-linear calibration function. Use of the Lyman-alpha hygrometer necessitates an independent measure of absolute humidity by another device to determine which portion of the Lyman-alpha calibration curve to use.

The krypton hygrometer radiation line is also attenuated to some degree by oxygen, which creates a problem if the oxygen concentration of the air fluctuates. The manufacturer recommended the use of an oxygen correction

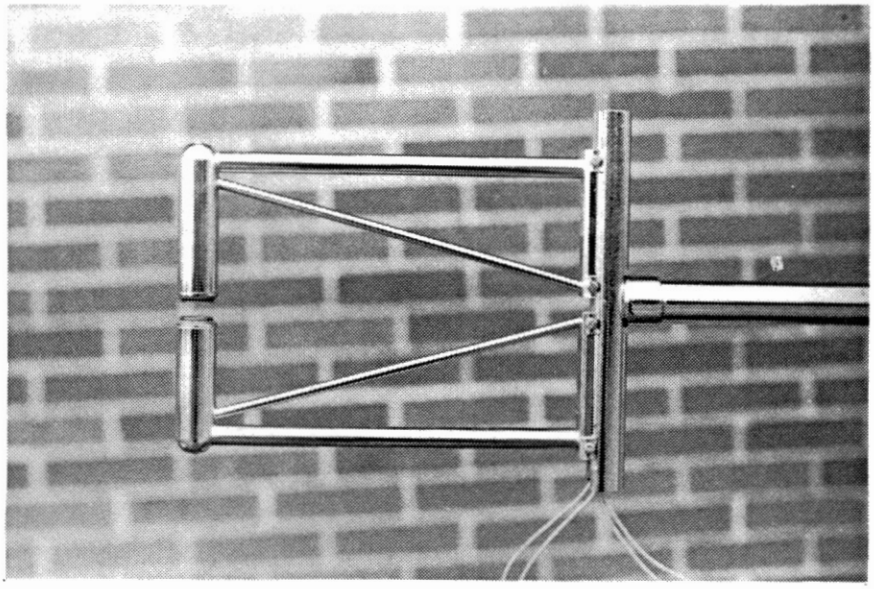

Figure 3. The KH-20 Krypton Ultraviolet Hygrometer

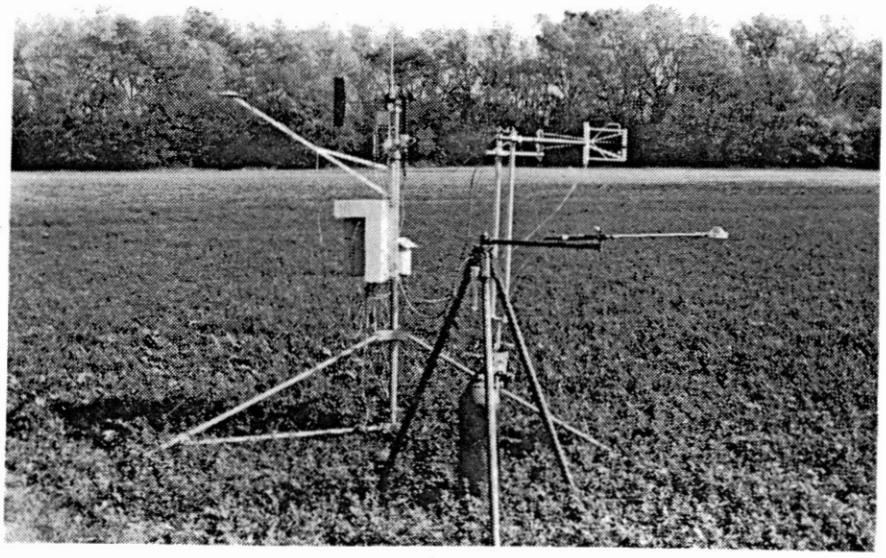

Figure 4. Deployment of the Instruments of the Portable Weather Station

factor based on air temperature and pressure. This was to prevent attributing a change in the measured signal to a change in water vapor content, when it was actually due to a change in the oxygen partial pressure of the air. This correction factor was initially computed, but was later discontinued, as it was always at least three orders of magnitude smaller than the uncorrected latent energy. It was therefore deemed that any fluctuation in output due to oxygen variability would be insignificant.

Conventional Weather Sensors

General

Other sensors deployed on the weather station included those required to obtain a complete set of input parameters for the Penman equation (Figure 4). These were a ventilated psychrometer, a net radiometer, a cup anemometer, a thermister for average ambient temperature, and a set of three soil heat flux plates. Also deployed were a solar pyranometer and a wind direction sensor.

Ventilated Psychrometer

Wet and dry bulb temperatures were measured by the Campbell Scientific WVU-7 ventilated psychrometer, manufactured by Delta T Devices. The temperatures were measured with wet and dry thermisters every 30 minutes, after being ventilated by a battery powered fan for two minutes. The psychrometer was mounted on the main tripod

mast at a height of two meters. The instrument was shielded by a polished stainless steel cover to prevent heating from solar radiation. The determination of the saturation vapor pressure from the dry bulb temperature was done using the approximation of Bosen (1960):

$$e_s=33.864[(0.00738T+0.8072)^8 - 0.000019|1.8T+48|+0.00132] \quad (4.1)$$

where

e_s = Saturation vapor pressure over water, (mb)

T = Ambient temperature, (C).

Ambient vapor pressure was determined from the wet and dry bulb temperatures in the manner outlined in Jensen (1973):

$$e = e_{sw}-g(T_a-T_w) \quad (4.2)$$

where

e = Ambient vapor pressure, (mb)

e_{sw} = Saturation vapor pressure at wet bulb, (mb)

g = Psychrometric constant, (mb/C)

T_a = Ambient air temperature, (C)

T_w = Wet bulb temperature, (C).

Net Radiometer

The net radiometer, a Swisstecho S-1, uses a thermopile embedded in a flat black collection disk covered by clear polyethylene domes. The radiometer was ventilated with dry nitrogen gas to prevent internal condensation on the domes. The instrument was mounted on a wooden theodolite tripod at the end of an arm approximately 1 m long. The instrument

height was approximately 1.3 m above the ground. The height of the instrument above the crop canopy varied with crop development, but was never less than 80 cm. The radiometer tripod was deployed approximately 3 m to 4 m from the weather station tripod to prevent shading effects. The device was factory calibrated before the season began.

Wind Speed Sensor

The horizontal wind speed sensor used was a Met-One 014A three cup anemometer. It uses a magnet-reed switch to produce a pulsed output whose frequency is proportional to wind speed. The anemometer has a threshold velocity of 0.447 m/s. It was mounted on the main axis cross arm at a height of 2 m.

Temperature Probe

Average ambient air temperature was measured by a Campbell Scientific 107 temperature probe. The probe thermister was excited continuously, and scanned every 15 seconds to obtain the 30 minute average temperature. It was felt that this would result in a value that more accurately reflected the actual average temperature than the single measurement taken with the psychrometer's dry thermister every 30 minutes. It was noted, however, that the two temperatures seldom differed by as much as one degree Celsius, except at sunrise and sunset. The temperature probe was positioned in the shade beneath the

data logger shelter to avoid temperature elevation due to solar radiation loading. The instrument height was approximately 1 m above the ground.

Soil Heat Flux Plates

The soil heat flux plates were manufactured by the Agronomy Department of Oklahoma State University. The differential thermopile is embedded in a rigid plastic resin wafer approximately 20 mm by 40 mm by 4 mm. The plates were calibrated by placing them in a pan of dry sand with three commercially produced Thornthwaite heat flux disks with known calibration factors. The pan was insulated on the sides with foam to ensure vertical heat flow through the sand. The pan was then heated evenly over the bottom surface, producing heat flux in the range of 20 W/m^2 to 300 W/m^2. The locally produced plates were found to have virtually a constant calibration factor over the range of heat flux measured.

Three heat flux plates were deployed for the duration of the growing season at each instrumentation site. A shallow hole approximately 20 cm in diameter was dug. A large flat-bladed knife was used to make a slit about 5 cm wide horizontally into the wall of the hole approximately 1 cm below the soil surface. A thin wooden splint was then used to push the heat flux plate into the slit until it was a minimum of 5 cm beyond the rim of the hole. The proceedure was repeated for two more plates at other positions on the

hole circumference. The excess lead wire was coiled in the hole and covered with the extracted soil. All six lead wires were terminated in a single waterproof coupler. A shielded cable from the data logger was then connected to the coupler during each measurement set-up. This arrangement assured rapid, correct connection to the plates with minimum disturbance to the soil and surrounding vegetation.

The placement of the soil heat flux plates at a depth of 1 cm below the soil surface has advantages and disadvantages. It makes them more susceptible to disturbance by surface traffic, which could alter their orientation or expose them directly to solar radiation. Their shallow placement can also have a potentially greater impact on crop root development. However, it is felt that shallow installation eliminates many difficulties associated with deeper installation. The damping effect of heat storage in the soil between the plates and the surface of the ground makes the correlation of readings from deep heat flux plates and surface instrumentation difficult. It was felt that careful location of the access hole and placement of the plates between individual plants minimized disturbance to the vegetation. Careful marking of the plate locations when measurements were not being taken prevented their disturbance by surface traffic.

Miscellaneous Sensors

Two sensors were deployed whose output was not directly needed for Penman equation computations. These were a wind direction sensor, and a solar pyranometer. The wind direction sensor, a Met-One 024A wind vane, uses a light-weight vane and a variable potentiometer to produce an electrical output that varies directly with the wind bearing. It was positioned on the main tripod cross arm at a height of 2 m. The sensor was used to determine when the wind was blowing from the proper direction to provide adequate fetch for valid eddy correlation measurements.

The solar pyranometer used was a Li-Cor LI-200S silicon pyranometer. It uses a silicon photodiode to produce an electrical output proportional to the intensity of incoming short-wave radiation. It was mounted on an arm extending from the main tripod mast at a height of approximately 2 m. It was deployed because it requires much less maintenance than a net radiometer and can be used on unattended weather stations. It is anticipated that with the development of a functional relationship between solar radiation and net radiation over reference crops, net radiometers may be replaced by pyranometers in future evapotranspiration prediction efforts.

Site Layout

Careful placement of instrumentation was necessary at each site. It was important to prevent the net radiometer

from being shaded by the weather station mast at any time during the day. Both of the tripods had to be positioned to avoid shading the location of the soil heat flux plates, as well. The eddy correlation instrumentation had to be positioned so that it was not in a wind shadow from any of the hardware at the instrumentation site.

The eddy correlation instruments were placed on a forked secondary mast attached to one of the weather station tripod legs, approximately 1 m from the main mast (Figure 5). The secondary mast was guyed to the tripod anchor stakes for stability using small cables and turnbuckles. The tripod was oriented so that the secondary mast was located upwind from the main mast. The hygrometer and sonic anemometer were attached on mounting arms in undisturbed air upwind of the secondary mast at a height of 1.8 m. The mounting arms were approximately 45 cm long, with the hygrometer arm being slightly shorter than the anemometer arm. The sensing heads of the two eddy correlation instruments were separated by a distance of approximately 10 cm (Figure 6). Closer spacing would have the advantage of reducing spatial variability of the eddy flux readings, but would increase the interference to air flow around one sensor by the other sensor (Kaimal, 1975). Placing the hygrometer on a shorter arm was felt to increase the angle of variation in horizontal wind that could be accepted. It was felt that the greatest interference to accurate readings would result from air

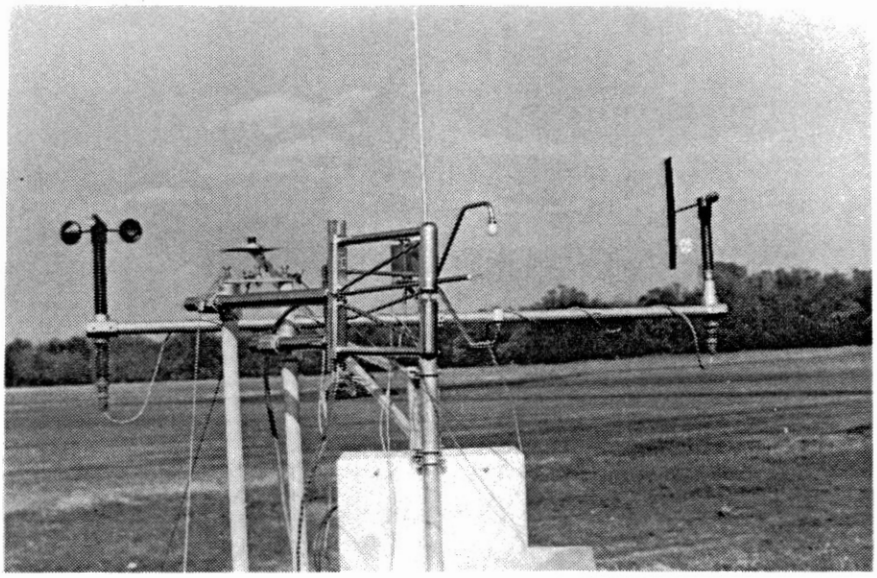

Figure 5. The Eddy Sensors Mounted Upwind of the Main Mast

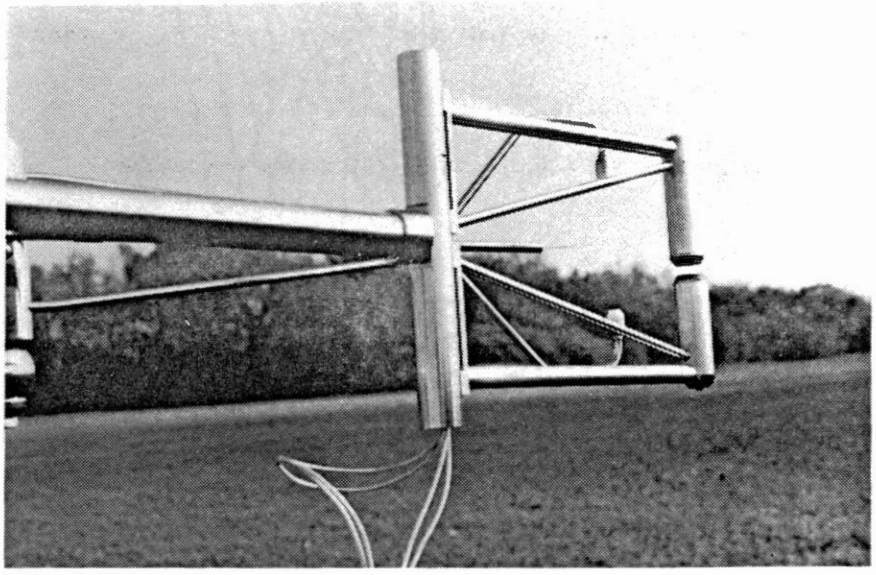

Figure 6. The Separation of the Anemometer and Hygrometer

flow across the hygrometer onto the thermocouple of the anemometer. The more massive hygrometer arms, heated by solar radiation, could in turn heat the air flow over the thermocouple and greatly affect the sensible heat measurements (Tanner, 1986).

Field Site Specifications

The physical site requirements for accurate eddy correlation measurements are fairly stringent. First of all, the field surface must be level and free of any local irregularities. This helps to assure that the long term mean vertical wind velocity is zero, which is a requirement of the eddy correlation theory. Next, the site must have adequate upwind fetch to ensure that the turbulent boundary layer over the crop canopy is completely developed to the height of the instruments. There is some debate as to the distance required for this. The sites chosen had at least 190 m of clear, relatively level fetch to the south of the instrumentation site. South winds predominate in the summer in the measurement area. Schematic diagrams of the instrumentation sites are given in Figures 7 through 10.

Datalogger

All of the instrumentation of the weather station is controlled by the Campbell Scientific CR21X datalogger. The datalogger reads the output of the various sensors, processes the data into a useable form, and stores the data

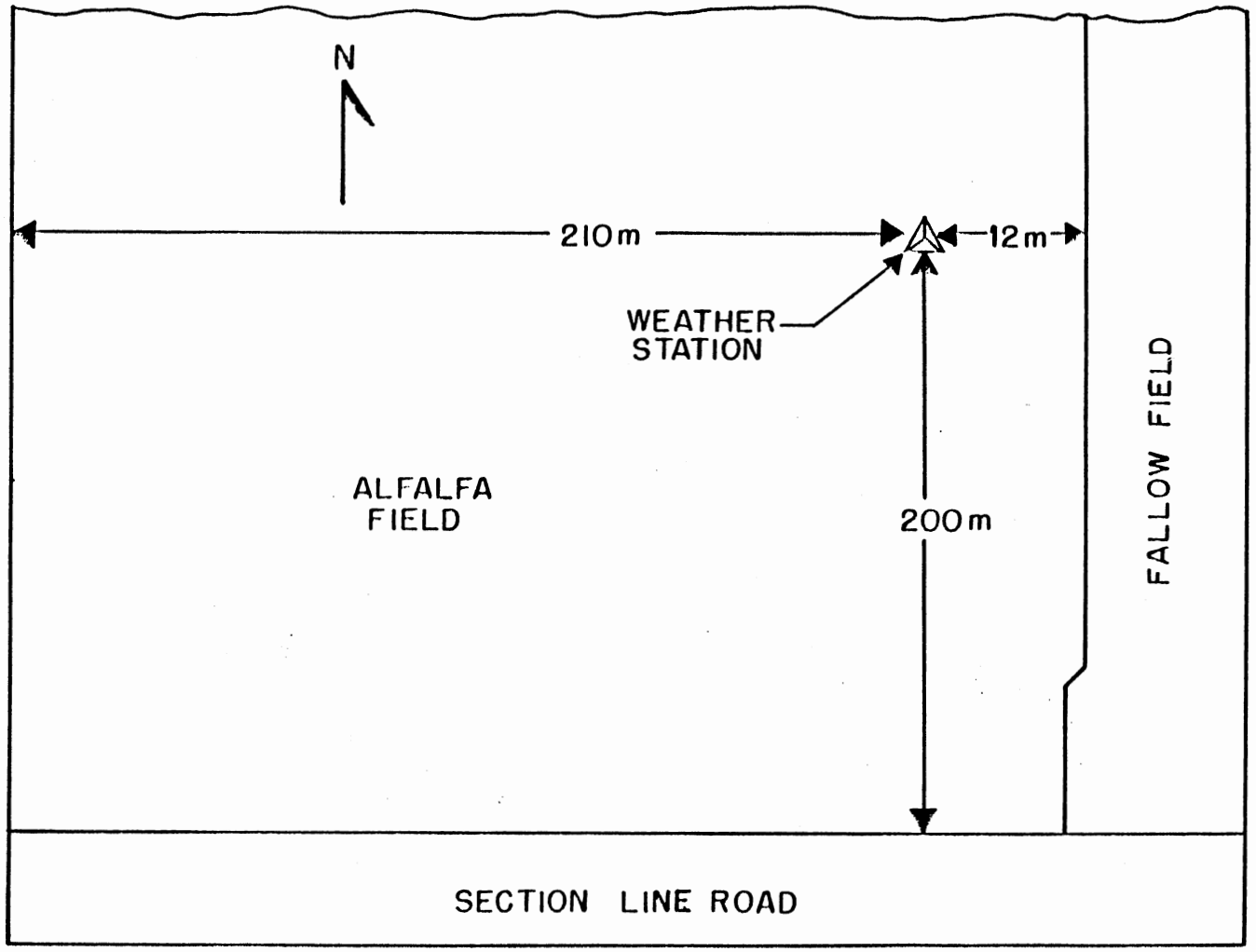

Figure 7. Spies Alfalfa Site

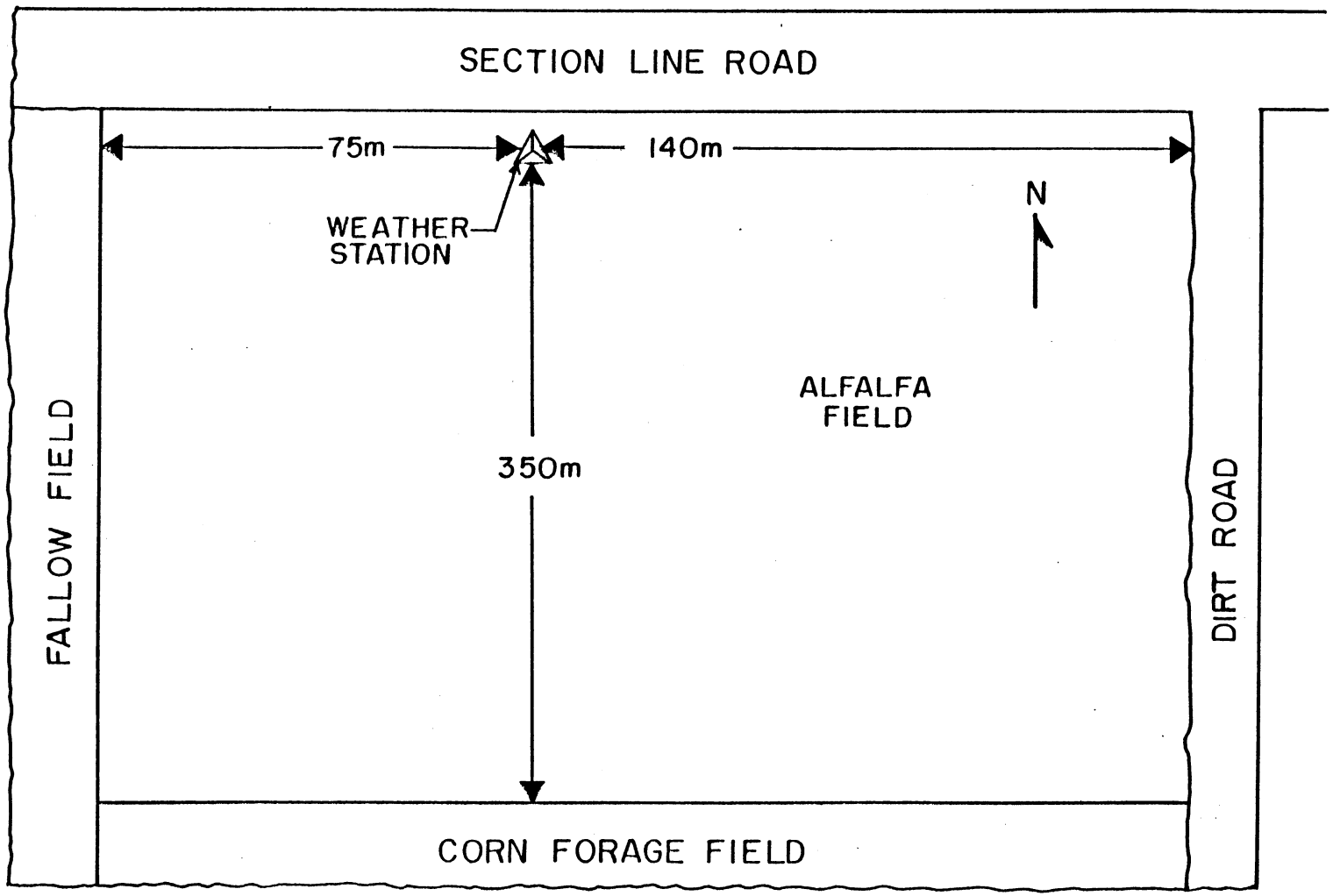

Figure 8. Farmer Alfalfa Site

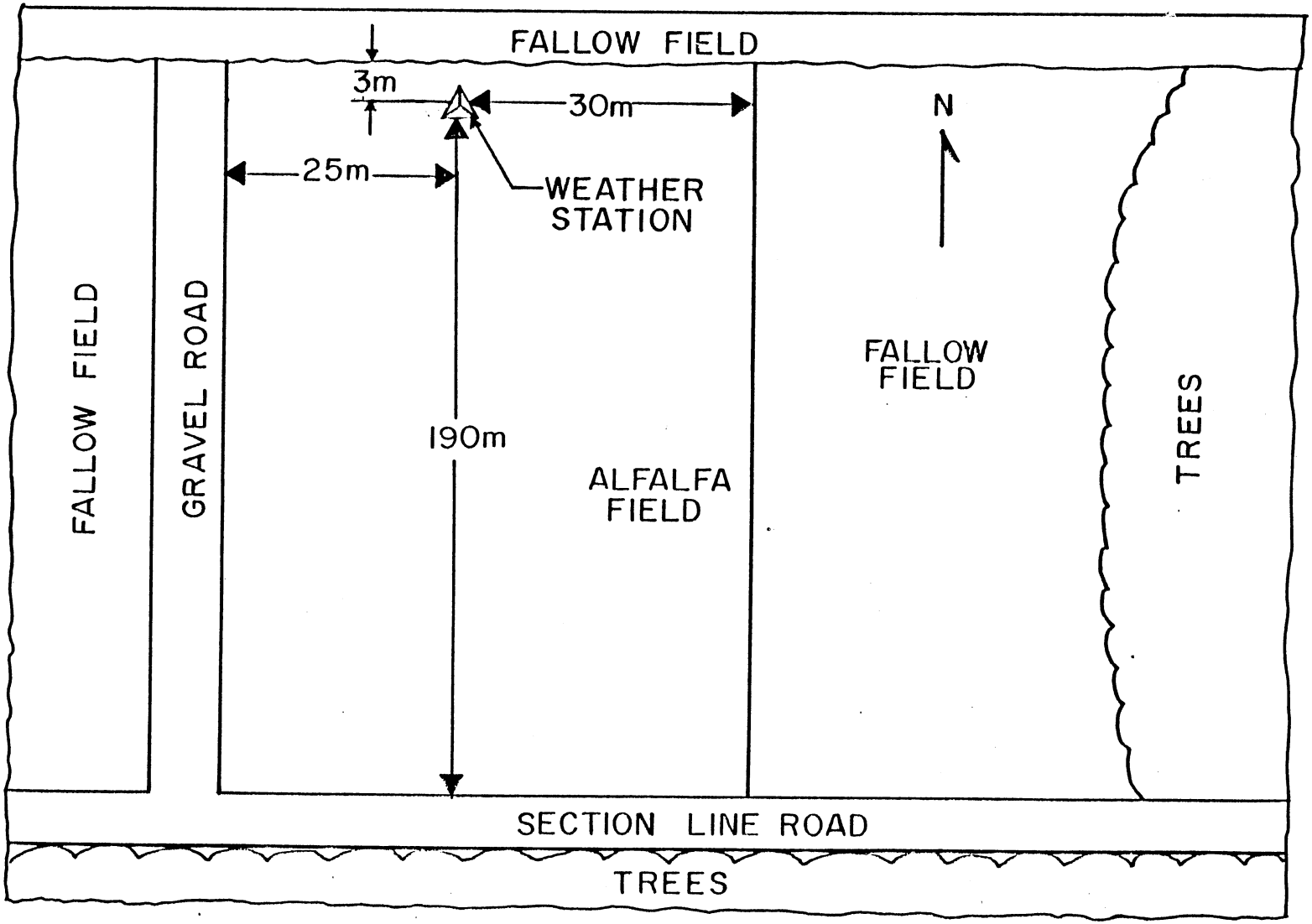

Figure 9. Agronomy Farm Alfalfa Site

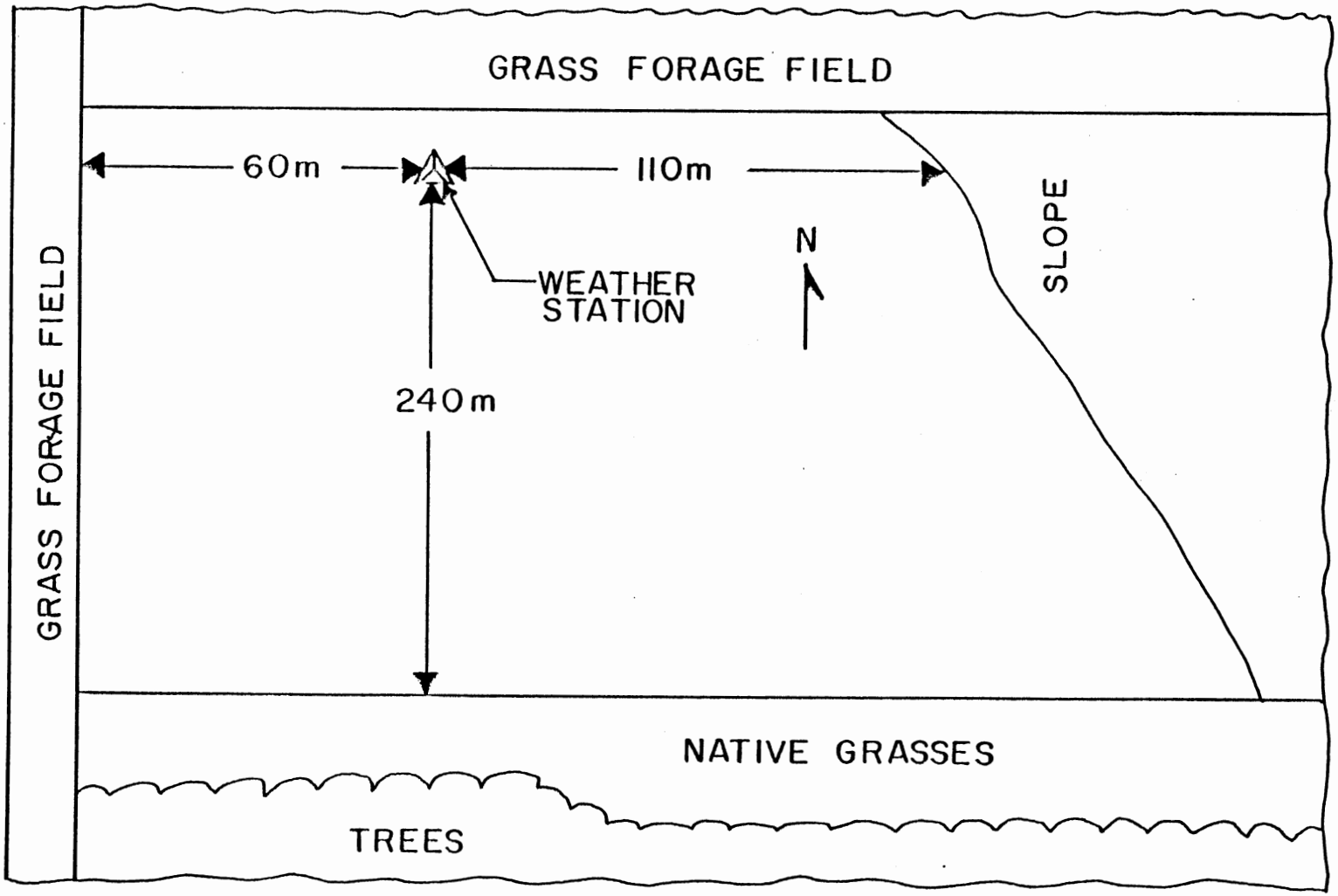

Figure 10. King Peanut Site

internally. It also transmits the data to a small thermal printer at the end of every output interval. Whenever an internal buffer in the datalogger is full the data are also sent, in a compressed binary form, for storage on magnetic cassette tape. The hygrometer, sonic anemometer, and psychrometer fan have external power supplies. All other power requirements for sensor operation are drawn from the datalogger.

The datalogger microprocessor is capable of scanning a sensor at intervals as short as 0.0125 sec. It cannot, however, do all of the necessary computations to put the eddy data in a useable form before such a short interval is over. The number of instruments being scanned by the datalogger limited the sampling frequency to 10 Hz. At this rate the CR21X ran out of processing time only once every half hour, when the data output occurred.

Datalogger Computations

The data logger has an extended software routine that computes the covariances of the appropriate quantities for eddy correlation measurements. During the averaging interval the datalogger simply maintains several accumulation locations where it stores the summations of vertical wind velocity, air temperature, and hygrometer voltage output. The values of each of the cross-products are also summed and stored, along with the number of observations during the interval. The covariance of

vertical wind and temperature is computed as follows:

$$\overline{w'T'} = [\Sigma wT]/N - [\Sigma w \cdot \Sigma T]/N^2 \qquad (4.3)$$

where

w = Vertical wind velocity, (m/sec)

T = Air temperature, (C)

N = Number of observations.

Multiplication by the density and specific heat of air yields the sensible heat component of the energy budget.

Eddy correlation computations with the krypton hygrometer output require special treatment. The output is not calibrated before making the covariance computation because of variation in the calibration intercept, caused by a deposit that builds up on the hygrometer windows. The build-up has virtually no effect on the hygrometer calibration slope. The rate of build-up of occluding material does not appear to be rapid enough to affect covariance computations with relatively short averaging periods. To reduce complications, the covariance computation for latent heat flux is made with the raw millivolt output of the hygrometer as follows:

$$\overline{w'V'} = [\Sigma wV]/N - [\Sigma w \cdot \Sigma V]/N^2 \qquad (4.4)$$

where

$\overline{w'V'}$ = Covariance of vertical wind and hygrometer millivolt output, (m-mV/s)

w = Vertical wind velocity, (m/sec)

V = Hygrometer millivolt output, (mV)

N = Number of observations.

The hygrometer calibration is given by:

$$q'/V' = 1/(VxK_w) \qquad (4.5)$$

where

q' = Fluctuation of absolute humidity, (g/m^3)

V' = Hygrometer voltage fluctuation, (mV)

V = Mean hygrometer voltage output, (mV)

x = Hygrometer path length, (m)

K_w = Hygrometer absorption coefficient, (m^2/g).

Multiplying the covariance, $\overline{w'V'}$, by the calibration factor, q'/V', yields the covariance of vertical wind velocity and absolute humidity, $\overline{w'q'}$. The product of this covariance and the mean latent heat of vaporization of water for the interval yields the latent heat component of the surface energy budget.

The averaging period used for the eddy correlation computations was 10 min. The final output interval of the datalogger was 30 min. The eddy correlation data placed in final storage every half hour were the average of the three 10 min periods that occurred during the interval. This approach has the advantage of removing the effects of variations due to lower frequencies in the input signals by acting as a high pass filter. This reduces the chance of errors during the longer output interval due to drift in the temperature of the thermocouple reference junction, anemometer calibration drift due to temperature change, or hygrometer encrustation.

Computation of Constants

The values of air density and latent heat of vaporization are computed for each 10 min averaging period. They are assumed to be independent of any fluctuations in barometric pressure, and are computed using a standard atmospheric pressure corresponding to an elevation of 370 m above mean sea level.

The density of air was adjusted for temperature according to the ideal gas law (Mortimer, 1967) as follows:

$$p_a = PM/RT \qquad (4.6)$$

where

p_a = Air density, (g/m^3)

P = Standard atmospheric pressure, (Pa)

M = Gram molecular weight of air, (g/mole)

R = Gas constant, (J/mole-K)

T = Absolute air temperature, (K).

For the elevation of Caddo County, OK the relationship reduces to:

$$p_a = 338484/T \; . \qquad (4.7)$$

The latent heat of vaporization of water is adjusted in the manner described by Brunt (1952), as a linear function of temperature:

$$L = 2491 - 2.135T \qquad (4.8)$$

where

L = Latent heat of vaporization of water, (J/g)

T = Temperature, (C).

CHAPTER V

RESULTS AND DISCUSSION

Energy Balance

Energy balance measurements were made over alfalfa and Florunner peanuts for 22 periods of 24 hr in length. The measurements ranged from as early in the season as calendar day 176 to as late as calendar day 304. The instruments were placed in the field on several other occasions, but measurement conditions deteriorated before more than a few hours data were gathered. Unsatisfactory conditions for measurement resulted from wind shifts which disrupted fetch requirements, and thunderstorms which interfered with the functioning of the eddy instruments.

The adequacy of the instrumentation in accounting for the energy fluxes above the crop canopy was evaluated by the closure ratio. The closure ratio is the ratio of the sum of sensible and latent heat fluxes to the sum of net radiation and soil heat flux. A sign convention of energy flow toward the canopy being positive and energy flow away from the canopy as negative is used. Since the major component in the numerator (LE) is negative and the major component of the denominator (R_n) is normally positive during the hours of greatest concern, the ratio is multiplied by -1 to make it positive. For the 22 periods

of measurement, the mean closure ratio was 0.661, with the low being 0.49 and the high being 0.90 (Table I). Appendix A contains the data from which these results were derived. Plots in Appendix B graphically represent the energy balance for selected 24 hr periods.

The errors in the balancing of the energy budget should be analyzed in reference to the limitations of the measurement system. The contribution of eddies of certain frequencies will not be measured because they lie outside the range of measurement of the system. These eddies are "cut off" by the system. Both sensible heat flux and latent heat flux will be underestimated because of failure to measure the contributions of extremely low and extremely high frequencies. With the system operating at a frequency of 10 Hz, at a height of 1.8 m, in winds as high as 5.56 m/s, the normalized frequency of the system reaches 3.24. According to McBean et al. (1972) the error from high frequency cut-off in neutral conditions would be approximately 5%. McBean's definition of neutral conditions is when the ratio of height of measurement, z, to the Monin-Obukhov length, L, is in the range $-0.04<z/L<0.1$. The stability of the atmosphere was not evaluated during these experiments, so L cannot be determined directly. However, the Monin-Obukhov length is given by:

$$L = (\rho_a \, C_p \, T \, u_*^3)/(k \, g \, H) \qquad (5.1)$$

where

L = Monin-Obukhov length, (m)

TABLE I

SUMMARY OF DAILY ENERGY BUDGET CLOSURE RATIOS

Day	Crop	Closure Ratio
176/177	Alfalfa	0.721
177/178	"	0.728
183/184	"	0.603
184/185	"	0.725
190/191	Peanuts	0.628
195/196	Alfalfa	0.645
196/197	"	0.706
197/198	"	0.725
198/199	Peanuts	0.655
209/210	Alfalfa	0.511
210/211	"	0.490
211/212	"	0.506
223/224	Peanuts	0.664
224/225	"	0.650
231/232	"	0.631
232/233	"	0.650
237/238	Alfalfa	0.637
240/241	Peanuts	0.821
251/252	Alfalfa	0.728
252/253	"	0.555
256/257	Peanuts	0.663
304	Alfalfa	0.900

$\overline{CR} = 0.661$

$S_{CR} = 0.097$

p_a = Air density, (g/m^3)

C_p = Specific heat of air, (J/g-K)

T = Absolute air temperature, (K)

u_* = Friction velocity, (m/sec)

k = von Karmen's constant, (0.4)

g = Acceleration of gravity, (m/sec^2)

H = Sensible heat flux, (J/m^2-sec).

Friction velocity is given by:

$$u_* = (U_z\ k)/\ln(z/z_0) \qquad (5.2)$$

where

U_z = Wind velocity at height z, (m/sec)

k = von Karmen's constant, (0.4)

z = Height of measurement, (m)

z_0 = Roughness length, (m).

As mentioned in Chapter II, roughness length of crops can be approximated using an empirical relationship developed by Szeicz et al. (1969). An alfalfa crop 20 cm tall has a roughness length of 0.06 m according to this relationship. This leads to a friction velocity of 0.65 m/s for a 5.56 m/s wind at a height of 1.8 m. From this we find that a sensible heat flux of 100 W/m^2 in 35 C air yields a z/L ratio of 0.0007, which is within the neutral region. Only when the sensible heat flux is extremely high, and the wind is very calm over short crop canopies does the atmospheric condition become stable. All of the daytime measurement conditions indicate that the atmosphere was either neutral or unstable when measurements were taken. Thus, from the

analysis of McBean it can be concluded that the errors due to high frequency cut-off should be 1% or less, from the curves in Figure 11.

The errors in flux measurement due to low frequency cut-off are also shown in Figure 5. An averaging period of 30 min is equivalent to a frequency of 0.00056 Hz. At a 1.8 m height, underestimation of eddy flux occurs when wind speed drops below 5 m/s. When wind speed drops to 1 m/s, the underestimation due to low frequency cut-off becomes approximately 2%.

There will be a further error due to the separation of sensors. The error in sensible heat flux should be extremely low, since the thermocouple is approximately 2 cm from the sonic anemometer path. However, the error in latent heat flux measurement should approach 7% at the maximum tolerable wind speed, as discussed in Chapter II.

It can be seen that in the extreme high frequency case, measured sensible heat flux would be 99% of actual flux, and measured latent heat flux would be only 92% of actual flux. This would result in a closure error of at least 8%, without taking into consideration random errors in measurement. In a typical low frequency error situation at a 1 m/s wind speed, a closure ratio of no higher than 87% would result.

The summary of the energy budget closures given earlier in this chapter lists closure errors that were somewhat higher than expected. Even after correction for known

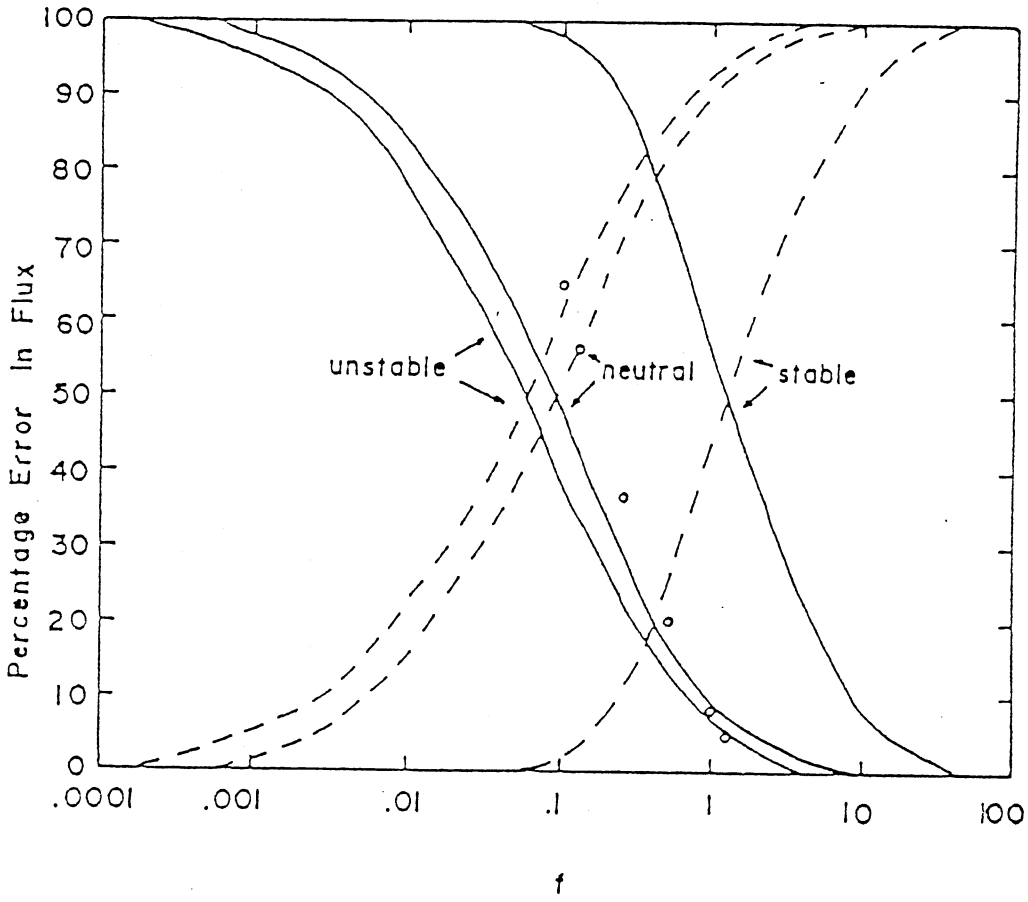

Figure 11. Relationship of Frequency Cut-off Errors to Normalized Frequency (from McBean et al., 1972)
- - - Low Frequency Errors
——— High Frequency Errors

systematic errors due to frequency cut-off and sensor separation, there is an approximate 25% underestimation of energy fluxes for all the days of measurement. Some of this error might be attributed to other types of measurement errors. For example, the manufacturer of the net radiometer rates it to be accurate to $\pm$2.5%. The soil heat flux plates do not have a published accuracy rating, but since they are based on the same measuring principle as the radiometer, they would not reasonably be expected to be any more accurate than the net radiometer. The sonic anemometer and the krypton hygrometer errors have been discussed to some extent earlier. Recent literature published by the manufacturer (Campbell Scientific, Inc., 1986) indicates the error in the calibration slope of the hygrometer may be as great as 10% when the windows of the source and sensor tube are severely scaled. The calibration shift after an extended period of operation is more typically in the range of 4% to 5%, however.

Most of the errors associated with the measurement of physical quantities are random in nature. As such, they would be expected to cancel each other to some degree, and to cause overestimation and underestimation with equal likelihood. The consistent, significant underestimation of the eddy fluxes required to balance the energy budget leads to the conclusion that there is a fault in the measurement of at least one of the energy fluxes. There is reason to believe that the error lies largely in the measurement of

latent energy flux.

On calendar day 257 it was discovered that the signal from the krypton hygrometer was erratic. Upon checking with the manufacturer and performing some diagnostic tests, it was found that there was a fault in the radiation source tube. For short periods, at irregular intervals, the tube had been giving essentially a zero output. The hygrometer was returned to the manufacturer, where the radiation tube was found to have a fabrication defect. The tube was replaced and the hygrometer was recalibrated. It was returned in time to permit field measurements over a plot of alfalfa for approximately 36 hrs before the first major frost of the season ended active vegetative growth. The energy budget closure for the one complete 24 hr period measured after hygrometer repair showed a closure ratio of .90. After correction for the expected errors due to frequency cut-off and sensor separation, a closure ratio of 1.005 was obtained.

The results from this late-season measurement lead to the belief that the latent energy flux was underestimated from the beginning. If this one measurement period can be construed as sufficient justification, latent energy flux underestimation appears to account for virtually all of the energy budget closure error. It follows then, that the residual of net radiation plus soil heat and sensible heat fluxes is an accurate evaluation of latent energy flux. This appears to be the only approach that can be taken, in

light of the uncertainty resulting from the hygrometer failure, and the subsequent improvement in readings after its repair.

All of the computations made in calibrating the Penman equation, and in determining crop coefficients utilize the residual of net radiation plus soil heat and latent heat fluxes in place of the measured latent energy flux. The residual is determined using a sensible heat flux that has been corrected for frequency cut-off using the empirical relationship of McBean et al. (1972). The correction to the sensible heat flux seldom amounts to as much as 1%.

Penman Parameter Estimation

Introduction

The estimation of net radiation and soil heat flux from other, more easily measured parameters was limited to daylight hours. It was apparent from the energy budget data that there was no significant contribution to daily ET made during the night. In addition, preliminary investigations showed very poor correlation of both net radiation and soil heat flux with air temperature. Since air temperature was the only parameter measured that could be reasonably expected to correlate with these two energy fluxes at night, a good prediction model could not be developed.

Net Radiation Estimation

The process of estimation of hourly net radiation was broken into two parts. During daylight hours estimates were made from measurements of direct and diffuse solar radiation, as sensed by a solar pyranometer.

Daytime net radiation for both the alfalfa and peanut crops was determined to be best approximated by a linear function of solar radiation, as previous investigators have done. The addition of quadratic and cubic terms to the linear solar radiation relationship produced no significant improvement in net radiation estimates. Nor did the addition of air temperature as a regression variable improve the prediction significantly.

For both crops it was observed that the greatest deviation of the predicted value from the measured value of net radiation occurred during the twilight hours of dawn and dusk. Investigation of the ratio of net to solar radiation showed that the ratio increased gradually from approximately 0.6 at sunrise to about 0.7 a few hours before solar noon, when the solar radiation was observed to be about 400 W/m^2. The ratio remained constant at about 0.7 until it dropped rapidly to about 0.6 at sunset. It was decided, upon inspection of the data, to break the daytime estimate of net radiation into two prediction equations--one equation for twilight hours, when solar radiation was less than 400 W/m^2, and another equation for periods when solar radiation was 400 W/m^2 or greater. The

plots of the data and the regression equations are shown in Figure 12 and Figure 13. Prediction equations for daily net radiation for alfalfa and peanuts are given in Figure 14 and Figure 15. The fit of the equations to data is quite good. Summaries of the analysis of variance table for each equation are found in Table II through Table VII. A summary of the net radiation models is given in Table X.

Soil Heat Flux Estimation

The estimation of soil heat flux was handled in a manner similar to net radiation estimation. Estimates of hourly soil heat flux were limited to periods when solar radiation was 1 W/m^2 or greater. The original attempt to produce a model included the measured variables air temperature and solar radiation, fraction of the growing season elapsed, and an artificial variable formed by averaging the air temperatures of the three previous hours. This last variable was defined in an attempt to approximate the temperatures of the vegetation and the soil surface. The results from this regression were promising, but not extremely good. When squares of each of the previous variables were added to the regression model, more satisfactory results were obtained. The final model contained only the square of solar radiation and the square of air temperature. No other variables were found to be significant. Plots of the predicted versus measured soil heat flux are given in Figure 16 and Figure 17. Summaries

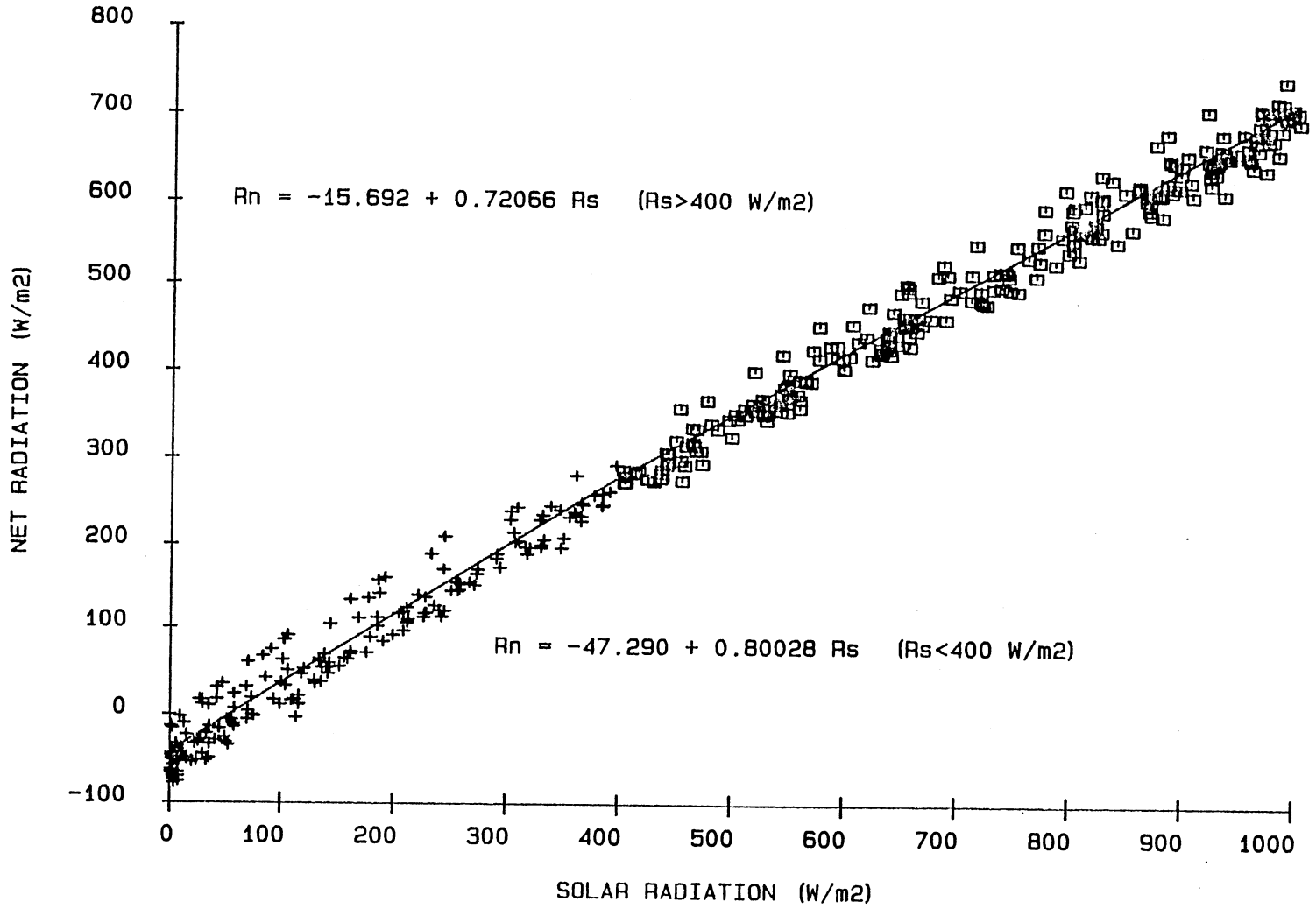

Figure 12. Hourly Alfalfa Net Radiation as a Function of Solar Radiation

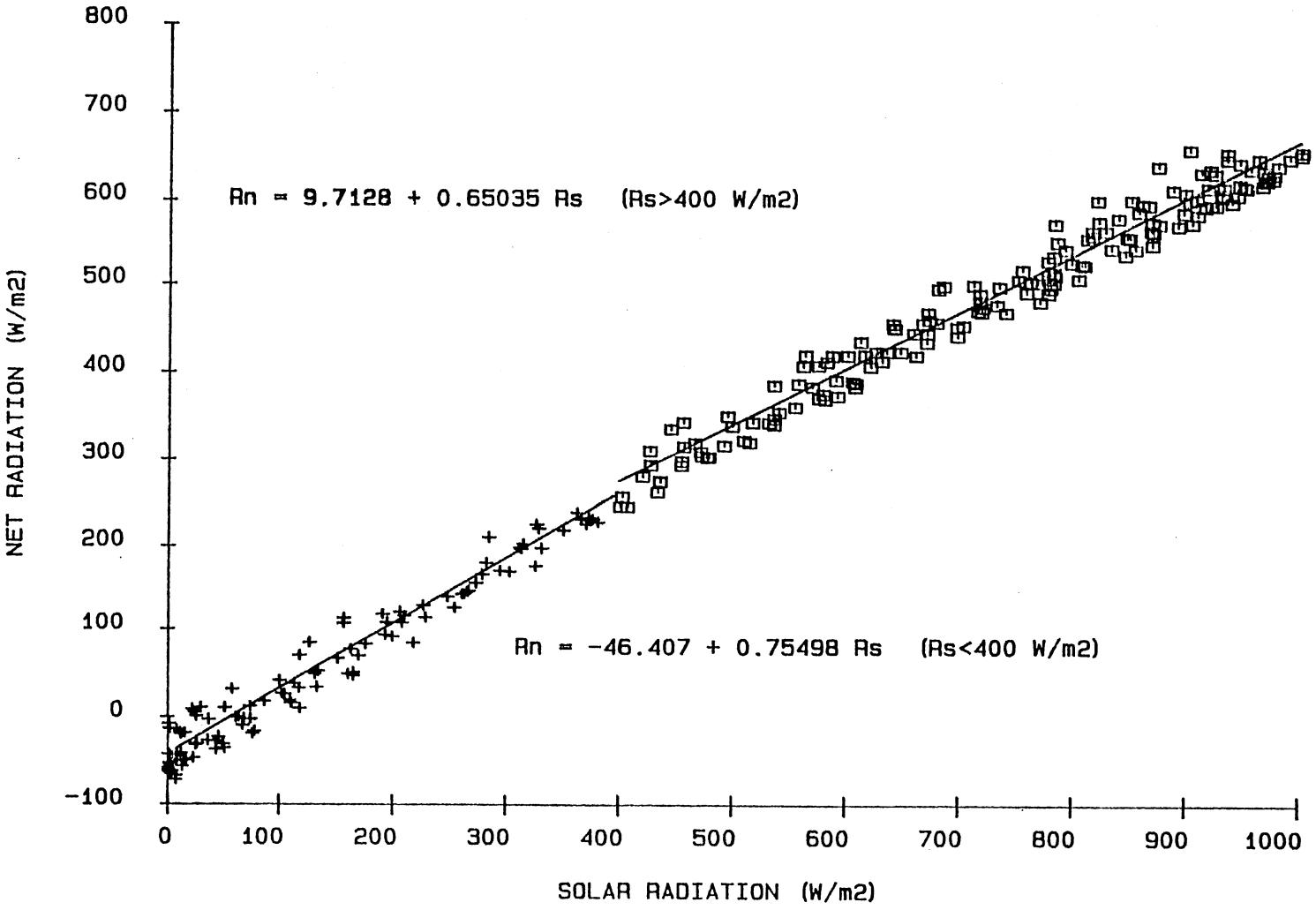

Figure 13. Hourly Peanut Net Radiation as a Function of Solar Radiation

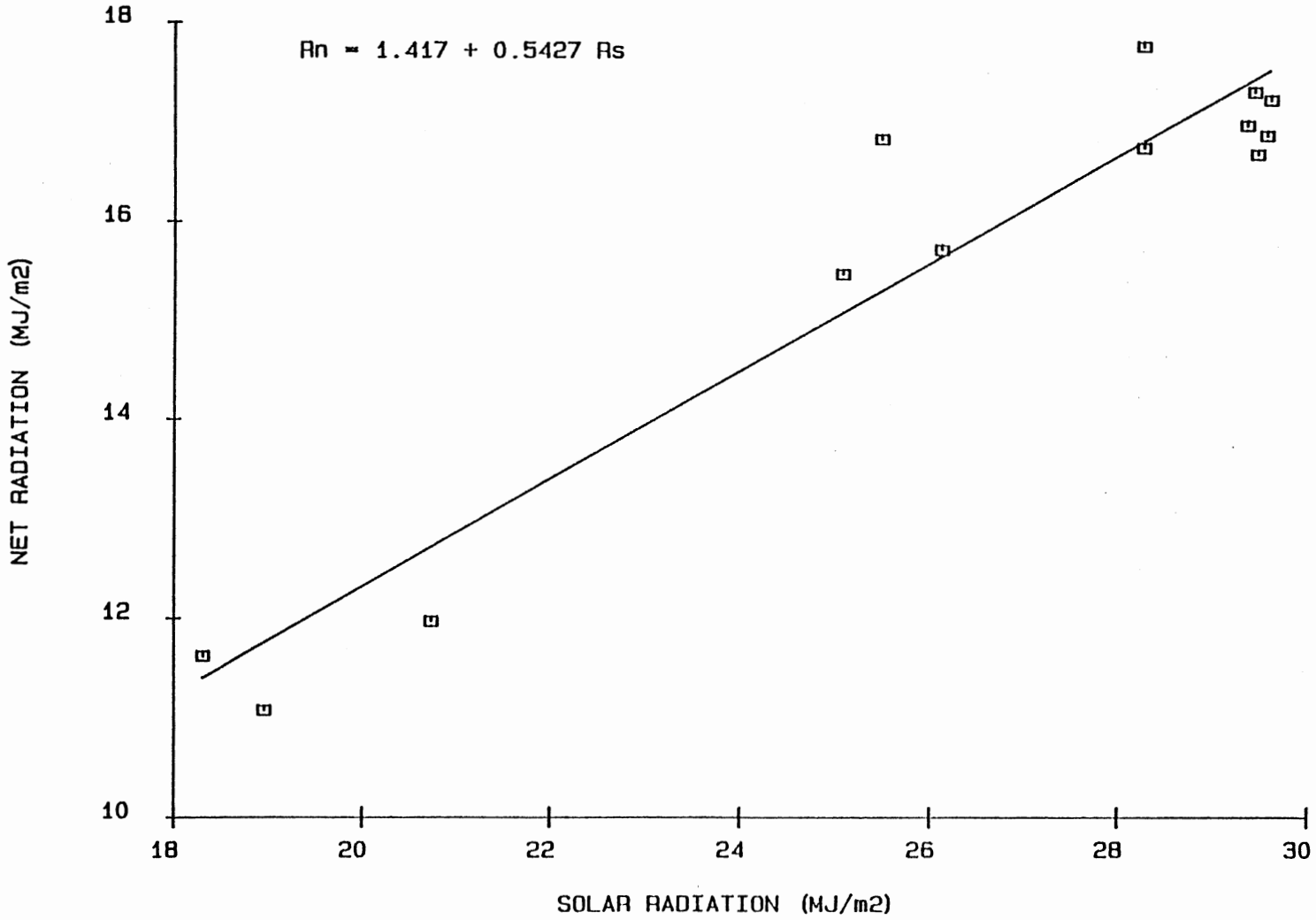

Figure 14. Daily Alfalfa Net Radiation as a Function of Solar Radiation

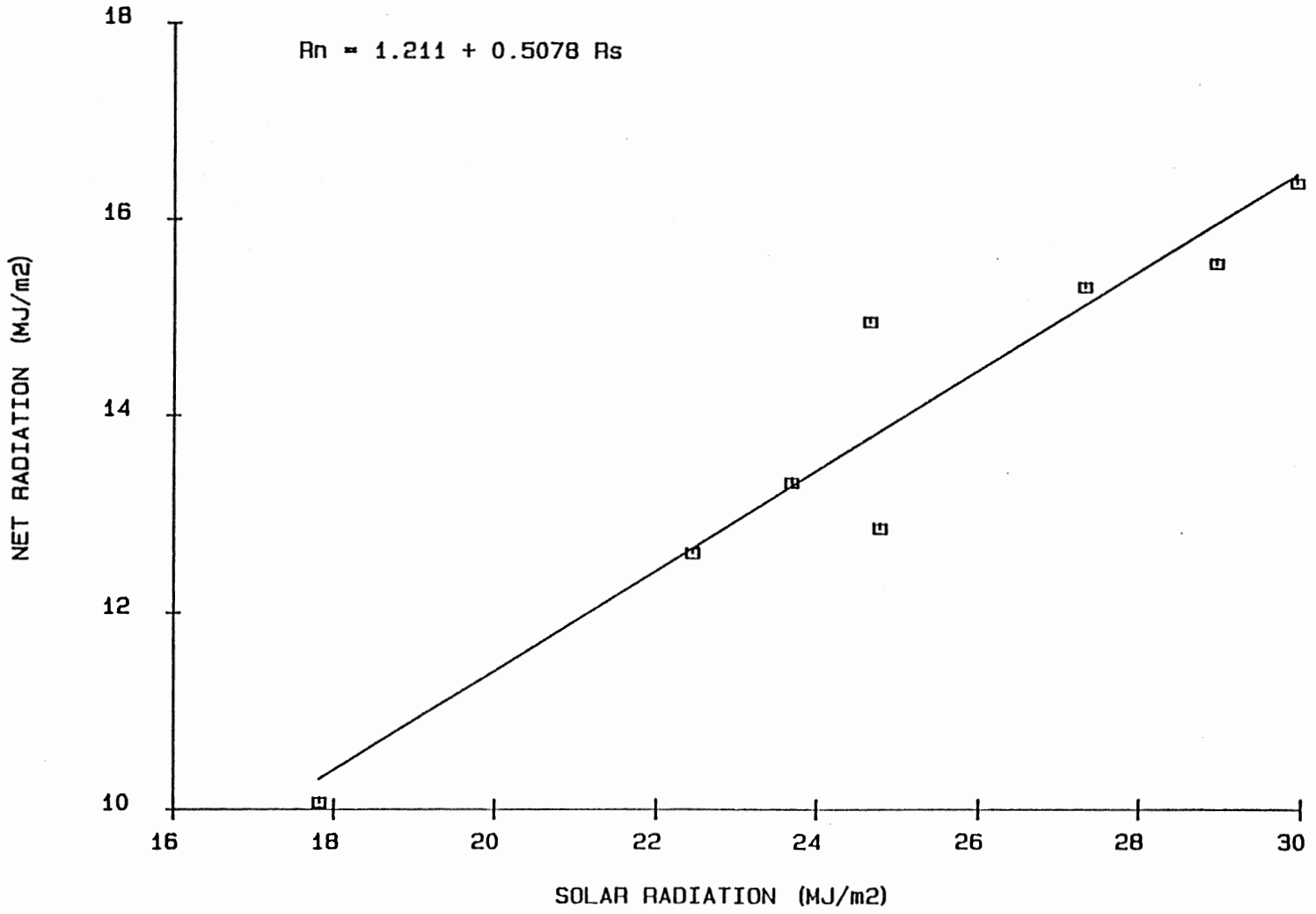

Figure 15. Daily Peanut Net Radiation as a Function of Solar Radiation

TABLE II

ANALYSIS OF VARIANCE TABLE - ALFALFA NET RADIATION-SOLAR RADIATION - DAYTIME HOURLY DATA

Source of Variation	Sum of Squares	Degrees of Freedom	Mean Square	F Ratio	r^2
Regression	4260687	1	4260687	9787	0.975
Error	111005	255	435		
Total	4371693	256			

The critical $F_{.01:1,255}=6.75$. Therefore, the model: $R_n=-15.692 +0.72066 R_s$ is statistically significant.

TABLE III

ANALYSIS OF VARIANCE TABLE - ALFALFA NET RADIATION-SOLAR RADIATION - TWILIGHT HOURLY DATA

Source of Variation	Sum of Squares	Degrees of Freedom	Mean Square	F Ratio	r^2
Regression	1769970	1	1769970	3427	0.950
Error	93995	182	516		
Total	1863965	183			

The critical $F_{.01:1,182}=6.79$. Therefore, the model: $R_n=-47.290 +0.80028 R_s$ is statistically significant.

TABLE IV

ANALYSIS OF VARIANCE TABLE - PEANUT NET RADIATION-SOLAR RADIATION - DAYTIME HOURLY DATA

Source of Variation	Sum of Squares	Degrees of Freedom	Mean Square	F Ratio	r^2
Regression	2068852	1	2068852	5077	0.967
Error	67234	165	407		
Total	2136086	166			

The critical $F_{.01:1,165}=6.80$. Therefore, the model: $R_n=9.713 +0.65035 R_s$ is statistically significant.

TABLE V

ANALYSIS OF VARIANCE TABLE - PEANUT NET RADIATION-SOLAR RADIATION - TWILIGHT HOURLY DATA

Source of Variation	Sum of Squares	Degrees of Freedom	Mean Square	F Ratio	r^2
Regression	1071923	1	1071923	3479	0.965
Error	38818	126	308		
Total	1110741	127			

The critical $F_{.01:1,126}=6.84$. Therefore, the model: $R_n=-46.407 +0.75498 R_s$ is statistically significant.

TABLE VI

ANALYSIS OF VARIANCE TABLE - ALFALFA NET RADIATION-SOLAR RADIATION - DAILY DATA

Source of Variation	Sum of Squares	Degrees of Freedom	Mean Square	F Ratio	r^2
Regression	61.45	1	61.45	117	0.914
Error	5.77	11	0.52		
Total	67.22	12			

The critical $F_{.01:1,11}=9.65$. Therefore, the model: $R_n=1.417 +0.5427\ R_s$ is statistically significant.

TABLE VII

ANALYSIS OF VARIANCE TABLE - PEANUT NET RADIATION-SOLAR RADIATION - DAILY DATA

Source of Variation	Sum of Squares	Degrees of Freedom	Mean Square	F Ratio	r^2
Regression	27.14	1	27.14	63	0.913
Error	2.60	6	0.43		
Total	29.74	7			

The critical $F_{.01:1,6}=13.74$. Therefore, the model: $R_n=1.211 +0.5078\ R_s$ is statistically significant.

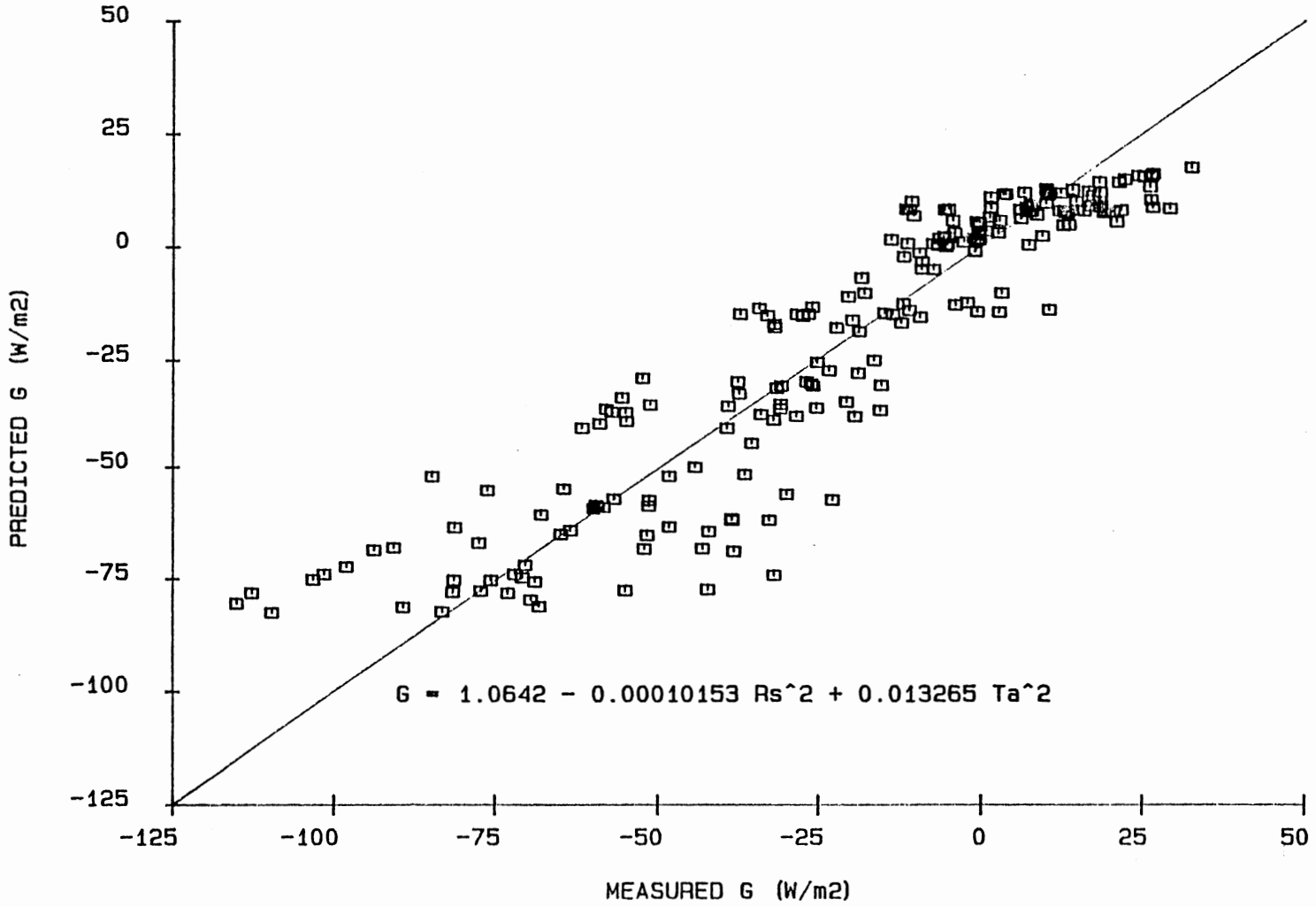

Figure 16. Hourly Alfalfa Soil Heat Flux as a Function of Solar Radiation and Air Temperature

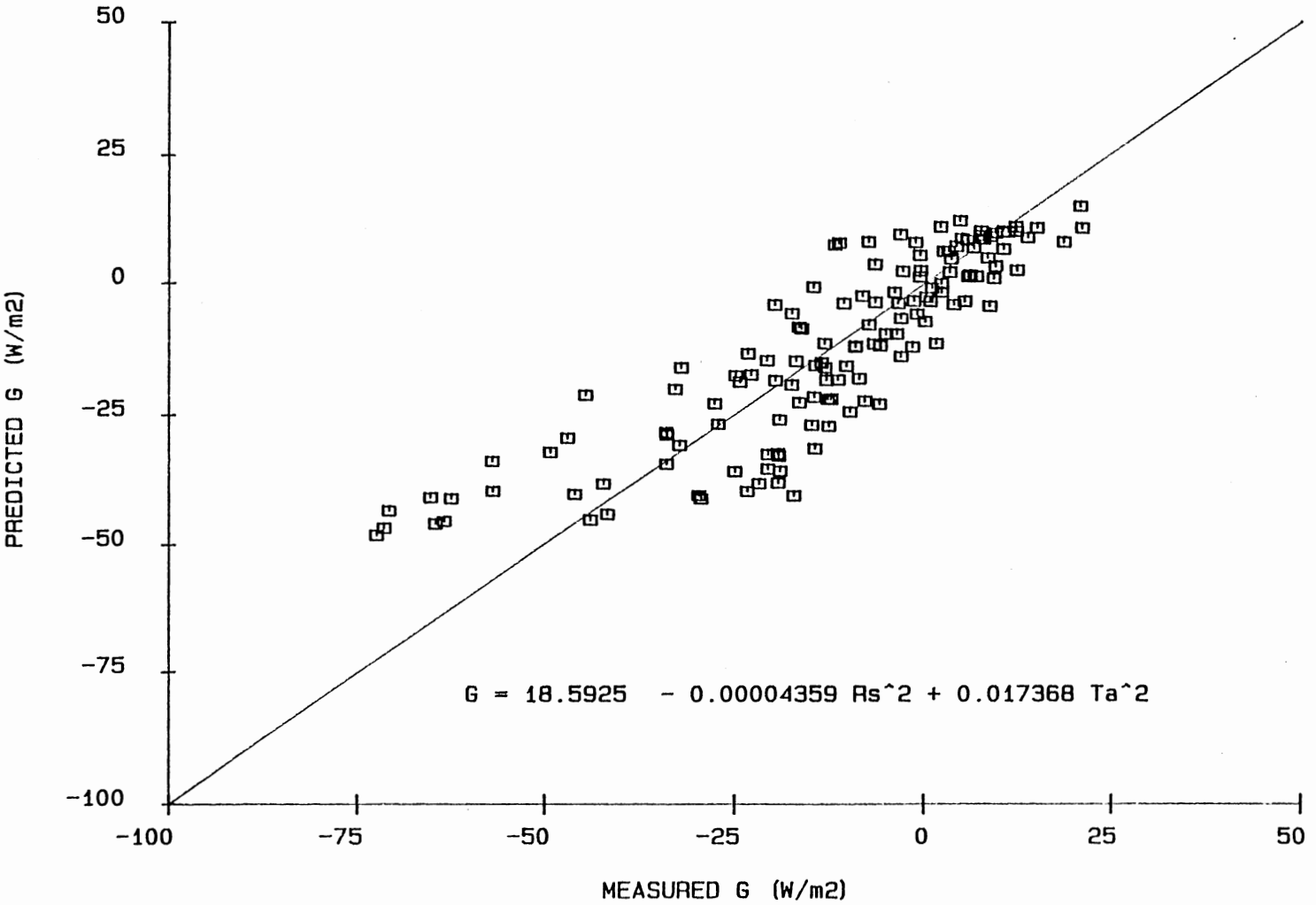

Figure 17. Hourly Peanut Soil Heat Flux as a Function of Solar Radiation and Air Temperature

of the analysis of variance for the models are given in Table VIII and Table IX. A summary of the soil heat flux models is given in Table XI.

While the estimates of these models are statistically significant, their fit is not outstanding. However, the contribution of soil heat flux to the driving energy of the process of evapotranspiration is such that a 10% error in soil heat flux estimation will result in an error in ET estimation on the order of only 1%.

Penman Calibration

Calibration Development

As previously outlined, the calibration of the Penman equation requires the simultaneous measurement of weather parameters and ET. The equation is then rearranged to solve for the wind function in terms of ET and the other weather parameters. A linear regression of the derived wind function on the horizontal wind run will then yield the wind function coefficients. The ET was measured over the alfalfa reference crop only when field conditions approximated potential conditions. This required the crop to be actively growing, well watered and at least 20 cm tall.

The plots of computed W_f versus hourly wind run are shown in Figures 18 and 19, along with the linear regression lines. The data were divided into two groups for calibration. Daytime calibration data were defined as

TABLE VIII

ANALYSIS OF VARIANCE TABLE - ALFALFA SOIL HEAT FLUX-
SOLAR RADIATION/AIR TEMPERATURE - HOURLY DATA

Source of Variation	Sum of Squares	Degrees of Freedom	Mean Square	F Ratio	r^2
Regression	197854	2	98927	551	0.846
Error	35925	200	180		
Total	233778	202			

The critical $F_{.01:2,200}=4.71$. Therefore, the model: $G=1.0642-0.0001015\ R_S^2+0.01327\ T_A^2$ is statistically significant.

TABLE IX

ANALYSIS OF VARIANCE TABLE - PEANUT SOIL HEAT FLUX-
SOLAR RADIATION/AIR TEMPERATURE - HOURLY DATA

Source of Variation	Sum of Squares	Degrees of Freedom	Mean Square	F Ratio	r^2
Regression	42416	2	21208	188	0.737
Error	15148	134	113		
Total	57564	136			

The critical $F_{.01:2,136}= 4.77$. Therefore, the model: $G=18.592-0.00004539\ R_S^2-0.01736\ T_A^2$ is statistically significant.

TABLE X

NET RADIATION PREDICTION EQUATIONS

Model	Intercept	R_s Coefficient	r^2	Std. Error of Estimate
Daytime, Hourly				
Alfalfa	-15.692	0.72066	0.975	20.9
Peanuts	9.713	0.65035	0.967	20.2
Twilight, Hourly				
Alfalfa	-47.290	0.80028	0.950	22.7
Peanuts	-47.407	0.75498	0.965	17.6
Daily				
Alfalfa	786.99	0.54267	0.914	402.3
Peanuts	672.64	0.50777	0.913	365.4

TABLE XI

SOIL HEAT FLUX PREDICTION EQUATIONS

Model	Intercept	R_s^2 Coefficient	T_A^2 Coefficient	r^2	Std. Error of Estimate
Alfalfa	1.0642	-0.0001015	0.01327	0.846	13.4
Peanuts	18.593	-0.00004359	0.01737	0.737	10.6

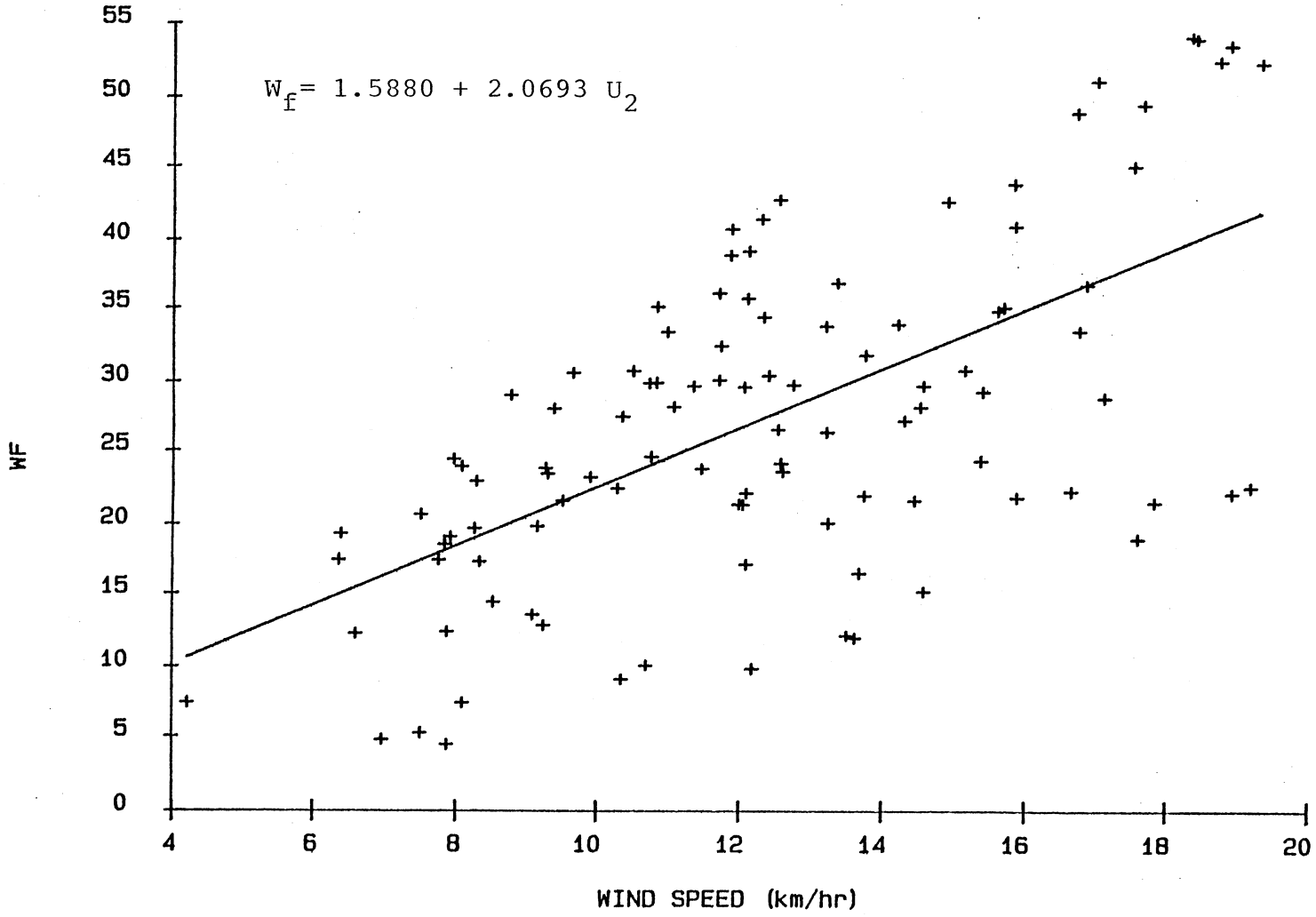

Figure 18. Hourly Calibrated Penman Wind Function as a Function of Daytime Hourly Wind Run

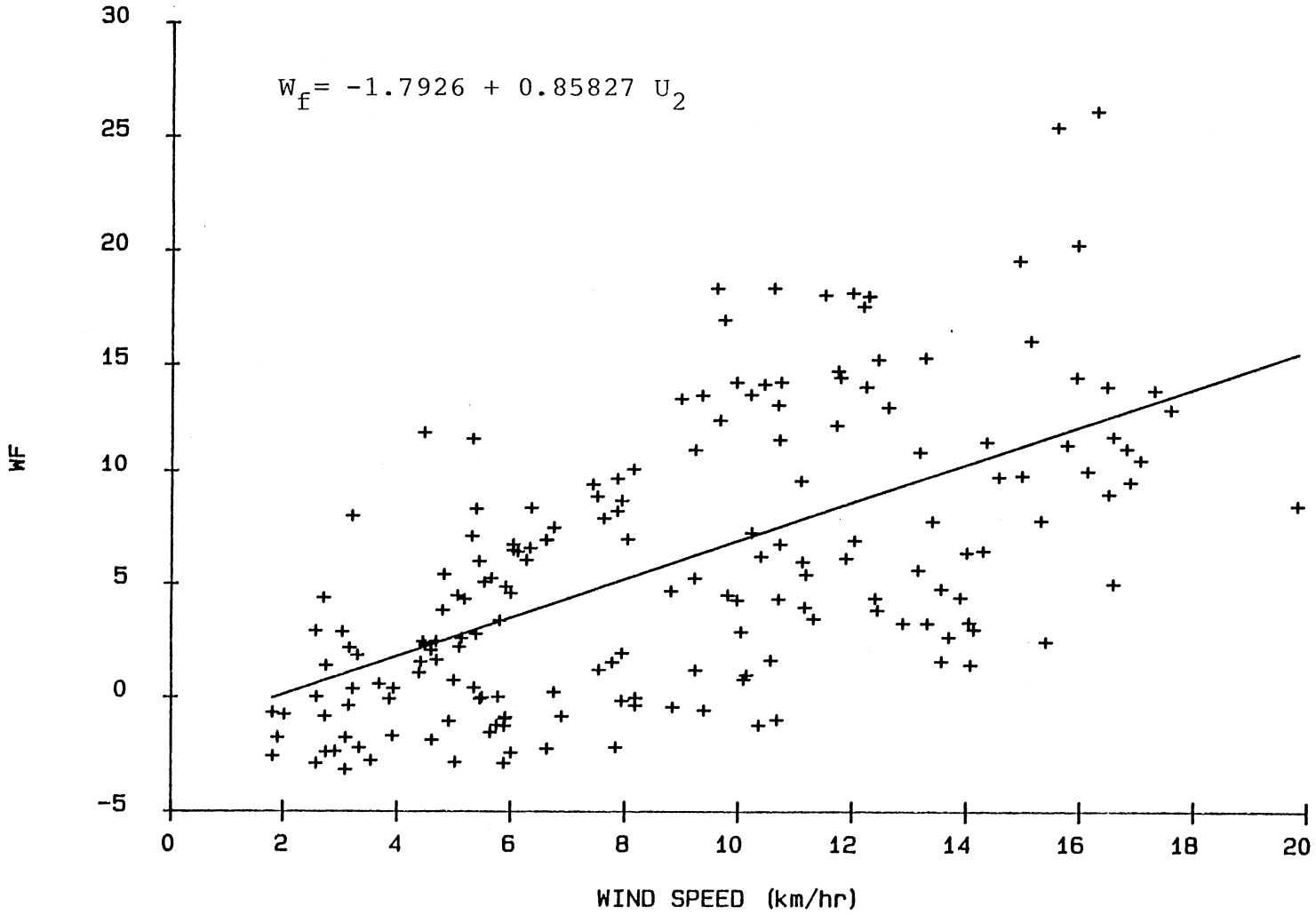

Figure 19. Hourly Calibrated Penman Wind Function as a Function of Nighttime Hourly Wind Run

readings taken during hourly periods when the solar radiation was 200 W/m^2 or greater in the morning, and 1 W/m^2 or greater in the evening. The choice of these divisions was based on observations of the wind function data. There is a definite difference in the behavior of the wind function between daytime and darkness. This makes sense, as one would expect daytime ET to be largely a function of energy availability. At night it would be expected that what little ET occurs would be affected differently by transport phenomena because of the limited energy input.

Originally, 1 W/m^2 of solar radiation was used as the dividing point for both morning and evening. However, it was noted that there were several points that were far outside the envelope of the other daytime data. Inspection showed that these points all occurred in the morning hours, before 9:00 AM local time. Moving these points into the night-time calibration group, it was found that they fit in the middle of the data set, centered about the previously computed regression line. It was reasoned that in the hours immediately after sunrise, the vegetation and soil surface are still cool and damp, and wind speeds are often relatively calm. Therefore, despite the presence of solar radiation the situation is more nearly like nighttime than the heat of the afternoon. Consequently, it was felt that adjustment of the morning division between day and night calibrations was justified.

After inspection of the data for the hours immediately after sunset, it was concluded that a similar sort of adjustment would not improve the fit of the data. This would lead to the conclusion that the start-up of ET in the hours after sunrise is more gradual than the cessation of ET after sunset. It can be seen from the summaries of the analysis of variance in Table XII and Table XIII, that the regression equations for the two wind function relationships have relatively low coefficients of determination. The F tests for both regressions do show that the relationships are significant.

It should be noted that the wind function coefficients used here are not identical to those used in the Penman equation cited in Chapter III. The coefficients developed here have the constant of proportionality for units conversion included internally, and are for input data with different units. The form of equation they are used in is:

$$LE_p = [d/(d+g)]\ (R_n+G) + [g/(d+g)]\ W_f\ (e_s-e) \qquad (5.3)$$

where

LE_p = Mean hourly potential latent energy flux, (W/m^2)

d = Slope of saturation vapor pressure curve, (mb/C)

g = Psychrometric constant, (mb/C)

R_n = Mean hourly net radiation, (W/m^2)

G = Mean hourly soil heat flux, (W/m^2)

W_f = Empirical wind function

e_s = Saturation vapor pressure, (mb)

e = Ambient vapor pressure, (mb).

TABLE XII

ANALYSIS OF VARIANCE TABLE - PENMAN WIND FUNCTION-
DAYTIME HOURLY DATA

Source of Variation	Sum of Squares	Degrees of Freedom	Mean Square	F Ratio	r^2
Regression	5385	1	5385	64	0.386
Error	8579	102	84		
Total	13963	103			

The critical $F_{.01:1,103}=6.90$. Therefore, the model: $W_f=1.5580 +2.0693\ U_2$ is statistically significant.

TABLE XIII

ANALYSIS OF VARIANCE TABLE - PENMAN WIND FUNCTION-
NIGHTTIME HOURLY DATA

Source of Variation	Sum of Squares	Degrees of Freedom	Mean Square	F Ratio	r^2
Regression	2463	1	2463	102	0.366
Error	4267	176	24		
Total	6730	177			

The critical $F_{.01:1,177}=6.78$. Therefore, the model: $W_f=-1.7926 +0.85827\ U_2$ is statistically significant.

The wind function, W_f, is given by:

$$W_f = a + bU_2 \qquad (5.4)$$

where

U_2 = Horizontal wind run at 2 m elevation, (km/hr)

a,b = Linear regression coefficients.

For comparison purposes, the Penman equation was also calibrated for use with daily meteorological data. The calibration procedure was the same as for the case of hourly data. Daily totals of net radiation, soil heat flux and wind run were used. Mean daily air temperature was used to compute the coefficients for the energy and the aerodynamic portions of the equation. The mean daily vapor pressure deficit was computed using the average of the hourly vapor pressure deficits derived from hourly wet and dry bulb temperatures. A plot of the daily wind function versus daily wind run is shown in Figure 20. The coefficient of determination for the daily data wind function was extremely low, and the F test showed the relationship was not statistically significant at the 75% confidence level (Table XIV).

Calibration Verification

The Penman equation was applied to the hourly data from which the net radiation and soil heat flux approximations and the wind function calibration were developed. The model used only the weather data that would be available from a centralized weather station for irrigation

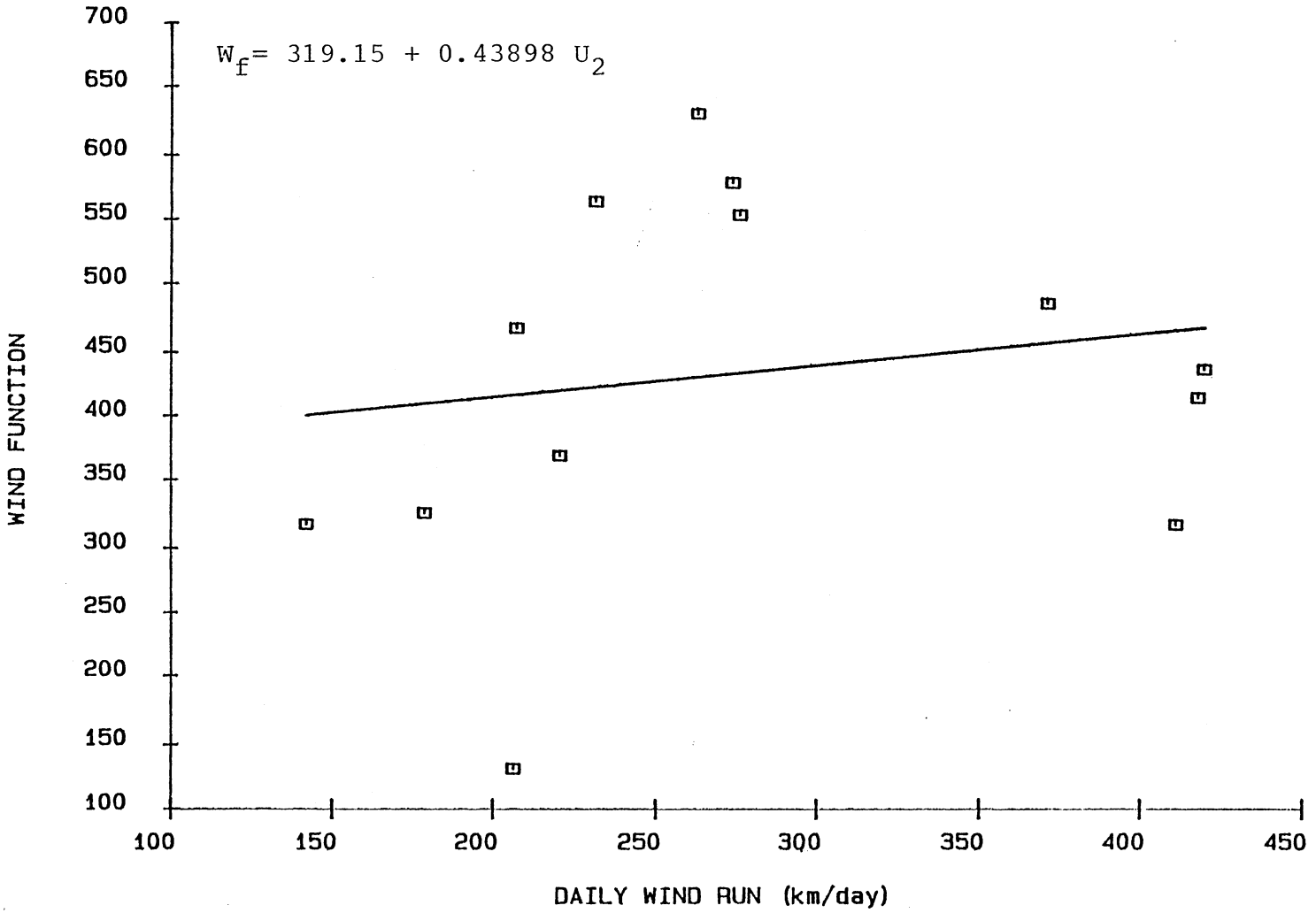

Figure 20. Daily Calibrated Penman Wind Function as a Function of Daily Wind Run

TABLE XIV

ANALYSIS OF VARIANCE TABLE - PENMAN WIND FUNCTION-
DAILY DATA

Source of Variation	Sum of Squares	Degrees of Freedom	Mean Square	F Ratio	r^2
Regression	6432	1	6432	.32	0.028
Error	222937	11	20267		
Total	229369	12			

The critical $F_{.25:1,12}=1.47$. Therefore, the model: $W_f=362.21 +0.2418\ U_2$ is not statistically significant at 75% confidence level.

scheduling purposes--hourly solar radiation, hourly wet and dry bulb temperatures, mean hourly air temperature and hourly wind run. The net radiation and soil heat flux inputs for the model were approximated from the models based on solar radiation and temperature. As would be expected, the plot of the predicted versus measured ET in Figure 21 falls in a balanced pattern about the equal value line. The measured ET in this plot is the residual of R_n+H+G. For both measured and predicted ET, any hour in which the value of ET was negative was assumed to be zero.

To better evaluate the validity of the model, it was applied to some independent data. Hourly weather data parameters were measured at the Ft. Cobb Research Station in both the 1984 and 1985 irrigation seasons. Soil water use data were measured at an alfalfa field approximately 5 kilometers away, using a neutron probe moisture meter. The soil moisture data were taken from three access tubes that monitored the top 1.2 m of the crop root zone. The data were taken at intervals of 2 to 4 days, the ET being derived from the difference between consecutive readings. Due to irrigation, rainfall events and field operations it was possible to obtain only 15 intervals from the data for which the ET was deemed to be accurate. Measurements for intervals during and immediately after irrigation and rainfall events had to be eliminated to avoid inaccuracies due to elevated surface evaporation, deep drainage and variability in gauging precipitation under sprinklers.

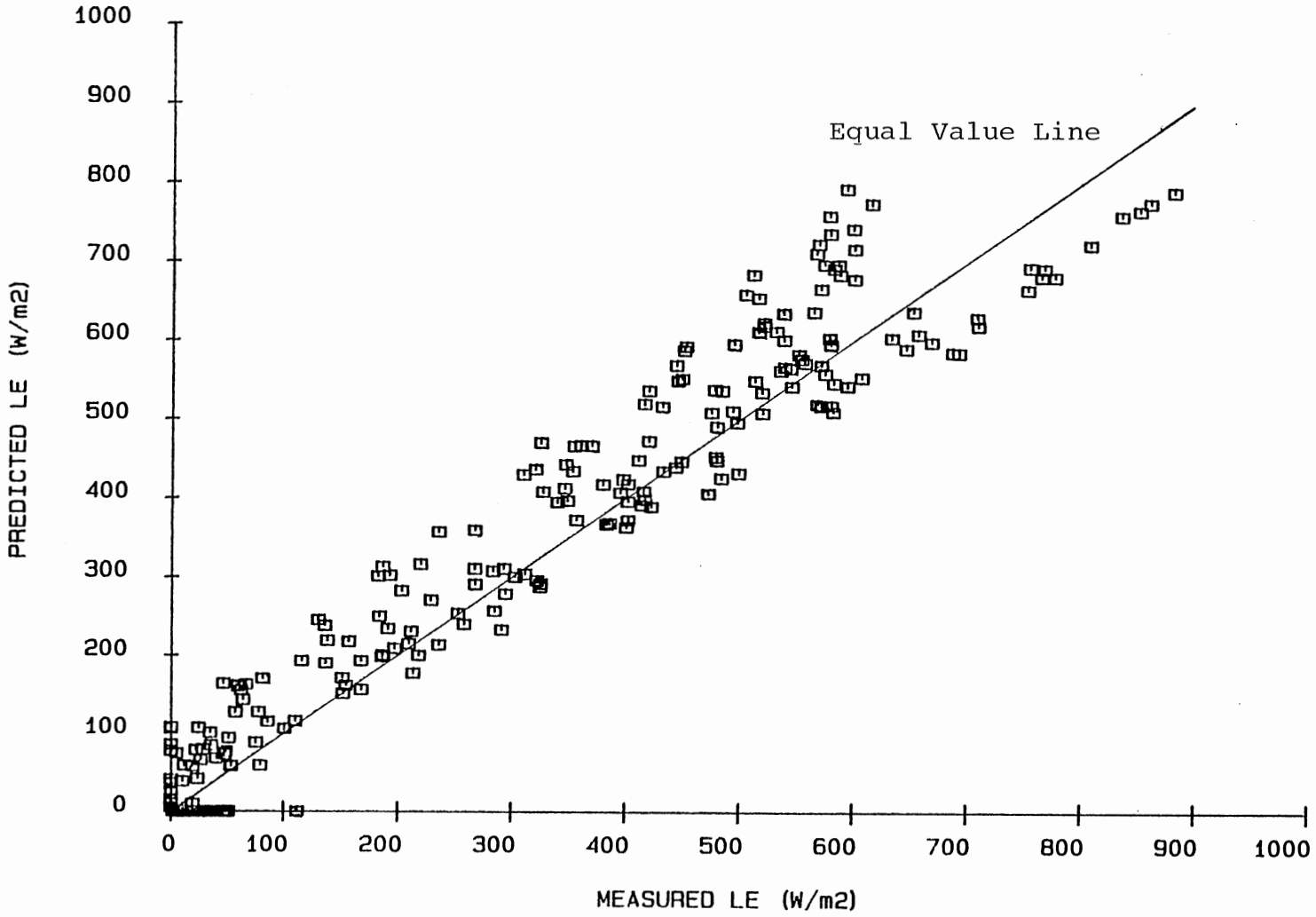

Figure 21. Penman Predicted Latent Energy Flux versus Residual Energy Balance Latent Energy Flux for Calibration Data

The model was applied to the hourly weather data, and the output was summed to obtain the total predicted ET for the interval for which the soil water was gauged with the neutron probe. During the computation of total ET, any hour for which the computed ET was negative was assumed to have a value of zero. Predicted versus measured data are plotted in Figure 22. Visually, the model seems to do an adequate job, perhaps underestimating ET slightly. The mean and the standard deviation of the difference between the measured and the predicted values for each interval were calculated, as shown in Table XV. The mean difference between the data pairs was tested to determine if it was significantly different from zero. Even at a 50% level of confidence the t test showed that the difference between the measured and predicted values was not significant.

Peanut Crop Coefficient

Coefficient Development

Measurements of the energy fluxes over a crop of Florunner peanuts were made at various stages of crop development. Due to equipment malfunctions and other limitations, only six separate measurement periods were completed. All measurements were made at the same field site, with the first measurements being made on calendar day 190, and the last on calendar day 257. As indicated in earlier discussion, the residual of net radiation plus soil heat and sensible heat fluxes was felt to most accurately

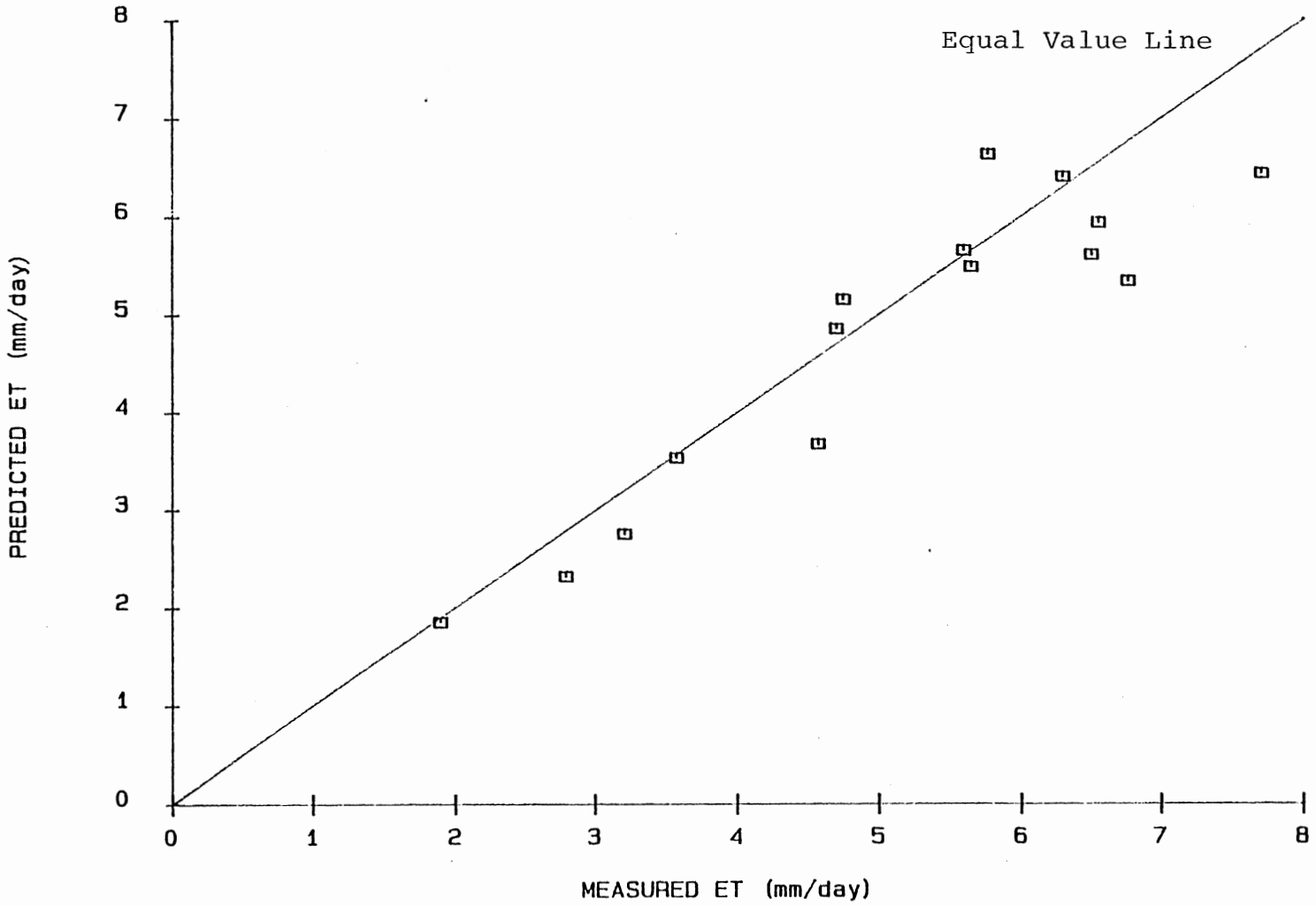

Figure 22. Calibrated Penman Model ET versus Neutron Probe Measured ET for 1984-1985 Alfalfa Data

TABLE XV

EVALUATION OF MODEL FIT TO 1984-1985
MEASURED ALFALFA ET

Mean Error	Standard Error of the Estimate	t	Critical t
Absolute:			
-0.102	1.016	0.1004	0.692
Relative:			
-0.0596	0.109	0.5468	0.692

Even at the 50% confidence level the mean error is not significantly different from zero.

reflect the actual latent energy flux of the crop. Consequently, all the crop coefficient computations were made using this residual equivalent of latent energy flux.

Since the purpose of the crop coefficient is to predict the ET of a given crop relative to the reference crop ET, some special adjustments were necessary. With only one set of instrumentation, it was impossible to measure the meteorological parameters over the alfalfa reference crop while measuring the latent energy flux over the peanut crop. This is of importance because the prediction equation computes reference ET with the parameters of net radiation and soil heat flux for the reference crop. The procedure that will eventually be used in applying the prediction equation for irrigation scheduling will be to determine the net radiation and soil heat flux from the empirical equations that use solar radiation and air temperature. The same procedure was used for peanut crop coefficient development. The net radiation and soil heat flux parameters used in the prediction equation were computed from the previously determined empirical relationships. ET was then computed using the calibrated Penman equation. At each stage of growth for which measurements were taken, the ratio of measured crop ET to reference crop ET was determined, giving the crop coefficient at that point.

Since the coefficients will be utilized to predict crop ET with a computer model, the coefficients must be in a

form that can readily be used in this type of application. The approach most commonly used to quantify the series of coefficients for the whole growing season is to develop a functional relationship based on the degree of crop development. In this case, the time elapsed since planting was used as the index of crop development. The approach of considering only elapsed time can lead to difficulty for crops planted early in the year when soil temperatures are low enough to retard germination and emergence. For peanuts planted in mid-May, this is not normally a problem. The elapsed time is normalized by dividing it by the length of the growing season, normally 160 days for Florunner peanuts. The resulting quantity is the fraction of the growing season elapsed, FGS.

After FGS has been determined for each day on which measurements have been taken, a regression program is used to fit a functional relationship to the data. The usual relationship is a third order polynomial. Experience has shown that the shape of rise and fall of the relative water use rate of most crops can be approximated by a third order polynomial. The best fit third order polynomial for the data is shown in Figure 23.

Coefficient Verification

There was not enough data available on water use by Florunner peanuts to independently verify the performance of the crop coefficient relationship. When the model was

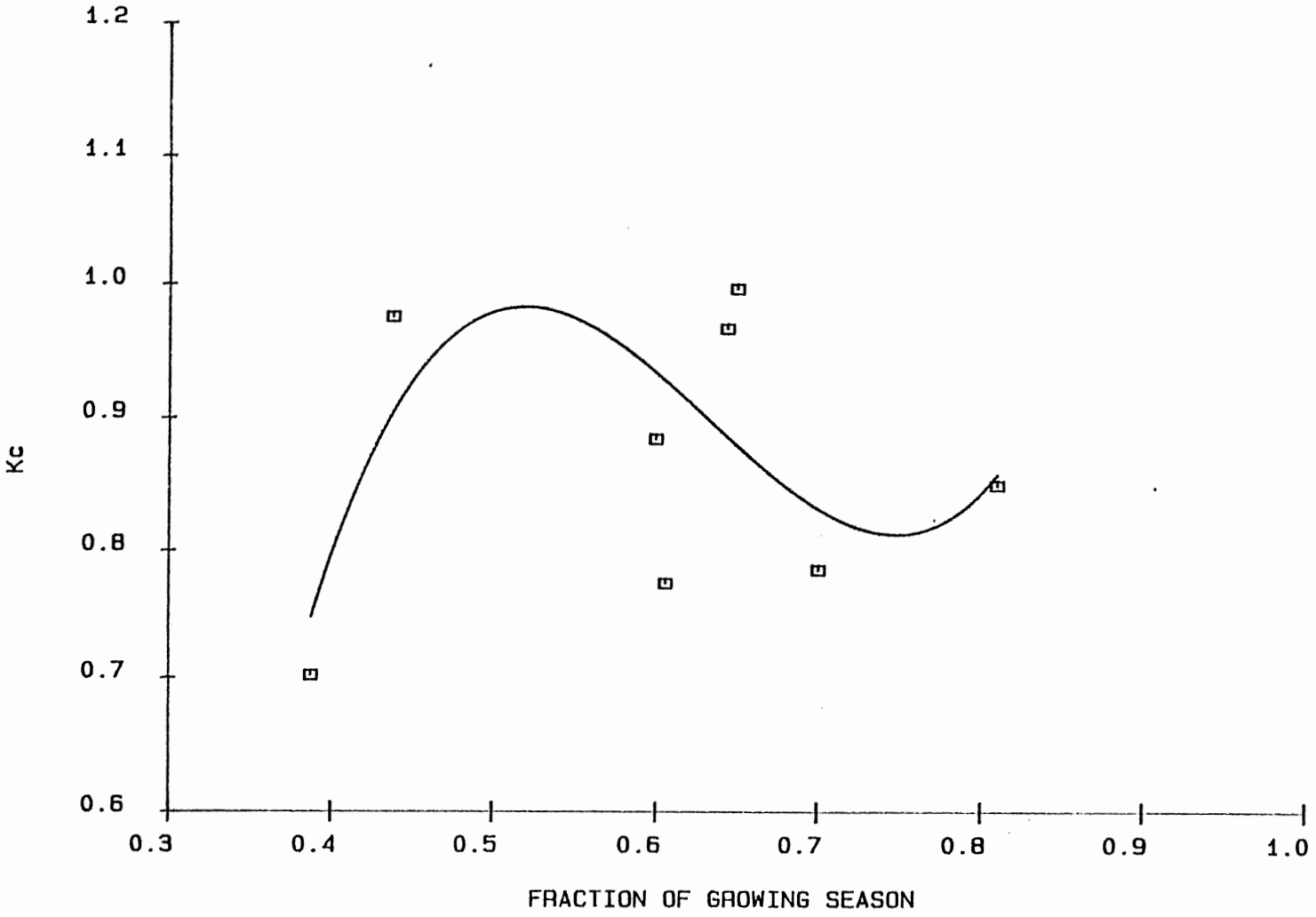

Figure 23. Florunner Peanut Crop Coefficient Curve

applied to the calibration data, it produced a balanced pattern of data points about the equal value line, as it should (Figure 24).

As might be expected in the field measurement of a parameter subject to the control of so many variables, the measured values of the crop coefficient do not form the desired smooth curve. It does show low relative water use early in the season when the leaf area index is low. It peaks near mid-season when vegetal growth has covered the ground densely and fruiting has begun. Late in the season, with the onset of senescence, water use declines. The best fit polynomial follows this basic trend, but because of a lack of data values near harvest, the curve begins an upward trend near FGS=0.75. In order to prevent this upturn, the curve was constrained by the addition of a ficticious extra point (K_C=0.9 at FGS=0.9). With little effect on the peak, the tail of the curve is kept from showing an increasing trend until FGS=0.8 (Figure 25). The use of this adjusted coefficient function produces estimates (Figure 26) which do not match the measured values as closely as the unadjusted function. However, it is felt that this relationship more accurately reflects the actual behavior of the crop coefficient in the range of measurement.

There are two data points near FGS=0.6, taken on consecutive days, which lie well below another pair of points taken a week later. Soil moisture conditions during

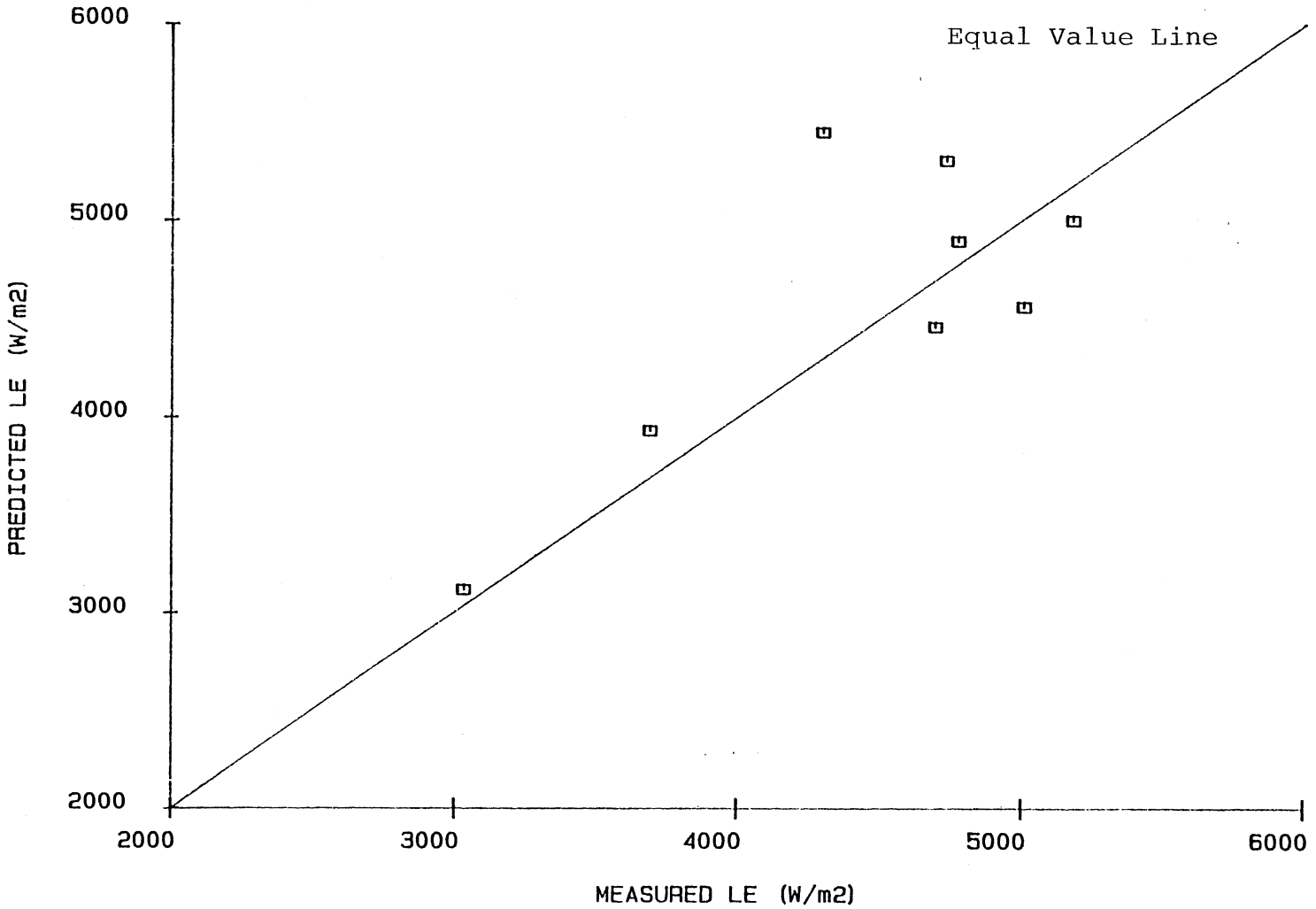

Figure 24. Calibrated Penman Model LE versus Measured Florunner Peanut LE Using Florunner Crop Coefficient

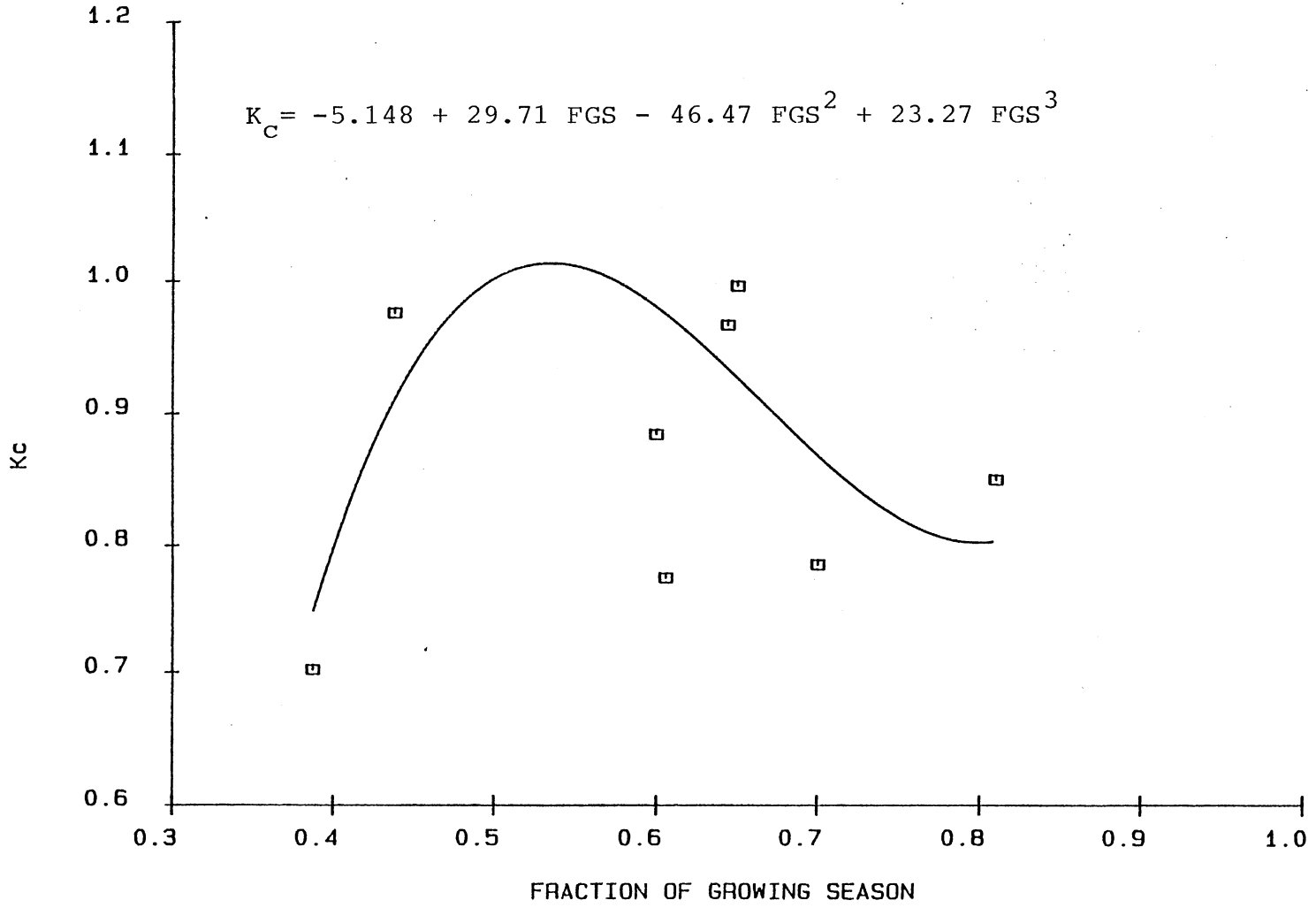

Figure 25. Adjusted Florunner Peanut Crop Coefficient Curve

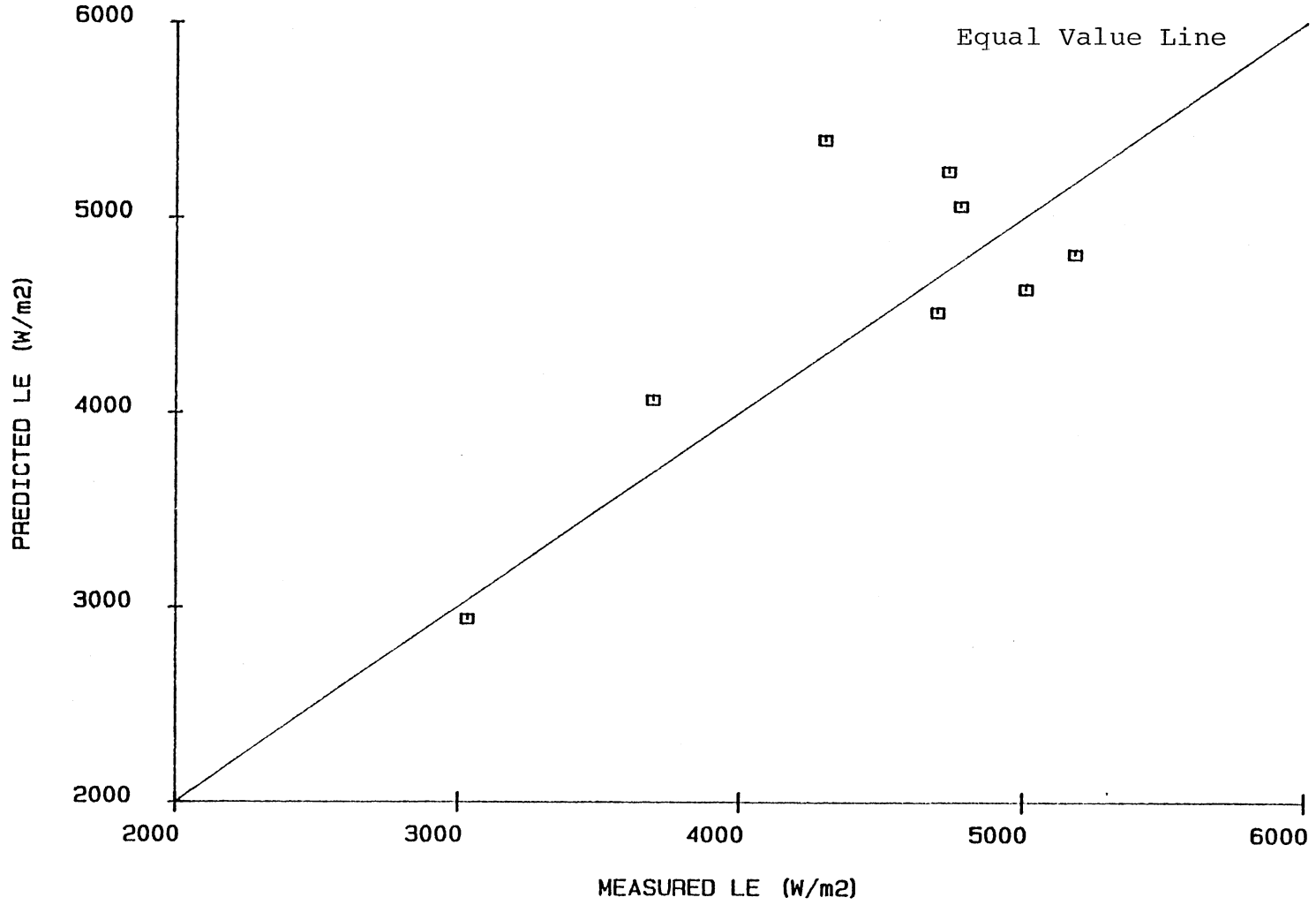

Figure 26. Calibrated Penman Model LE versus Measured Florunner Peanut LE Using Adjusted Florunner Crop Coefficient

this period were drier than potential conditions, and measured ET was depressed as a result. For this particular instrument set-up, the eddy correlation instruments operated at 13.3 Hz. It was found that the microprocessor did not have time to complete all of the eddy correlation calculations and scan all of the weather instruments within the allowed processing interval. These aspects, plus the fact that the data measured on two consecutive days exhibit such widely divergent values, cast some doubt upon the accuracy of at least one of the points. The point at FGS=0.7 is lower than would be expected, but not unreasonably so. The positioning of the five upper points forms a relatively smooth curve that suggests an "upper envelope" for the coefficient.

A comparison of these data with some some Spanco peanut data gathered in the same area during 1984 and 1985 (Harp et al., 1986) revealed some interesting features. The four upper points of the 1986 Florunner data fall quite close to the best fit curve for the Spanco data developed from neutron probe readings (Figure 27). This might suggest that despite the 140 day growing season for the Spanco variety, and the 160 day growing season for the Florunner variety, there is no difference in the crop coefficients for the two cultivars. Once the time variable in the crop coefficient relationship is normalized, there is little difference between the curves, as is seen in Figure 28.

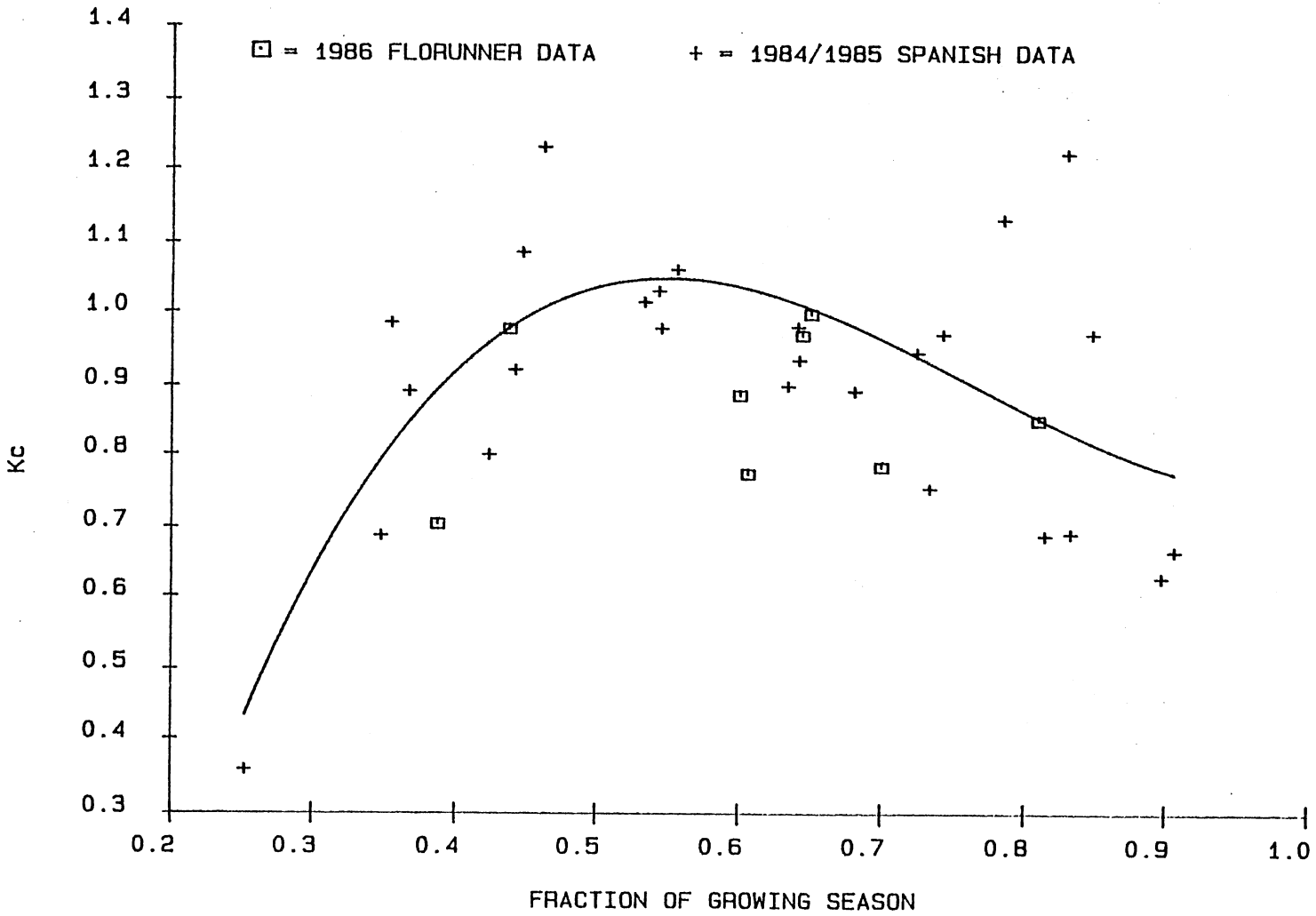

Figure 27. 1986 Florunner Crop Coefficient Data Superimposed on 1984-1985 Spanco Crop Coefficient Curve and Data

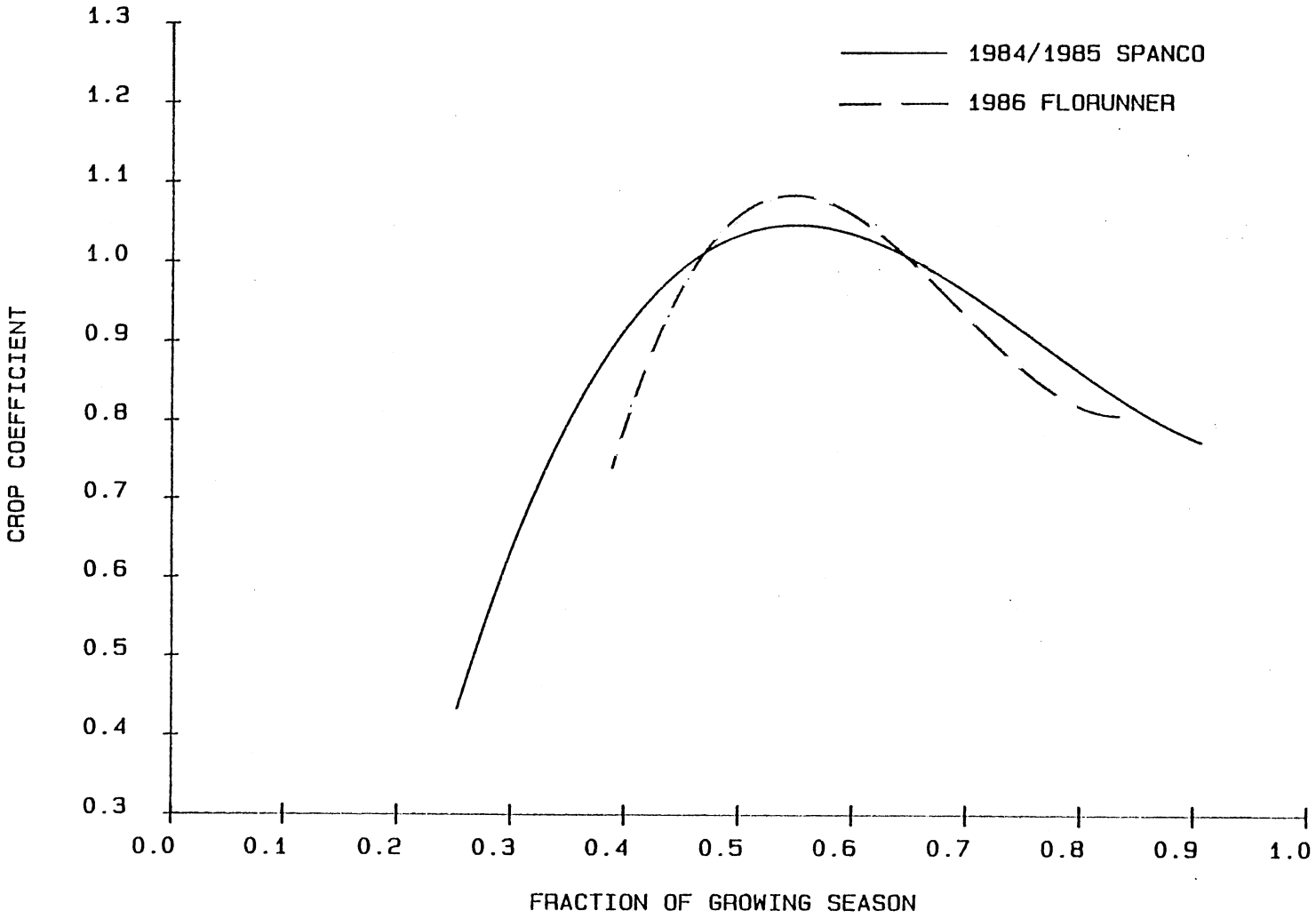

Figure 28. Comparison of Adjusted Florunner and Spanco Crop Coefficient Curves

CHAPTER VI

SUMMARY, CONCLUSIONS AND RECOMMENDATIONS

Summary

With the aim of developing an integrated system of accurately predicting crop water use for irrigation scheduling purposes, measurements of energy fluxes and meteorological parameters were made over alfalfa and peanut crops. The ability of the eddy correlation equipment to measure the components of the surface energy budget of the crops was evaluated by examining the closure of the energy balance equation. The early season results of the energy budget closure indicated that the equipment was not measuring the energy fluxes above the crops as accurately as other experimenters have indicated is possible. After applying correction factors based on the operating parameters of the system, the average closure ratio was only 0.75. Late in the growing season, it was discovered that the krypton hygrometer was defective. A single day of measurement, late in the growing season, yielded a closure ratio of 0.90 after repairs were made to the hygrometer. After the appropriate correction factors for sensor separation and frequency cut-off were applied, the closure ratio was 1.005. From this it was determined that the measurements of net radiation, soil heat flux and sensible

heat flux were of acceptable accuracy, and that the latent heat flux was responsible for the large closure errors earlier in the season. To recover useable data from the early season measurements, the residual of net radiation, soil heat and sensible heat fluxes from the energy balance equation was used to represent the latent heat flux.

Empirical relationships were developed that relate the net radiation and soil heat flux of alfalfa and peanut crops to parameters that are easily measured by centralized, automated weather stations. Excellent linear relationships between hourly net radiation and solar radiation were developed for both alfalfa and peanuts. Separate prediction equations were developed for twilight and midday hours. Acceptable relationships for predicting daytime soil heat flux for both alfalfa and peanuts were developed from hourly solar radiation and air temperature.

The modified Penman equation was calibrated for an alfalfa reference crop in Caddo County, in southwest Oklahoma. The linear calibration coefficients for the Penman wind function were developed for hourly weather data for both day and night. Coefficients for daily weather data were developed also, but they were not found to be statistically significant.

A functional relationship between fraction of growing season elapsed and crop coefficient was determined for Florunner peanuts. The ratio of measured ET for Florunner peanuts to computed Penman reference ET was found at

several stages of crop development. The best fit third order polynomial function was determined for the ratios as a function of the fraction of growing season elapsed. An adjustment to the empirical polynomial was made to force it to monotonically decrease late in the measurement period.

Conclusions

Because of problems with the krypton hygrometer, there is some doubt about the validity of the early season latent heat flux measured directly by the covariance of absolute humidity and vertical wind velocity. For that reason, the use of the residual latent heat from the energy balance equation is deemed more satisfactory for use in this study. The performance of the system during the last instrument set-up shows the equipment is capable of measuring ET as accurately as other methods currently available. The fact that all components of the energy balance are measured does give some degree of assurance that useable data can be obtained despite failure of one instrument.

The ability of the system to measure ET for short intervals reveals some information about the contributions of nighttime hours to the total daily water use of a crop. The maximum half-hourly ET at night was on the order of 5% of the typical daytime half-hourly ET. From this it can be concluded that for ET prediction from hourly meteorological data, modelling of the hours when solar radiation is greater than zero will give satisfactory results.

It is possible to determine net radiation (R_n) from the more easily measured parameter of solar radiation (R_S). The prediction of hourly values is done with equations for each crop for both twilight and midday hours. The equations, which have high correlation coefficients, are:

Hourly Net Radiation:

Alfalfa,Midday:

$$R_n = -15.692 + 0.72066\ R_S$$

Alfalfa,Twilight:

$$R_n = -47.290 + 0.80028\ R_S$$

Peanuts,Midday:

$$R_n = 9.7128 + 0.65035\ R_S$$

Peanuts,Twilight:

$$R_n = -46.407 + 0.75498\ R_S$$

Daily Net Radiation:

Alfalfa:

$$R_n = 786.99 + 0.54267\ R_S$$

Peanuts:

$$R_n = 672.64 + 0.50777\ R_S$$

Soil heat flux (G) can be determined with a satisfactory level of correlation from solar radiation (R_S) and air temperature (T_A). The hourly values are determined from the following equations:

Hourly Soil Heat Flux:

Alfalfa:

$$G = 1.0642 - 0.00010153\ R_S^2 + 0.013265\ T_A^2$$

Peanuts:

$$G= 18.5925 - 0.00004359\ R_S^2 + 0.017368\ T_A^2$$

All hourly equations are for mean energy flux density with the parameters in units of W/m^2. The daily equations are for total energy density with parameters given in units of MJ/m^2. These relationships permit the estimation of Penman input parameters from simple meteorological data gathered at a centralized weather station.

The calibration factors for the modified Penman equation for an alfalfa reference crop were determined. The relationship between wind function ,W_f, and hourly wind run at a 2 m elevation ,U_2, while not highly correlated, is statistically significant. The correlation for daily data was not found to be significant, even at a low level of confidence. The hourly relationships are:

Hourly, Daytime:

$$W_f= 1.5880 + 2.0693\ U_2$$

Hourly, Nighttime:

$$W_f= -1.7926 + 0.85827\ U_2$$

The hourly wind function calibrations are based on wind run, U_2, in km/hr. U_2 in daily calibration is in km/day.

The crop coefficient (K_c) relating ET for a specific crop to computed Penman reference ET can be determined as a function of the stage of crop development. Crop development can be quantified in terms of the fraction of the normalized growing season that has elapsed (FGS). For Florunner peanuts the relationship is:

$$K_c = -5.148 + 29.71\ FGS - 46.47\ FGS^2 + 23.27\ FGS^3$$

It has been observed that the crop coefficient curve for Florunner peanuts in 1986 is quite similar to that determined for the spanish variety, Spanco, in 1984 and 1985. It is concluded that there may not be a varietal difference in the rate of water use at the same relative stage of growth.

Despite the difficulties that developed with the krypton hygrometer, the eddy correlation system is a viable tool for the direct measurement of evaporative flux. If the end of the season performance can be sustained on a continued basis, it can measure ET with sufficient accuracy for virtually all agricultural purposes. The measurement of all of the fluxes of the surface energy budget is probably necessary to confirm the accuracy of the latent heat flux as measured by the hygrometer and sonic anemometer. The measurements made during the 1986 season show that the apparatus can be set up and operating within two hours after arrival in the field. Removal can be accomplished in one hour. This offers a degree of portability that is unmatched by any other apparatus that is capable of measuring evaporative flux for intervals of one day or less in length.

Recommendations

It is recommended that the apparatus be used to measure the terms of the energy balance equation during the 1987

season to confirm the accuracy of the closure ratio with a properly functioning hygrometer. If eddy correlation equipment is used in the future to develop crop coefficients for other crops, the performance and ease of use of the system can be improved through several changes. Operation of the basic meteorological sensors on a separate datalogger would permit the CR21X to drive the eddy sensors at a higher frequency. The system would certainly be able to operate at 13.3 Hz, and perhaps at 16 Hz, without the microprocessor running out of processing time. At 16 Hz, normalized frequencies as high as 0.86 can be measured without cut-off errors. Raising the sensors to a height of 3 m, fetch distances permitting, will allow measurement of normalized frequencies of as high as 1.4.

Raising the instruments will increase the low frequency cut-off errors at low wind speeds. If internal memory permits, the averaging period should be lengthened to 15 minutes. The output interval can be increased to 60 minutes. This will keep low frequency cut-off errors down to present levels, or lower, at a 3 m sensor height.

In order to ensure that the hygrometer is functioning properly, the printed output should include the standard deviation of the hygrometer signal. Though this will slow down the processing speed of the datalogger slightly, it will indicate any unusual variability in the hygrometer signal. This will give the operator warning of decay in the krypton glow tube integrity.

There were difficulties in keeping the sensing units oriented into the wind within acceptable tolerances without disturbing the vertical alignment of the sonic anemometer. In the future, the sensor mast should have a swivel head above the point of attachment of the guy wires. This will permit the apparatus to be pivoted, accomodating wind shifts, without disturbing the plumb of the sonic anemometer head.

With the previously cited relationships, it should be possible to predict water use and to accurately schedule irrigations. The prediction equation can be applied to the same crop over a wide area if it is meteorologically homogeneous. Water use rates can be determined for the whole area from data gathered at a single, automatic weather station without the need for intensive measurements at individual field sites.

CHAPTER VII

REFERENCES CITED

Anderson, D. E., S. B. Verma and N. J. Rosenberg. 1984. Eddy-correlation measurements of CO-2, latent heat, and sensible heat fluxes over a crop surface. Boundary-Layer Meteorology 29:263-272.

Bosen, J. F. 1960. A formula for approximation of the saturation vapor pressure over water. Monthly Weather Review 88(8):275-276.

Bottemanne, F. A. 1979. Eddy correlation measurements above a maize crop using a simple cruciform hot-wire anemometer. Agricultural Meteorology 20(9):397-410.

Brunt, D. 1952. Physical and dynamical meteorology. 2nd ed. University Press, Cambridge, 428 p.

Buck, A. L. 1976. The variable path Lyman-alpha hygrometer and its operating characteristics. Amer. Meteorological Soc. Bulletin 57(9):1113-1118.

Burman, R. D., P. R. Nixon, J. L. Wright and W. O. Pruitt. 1980. Water requirements. In: Design and Operation of Farm Irrigation Systems. M. E. Jensen (ed.) ASAE Monograph No. 3. ASAE, St. Joseph, MI. pp. 189-232.

Campbell, G. S. and M. H. Unsworth. 1979. An inexpensive sonic anemometer for eddy correlation. Journal of Applied Meteorology 18:1072-1077.

Campbell, G. S. and B.D. Tanner. 1985. A krypton hygrometer for measurement of atmospheric water vapor concentration. Moisture and Humidity 1985. Proc. of the International Symposium on Moisture and Humidity, Washington, D.C. April 15-18, 1985. pp. 609-612.

Campbell Scientific, Inc. 1986. CSI Eddy Correlation and Bowen Ratio Instrumentation. (Preliminary Version). Logan, UT. 9 p.

Cuenca, R. H. and M. T. Nicholson. 1982. Application of Penman equation wind function. Journal of the Irrigation and Drainage Division, Proc. of the ASCE 108(IR1):13-23.

Doorenbos, J. and W. O. Pruitt. 1977. Crop water requirements, Food and Agriculture Organization of the United Nations Irrigation and Drainage Paper 24, Revised, Rome, Italy, 144 pp.

Dyer, A. J. 1961. Measurement of evaporation and heat transfer in the lower atmosphere by an automatic eddy correlation technique. Quarterly Journal of the Royal Meteorological Society 87:401-412.

Dyer, A. J. and W. O. Pruitt. 1962. Eddy flux measurements over a small, irrigated area. Journal of Applied Meteorology 1:471-473.

Dyer, A. J., B. B. Hicks and K. M. King. 1967. The fluxatron--A revised approach to the measurement of eddy fluxes in the lower atmosphere. Journal of Applied Meteorology 6:408-413.

Dyer, A. J. and B. B. Hicks. 1972. The spatial variability of eddy fluxes in the constant flux layer. Quarterly Journal of the Royal Meteorological Society 98:206-212.

Dyer, A. J., J. R. Garratt, R. J. Francey, I. C. McIlroy, N.E. Bacon, P. Hyson, E. F. Bradley, O. T. Denmead, L. R. Tsvang, Y. A. Volkov, B. M. Koprov, L. G. Elagina, K. Sahashi, N. Monji, T. Hanafusa, O. Tsukamoto, P. Frenzen, B. B. Hicks, M. Wesely, M. Miyake and W. Shaw. 1983. An international turbulence comparison experiment (ITCE 1976). Boundary Layer Meteorology 24:181-209.

Fritschen, L. J. 1967. Net and solar radiation relations over irrigated field crops. Agricultural Meteorology 4:55-62.

Harp, S. L., R. L. Elliott, D. P. Schwab, G.D. Grosz and M. A. Kizer. 1986. Irrigation Scheduling Program. Project completion report for contract numbers: 291-68-G83/SECP-62039-07A, 291-45-G84/EES-69119-407A and 291-49-G85/EES-69119-407 to the Corporation Commission of Oklahoma.

Hicks, B.B. 1973. Eddy fluxes over a vinyard. Agricultural Meteorology 12:203-215.

Hicks, B. B., P. Hyson and C. J. Moore. 1975. A study of eddy fluxes over a forest. Journal of Applied Meteorology 14:58-66.

Jensen, M. E. 1968. Water consumption by agricultural plants. In: Water Deficits and Plant Growth, Vol. II, T. T. Kozlowski (ed.) Academic Press, New York, pp. 1-22.

Jensen, M. E. (ed.). 1973. Consumptive use of water and irrigation water requirements. Report of the Technical Committee on Irrigation Water Requirements, Irrigation and Drainage Division, ASCE, New York, 215 p.

Jensen, M. E., J. L. Wright and B. J. Pratt. 1971. Estimatimg soil moisture depletion from climate, crop and soil data. Transactions of ASAE 14(5):954-959.

Kaimal, J. C. 1969. Measurement of momentum and heat flux in the surface boundary layer. Radio Science 4(12):1147-1153.

Kaimal, J. C. 1975. Sensors and techniques for direct measurement of fluxes and profiles in the atmospheric surface layer. Atmospheric Technology 7:7-14.

Kaimal, J. C. and J. A. Businger. 1963. A continuous wave sonic anemometer-thermometer. Journal of Applied Meteorology 2:156-167.

Kanemasu, E. T., M.L. Wesley, B. B. Hicks, and J. L. Heilman. 1979. Techniques for calculating energy and mass fluxes. In: Modification of the Aerial Environment of Crops. B. J. Barfield and J. F. Gerber, (eds.). ASAE Monograph No. 2. ASAE, St. Joseph, MI. pp. 156-182.

Kincaid, D. C. and D. F. Heerman. 1974. Scheduling irrigations using a programmable calculator. Nebrasba Agricultural Experiment Station, Journal Series Paper No. 3604.

Koprov, B. M. and D. Yu. Sokolov. 1973. Spatial correlation functions of velocity and temperature components in the surface layer of the atmosphere. Izv. Atmospheric and Oceanic Physics 9:178-182.

Lloyd, C. R., W. J. Shuttleworth, J. H. C. Gash and M. Turner. 1984. A microprocessor system for eddy-correlation. Agriculture and Forest Meteorology 33:67-80.

McBean, G. A. 1972. Instrument requirements for eddy-correlation measurements. Journal of Applied Meteorology 11:1078-1084.

Miyake, M. and G. McBean. 1970. On the measurement of vertical humidity transport over land. Boundary-Layer Meteorology 1:88-101.

Monteith, J. L. 1963. Gas exchange in plant communities. In: Environmental Control of Plant Growth, L. T. Evans (ed.). Academic Press, New York, pp. 95-112.

Monteith, J. L. 1964. Evaporation and environment: The state and movement of water in living organisms. 19th Symp. Soc. Exp. Biology, Academic Press, New York, pp. 205-234.

Moore, C. J. 1976. Eddy flux measurement above a pine forest. Quarterly Journal of the Royal Meteorological Society 102:913-918.

Mortimer, C. E. 1967. Chemistry: A conceptual approach. Reinhold Publishing Inc., New York, 692 p.

Munro, D. S. and T. R. Oke. 1975. Aerodynamic boundary layer adjustment over a crop in neutral stability. Boundary-Layer Meteorology 9:53-61.

Neumann, H. H. and G. den Hartog. 1985. Eddy correlation measurements of atmospheric fluxes of ozone, sulphur, and particles during the Champaign intercomparison study. Journal of Geophysical Research 90(D1):2079-2110.

Penman, H. L. 1948. Natural evaporation for open water bare soil, and grass. Proceedings Royal ciety of London, A193:120-146.

Penman, H. L. 1963. Vegetation and hydrology. Tech. Communication No. 53. Commonwealth Bureau of Soils. Harpenden, England. 125 p.

Pruitt, W. O. and J. Doorenbos. 1977. Empirical calibration, a requisite for evapotranspiration formulae based on daily or longer mean climatic data. Presented at the International Round Table Conference of Evapotranspiration, International Commission on Irrigation and Drainage, Budapest, Hungary. 20 p.

Randall, D. L., T. E. Hanley and O. K. Larison. 1965. The NRL Lyman-alpha humidiometer. In: Humidity and Moisture: Measurement and Control in Science and Industry. A. Wexler (ed.). Reinhold Publishing, Inc. New York, pp. 444-454.

Redford, T. G., S. B. Verma and N. J. Rosenberg. 1980. Humidity fluctuations over a vegetated surface measured with a Lyman-alpha hygrometer and a fine-wire thermocouple psychrometer. Journal of Applied Meteorology 19:860-867.

Rosenberg, N. J., B. L. Blad and S. B. Verma. 1983. Microclimate: The biological environment. 2nd ed. John Wiley and Sons, New York, 495 p.

Slatyer, R. O. and McIlroy. 1961. Practical microclimatology. CSIRO, Melbourne, Vic. 310 p.

Spittlehouse, D. L. and T. A. Black. 1979. Determination of forest evapotranspiration using Bowen ratio and eddy correlation measurements. Journal of Applied Meteorology 18:647-653.

Staats, W. F., L. W. Foskett and H. P. Jensen. 1965. Infrared absorption hygrometer. In: Humidity and Moisture: Measurement and Control in Science and Industry. A. Wexler (ed.). Reinhold Publishing, Inc. New York, pp. 465-477.

Swinbank, W. C. 1951. The measurement of vertical transfer of heat and water vapor by eddies in the lower atmosphere. Journal of Meteorology 8:135-145.

Szeicz, G., G. Endrodi and S. Tajchman. 1969. Aerodynamic and surface factors in evaporation. Water Resources Research 5:380-394.

Tanner, B. D. 1984. Measurements with a portable eddy correlation system. Presented at: International Symposium in Memory of Dr. Franz Sauberer. Vienna, Austria. October 23-25, 1984.

Tanner, B. D. 1986. Telephone conversation. June 15,1986.

Tanner, B. D., M. S. Tanner, W. A. Dugas, E. C. Campbell and B. L. Bland. 1985. Evaluation of an operational eddy-correlation system for evapotranspiration measurement. In: Advances in Evapotranspiration. Proc. of the National Conference on Advances in Evapotranspiration. ASAE Pub. No. 14-85, pp. 87-99.

van Bavel, C. H. M. 1966. Potential evaporation: The combination concept and its experimental verification. Water Resources Research 2:455-467.

Verma, S. B., D. D. Baldocchi, D. E. Anderson, D. R. Matt and R. J. Clement. 1986. Eddy fluxes of CO_2, water vapor, and sensible heat over a deciduous forest. Boundary-Layer Meteorology 36:71-91.

Wesley, M. L., G. W. Thurtell and C. B. Tanner. 1970. Eddy-correlation measurements of sensible heat flux near the earth's surface. Journal of Applied Meteorology 9:45-50.

Wesley, M. L., J. A. Eastman, D. H. Stedman and E. D. Yalvac. 1981. An eddy-correlation measurement of NO_2 flux to vegetation and comparison to O_3 flux. Atmospheric Environment 16(4):815-820.

Wright, J. L. 1979. Recent developments in determining crop coefficient values. Proc. ASCE Irrigation and Drainage Specialty Conf. July, 1979. pp. 161-162.

Wright, J. L. 1981. Crop coefficients for estimates of daily crop evapotranspiration. In: Irrigation Scheduling for Water and Energy Conservation in the 80's. ASAE Pub. No. 23-81. ASAE, St. Joseph, MI. pp. 18-26.

Wright, J. L. and M. E. Jensen. 1972. Peak water requirements in southern Idaho. Proc. ASCE, Journal of Irrigation and Drainage Division 98(IR2):193-201.

APPENDIXES

APPENDIX A

ENERGY FLUX SUMMARIES

MEAN HALF-HOURLY ENERGY FLUX DENSITY

DAY	TIME	RN	H	G	LE	ET	CLOSURE
	(HR)	(W/M2)	(W/M2)	(W/M2)	(W/M2)	(MM)	
176.000	930.000	297.100	-25.190	-22.947	-141.800	0.105	0.609
176.000	1000.000	371.700	-24.640	-29.160	-116.300	0.086	0.411
176.000	1030.000	432.200	-27.490	-33.413	-253.600	0.188	0.705
176.000	1100.000	485.700	-25.190	-41.463	-224.100	0.166	0.561
176.000	1130.000	566.400	-30.100	-58.133	-222.100	0.165	0.496
176.000	1200.000	385.700	-7.490	-52.780	-213.700	0.159	0.664
176.000	1230.000	465.700	-3.885	-44.473	-207.200	0.154	0.501
176.000	1300.000	570.000	-16.450	-73.347	-298.100	0.222	0.633
176.000	1330.000	563.900	3.212	-78.387	-304.100	0.226	0.620
176.000	1400.000	615.600	-80.000	-74.253	-602.500	0.448	1.261
176.000	1430.000	647.300	-10.160	-95.570	-365.600	0.272	0.681
176.000	1500.000	632.000	-10.140	-91.950	-319.000	0.237	0.609
176.000	1530.000	611.700	-2.798	-92.640	-296.200	0.220	0.576
176.000	1600.000	534.400	13.130	-76.990	-355.500	0.264	0.748
176.000	1630.000	488.300	19.770	-63.133	-289.300	0.215	0.634
176.000	1700.000	449.200	34.460	-41.393	-266.400	0.198	0.569
176.000	1730.000	418.700	46.690	-35.113	-287.800	0.214	0.629
176.000	1800.000	333.400	61.270	-21.750	-251.200	0.187	0.609
176.000	1830.000	270.800	65.220	-9.724	-239.800	0.178	0.669
176.000	1900.000	187.900	75.500	-1.643	-196.600	0.146	0.650
176.000	1930.000	104.100	85.300	7.549	-168.000	0.125	0.741
176.000	2000.000	34.550	59.030	13.117	-97.300	0.072	0.803
176.000	2030.000	-14.450	30.210	16.117	-47.360	0.035	10.290
176.000	2100.000	-45.560	15.730	18.347	-23.870	0.018	-0.299
176.000	2130.000	-53.380	8.310	20.530	-11.640	0.009	-0.101
176.000	2200.000	-53.390	10.980	20.537	-16.370	0.012	-0.164
176.000	2230.000	-55.550	10.950	20.800	-15.670	0.012	-0.136
176.000	2300.000	-56.560	7.440	20.893	-12.460	0.009	-0.141
176.000	2330.000	-55.820	8.360	21.063	-10.760	0.008	-0.069
177.000	0.000	-56.030	16.410	20.993	-25.030	0.018	-0.246
177.000	30.000	-55.060	8.990	20.360	-13.670	0.010	-0.135
177.000	100.000	-54.000	0.880	20.900	-0.403	0.000	0.014
177.000	130.000	-54.890	3.296	20.203	-2.529	0.002	0.022
177.000	200.000	-54.430	2.188	19.520	-0.964	0.001	0.035
177.000	230.000	-53.080	4.407	18.527	0.017	0.000	0.128
177.000	300.000	-53.670	5.285	17.937	-6.483	0.005	-0.034
177.000	330.000	-55.180	8.800	17.513	-19.050	0.014	-0.272
177.000	400.000	-55.480	10.190	17.393	-21.230	0.016	-0.290
177.000	430.000	-55.930	9.450	17.450	-17.690	0.013	-0.214
177.000	500.000	-56.440	9.850	17.363	-21.240	0.016	-0.291
177.000	530.000	-56.470	7.370	17.023	-16.630	0.012	-0.235
177.000	600.000	-55.090	3.980	16.963	-0.161	0.000	0.100
177.000	630.000	-49.870	1.983	17.180	-0.792	0.001	0.036
177.000	700.000	-32.160	3.476	14.487	4.089	0.000	0.428
177.000	730.000	5.897	-0.733	9.483	-17.140	0.013	1.162
177.000	800.000	62.750	-10.520	5.004	-39.000	0.029	0.731
177.000	830.000	126.100	-17.990	-0.655	-51.960	0.038	0.558
177.000	900.000	203.000	-29.410	-7.544	-88.700	0.066	0.604

DAILY TOTAL ENERGY DENSITY

	(HR)	(MJ/M2)	(MJ/M2)	(MJ/M2)	(MJ/M2)	(MM)	
176.000	2400.000	15.717	0.594	-1.079	-11.147	4.601	0.721

MEAN HALF-HOURLY ENERGY FLUX DENSITY

DAY	TIME	RN	H	G	LE	ET	CLOSURE
	(HR)	(W/M2)	(W/M2)	(W/M2)	(W/M2)	(MM)	
177.000	930.000	284.700	-34.000	-14.767	-122.100	0.090	0.578
177.000	1000.000	357.600	-37.980	-21.153	-181.900	0.135	0.654
177.000	1030.000	435.900	-37.110	-29.943	-228.900	0.170	0.655
177.000	1100.000	515.200	-28.780	-33.220	-280.700	0.208	0.642
177.000	1130.000	564.800	-13.340	-40.017	-302.300	0.224	0.601
177.000	1200.000	604.900	-21.370	-56.423	-325.600	0.242	0.633
177.000	1230.000	590.500	-26.410	-63.740	-329.700	0.245	0.676
177.000	1300.000	715.000	-45.800	-91.443	-358.000	0.266	0.648
177.000	1330.000	649.000	-27.490	-92.580	-331.800	0.247	0.646
177.000	1400.000	708.000	-23.720	-110.300	-370.200	0.275	0.659
177.000	1430.000	662.400	-10.590	-92.793	-370.100	0.275	0.668
177.000	1500.000	644.100	-6.165	-88.580	-378.400	0.281	0.692
177.000	1530.000	653.600	-7.670	-85.207	-367.800	0.274	0.661
177.000	1600.000	618.300	12.020	-77.380	-394.800	0.294	0.708
177.000	1630.000	549.300	21.190	-63.210	-351.900	0.262	0.680
177.000	1700.000	496.600	36.810	-46.280	-307.100	0.228	0.600
177.000	1730.000	417.100	44.570	-32.110	-299.100	0.222	0.661
177.000	1800.000	350.800	73.500	-21.143	-281.100	0.209	0.630
177.000	1830.000	281.400	79.400	-8.740	-265.300	0.197	0.682
177.000	1900.000	201.500	72.700	-4.189	-209.700	0.156	0.694
177.000	1930.000	119.100	68.740	1.811	-155.400	0.115	0.717
177.000	2000.000	48.100	58.610	5.764	-114.300	0.085	1.034
177.000	2030.000	-14.320	55.240	9.419	-80.200	0.059	-5.093
177.000	2100.000	-47.320	39.220	10.630	-51.310	0.038	-0.330
177.000	2130.000	-58.720	33.580	12.553	-42.180	0.031	-0.186
177.000	2200.000	-60.540	18.270	13.760	-18.230	0.013	0.001
177.000	2230.000	-59.350	11.800	14.613	-15.390	0.011	-0.080
177.000	2300.000	-56.190	9.140	15.277	-13.900	0.010	-0.116
177.000	2330.000	-58.540	10.530	15.230	-16.530	0.012	-0.139
178.000	0.000	-57.920	7.100	15.250	-12.020	0.009	-0.115
178.000	30.000	-57.660	8.180	15.350	-13.730	0.010	-0.131
178.000	100.000	-57.130	7.830	15.500	-11.480	0.008	-0.088
178.000	130.000	-55.620	9.950	15.787	-14.060	0.010	-0.103
178.000	200.000	-54.350	5.313	15.430	-8.430	0.006	-0.080
178.000	230.000	-51.400	2.866	15.673	-1.548	0.001	0.037
178.000	300.000	-52.840	2.380	15.397	-12.100	0.009	-0.260
178.000	330.000	-54.070	4.944	14.653	-14.510	0.011	-0.243
178.000	400.000	-54.250	5.616	14.543	-11.190	0.008	-0.140
178.000	430.000	-53.940	5.297	14.500	-7.560	0.006	-0.057
178.000	500.000	-51.980	4.755	14.643	-5.054	0.004	-0.008
178.000	530.000	-51.820	4.520	14.630	-5.654	0.004	-0.030
178.000	600.000	-51.730	3.708	14.590	0.072	0.000	0.102
178.000	630.000	-46.330	1.114	15.573	-1.086	0.001	0.001
178.000	700.000	-27.410	-0.660	13.963	-27.370	0.020	-2.085
178.000	730.000	18.840	-4.346	8.232	-18.410	0.014	0.841
178.000	800.000	91.500	-14.710	3.859	-47.050	0.035	0.648
178.000	830.000	170.100	-13.480	-1.237	-79.900	0.059	0.553
178.000	900.000	256.400	15.460	-4.244	-167.300	0.124	0.602

DAILY TOTAL ENERGY DENSITY

	(HR)	(MJ/M2)	(MJ/M2)	(MJ/M2)	(MJ/M2)	(MM)	
177.000	2400.000	17.768	0.685	-1.336	-12.640	5.214	0.728

MEAN HALF-HOURLY ENERGY FLUX DENSITY

DAY	TIME	RN	H	G	LE	ET	CLOSURE
	(HR)	(W/M2)	(W/M2)	(W/M2)	(W/M2)	(MM)	
183.000	930.000	293.100	-3.592	-19.170	-10.300	0.008	0.051
183.000	1000.000	324.400	-3.754	-21.777	-9.470	0.007	0.044
183.000	1030.000	415.500	-80.100	-26.453	-475.800	0.353	1.429
183.000	1100.000	462.500	-51.980	-27.430	-309.500	0.230	0.831
183.000	1130.000	448.400	-34.190	-25.953	-251.900	0.187	0.677
183.000	1200.000	465.200	-32.200	-26.050	-226.300	0.168	0.589
183.000	1230.000	583.700	-67.690	-35.283	-339.300	0.252	0.742
183.000	1300.000	632.800	-46.070	-41.227	-284.700	0.211	0.559
183.000	1330.000	574.700	-32.210	-37.377	-311.000	0.231	0.639
183.000	1400.000	658.100	-25.490	-46.793	-324.700	0.241	0.573
183.000	1430.000	564.800	-4.527	-35.793	-318.500	0.237	0.611
183.000	1500.000	564.000	-12.450	-37.320	-281.000	0.209	0.557
183.000	1530.000	456.900	19.890	-27.367	-236.500	0.176	0.504
183.000	1600.000	344.300	50.770	-17.167	-231.700	0.172	0.553
183.000	1630.000	271.400	41.540	-12.327	-158.600	0.118	0.452
183.000	1700.000	260.600	50.850	-6.743	-189.400	0.141	0.546
183.000	1730.000	369.500	53.960	-9.723	-254.600	0.189	0.558
183.000	1800.000	374.300	52.130	-9.041	-253.100	0.188	0.550
183.000	1830.000	294.600	86.800	-3.170	-251.800	0.187	0.566
183.000	1900.000	182.700	80.400	1.894	-142.000	0.105	0.334
183.000	1930.000	138.000	60.710	2.463	-135.200	0.100	0.530
183.000	2000.000	38.600	64.310	4.456	-82.600	0.061	0.425
183.000	2030.000	-20.190	52.730	5.279	-32.630	0.024	1.348
183.000	2100.000	-47.530	21.700	8.013	-11.860	0.009	0.249
183.000	2130.000	-52.950	5.825	12.383	-3.093	0.002	0.067
183.000	2200.000	-51.890	0.140	16.103	-1.993	0.001	-0.052
183.000	2230.000	-52.280	1.172	18.273	-1.474	0.001	-0.009
183.000	2300.000	-51.620	2.523	16.220	0.397	0.000	0.082
183.000	2330.000	-48.480	0.888	17.487	-1.238	0.001	-0.011
184.000	0.000	-45.860	0.703	17.207	-0.981	0.001	-0.010
184.000	30.000	-43.400	0.636	16.763	-1.244	0.001	-0.023
184.000	100.000	-29.630	1.618	13.970	-1.186	0.001	0.028
184.000	130.000	-33.920	1.612	10.324	-0.279	0.000	0.056
184.000	200.000	-38.470	1.761	16.240	6.653	0.000	0.378
184.000	230.000	-24.770	-0.649	20.287	0.566	0.000	-0.019
184.000	300.000	-21.340	2.228	20.370	-3.492	0.003	-1.303
184.000	330.000	-19.030	3.676	20.843	8.500	0.000	-6.715
184.000	400.000	-17.960	-1.402	22.860	-16.220	0.012	3.596
184.000	430.000	-20.670	5.024	18.737	6.686	0.000	6.057
184.000	500.000	-19.710	4.200	18.837	3.432	0.000	8.739
184.000	530.000	-18.790	4.540	19.080	6.379	0.000	-37.652
184.000	600.000	-17.070	3.898	19.273	-1.603	0.001	-1.042
184.000	630.000	-14.090	2.462	19.160	-1.460	0.001	-0.198
184.000	700.000	13.510	-0.854	18.650	-8.220	0.006	0.282
184.000	730.000	52.690	-4.046	12.283	-38.510	0.028	0.655
184.000	800.000	86.600	-1.118	4.762	-30.110	0.022	0.342
184.000	830.000	165.000	-18.700	-2.749	-63.740	0.047	0.508
184.000	900.000	248.000	-9.870	-8.229	-115.300	0.085	0.522

DAILY TOTAL ENERGY DENSITY

	(HR)	(MJ/M2)	(MJ/M2)	(MJ/M2)	(MJ/M2)	(MM)	
183.000	2400.000	15.470	0.446	-0.153	-9.684	4.019	0.603

MEAN HALF-HOURLY ENERGY FLUX DENSITY

DAY	TIME	RN	H	G	LE	ET	CLOSURE
	(HR)	(W/M2)	(W/M2)	(W/M2)	(W/M2)	(MM)	
184.000	930.000	333.700	8.650	-11.170	-213.800	0.158	0.636
184.000	1000.000	430.600	17.830	-13.417	-254.400	0.188	0.567
184.000	1030.000	456.000	24.370	-14.247	-316.900	0.234	0.662
184.000	1100.000	514.400	-4.166	-16.573	-311.700	0.231	0.634
184.000	1130.000	609.000	-13.440	-20.987	-342.300	0.254	0.605
184.000	1200.000	625.400	-9.830	-24.977	-355.000	0.263	0.608
184.000	1230.000	630.600	-33.190	-30.987	-368.300	0.273	0.670
184.000	1300.000	678.500	-49.280	-46.110	-407.600	0.302	0.722
184.000	1330.000	705.000	-3.961	-46.207	-395.300	0.293	0.606
184.000	1400.000	594.100	-3.729	-30.913	-429.500	0.319	0.769
184.000	1430.000	740.000	-9.410	-34.523	-436.900	0.324	0.633
184.000	1500.000	666.400	-18.760	-29.457	-394.000	0.293	0.648
184.000	1530.000	591.400	-2.842	-24.570	-388.200	0.288	0.690
184.000	1600.000	400.600	6.024	-13.327	-269.300	0.200	0.680
184.000	1630.000	513.000	-34.470	-18.457	-441.700	0.328	0.963
184.000	1700.000	425.800	-5.969	-14.553	-299.200	0.222	0.742
184.000	1730.000	279.500	61.600	-0.322	-247.000	0.183	0.664
184.000	1800.000	142.300	92.200	6.012	-182.000	0.135	0.605
184.000	1830.000	237.700	76.100	2.440	-213.900	0.159	0.574
184.000	1900.000	243.800	87.300	2.752	-254.500	0.189	0.678
184.000	1930.000	140.400	105.400	8.408	-194.400	0.144	0.598
184.000	2000.000	71.400	89.100	11.621	-133.400	0.099	0.534
184.000	2030.000	33.140	77.000	9.396	-109.700	0.081	0.769
184.000	2100.000	-42.140	69.340	11.818	-57.360	0.042	0.395
184.000	2130.000	-55.630	54.020	11.808	-39.170	0.029	0.339
184.000	2200.000	-56.270	52.280	12.166	-36.500	0.027	0.358
184.000	2230.000	-56.090	44.740	11.797	-30.190	0.022	0.328
184.000	2300.000	-55.670	40.630	12.441	-29.660	0.022	0.254
184.000	2330.000	-54.300	42.790	12.637	-29.840	0.022	0.311
185.000	0.000	-53.300	25.650	12.577	-16.490	0.012	0.225
185.000	30.000	-51.420	15.170	13.120	-10.720	0.008	0.116
185.000	100.000	-51.530	14.480	13.170	-9.810	0.007	0.122
185.000	130.000	-54.160	20.760	11.450	-13.450	0.010	0.171
185.000	200.000	-56.920	18.440	11.447	-14.200	0.010	0.093
185.000	230.000	-56.270	12.370	12.143	-11.390	0.008	0.022
185.000	300.000	-54.460	10.640	13.390	-12.290	0.009	-0.040
185.000	330.000	-48.590	10.740	14.250	-16.780	0.012	-0.176
185.000	400.000	-56.270	13.390	15.870	-18.150	0.013	-0.118
185.000	430.000	-56.620	15.580	16.480	-18.570	0.014	-0.074
185.000	500.000	-57.980	15.470	16.130	-18.890	0.014	-0.082
185.000	530.000	-57.200	10.990	15.543	-15.510	0.011	-0.109
185.000	600.000	-57.180	10.010	15.490	-13.710	0.010	-0.089
185.000	630.000	-43.480	6.587	14.050	-43.670	0.032	-1.260
185.000	700.000	-21.800	2.120	11.517	-13.990	0.010	-1.154
185.000	730.000	20.700	-4.784	8.200	-21.050	0.016	0.894
185.000	800.000	8.700	-1.379	7.337	-19.980	0.015	1.332
185.000	830.000	114.600	-15.900	3.868	-63.100	0.047	0.667
185.000	900.000	239.400	-23.820	-4.424	-116.200	0.086	0.596

DAILY TOTAL ENERGY DENSITY

	(HR)	(MJ/M2)	(MJ/M2)	(MJ/M2)	(MJ/M2)	(MM)	
184.000	2400.000	16.828	1.650	-0.101	-13.769	5.670	0.725

MEAN HALF-HOURLY ENERGY FLUX DENSITY

DAY	TIME	RN	H	G	LE	ET	CLOSURE
	(HR)	(W/M2)	(W/M2)	(W/M2)	(W/M2)	(MM)	
190.000	1130.000	526.600	-28.430	-25.723	-236.500	0.176	0.529
190.000	1200.000	563.400	-37.040	-38.913	-286.700	0.213	0.617
190.000	1230.000	590.600	-39.790	-43.563	-330.300	0.246	0.677
190.000	1300.000	612.400	-38.020	-48.697	-285.500	0.212	0.574
190.000	1330.000	620.400	-32.480	-46.480	-267.100	0.199	0.522
190.000	1400.000	622.300	-22.630	-41.620	-293.800	0.219	0.545
190.000	1430.000	614.900	-20.180	-42.183	-355.500	0.265	0.656
190.000	1500.000	595.500	-13.720	-41.417	-331.500	0.247	0.623
190.000	1530.000	571.400	-6.277	-43.490	-315.300	0.235	0.609
190.000	1600.000	535.400	10.800	-41.183	-364.400	0.272	0.715
190.000	1630.000	491.600	25.100	-38.403	-358.700	0.267	0.736
190.000	1700.000	442.000	33.990	-29.648	-246.400	0.184	0.515
190.000	1730.000	383.200	44.260	-26.007	-196.000	0.146	0.425
190.000	1800.000	318.800	42.540	-19.625	-182.000	0.136	0.466
190.000	1830.000	243.900	53.570	-9.971	-171.600	0.128	0.505
190.000	1900.000	168.700	46.850	-4.430	-139.100	0.104	0.562
190.000	1930.000	93.600	55.970	0.059	-112.500	0.084	0.604
190.000	2000.000	20.600	54.140	4.839	-84.800	0.063	1.205
190.000	2030.000	-35.920	45.800	9.776	-59.900	0.044	-0.539
190.000	2100.000	-65.870	36.100	14.967	-25.910	0.019	0.200
190.000	2130.000	-71.400	37.950	18.170	-26.230	0.019	0.220
190.000	2200.000	-71.700	41.920	19.477	-29.100	0.022	0.245
190.000	2230.000	-70.000	35.120	20.730	-23.110	0.017	0.244
190.000	2300.000	-67.520	33.510	21.087	-23.900	0.018	0.207
190.000	2330.000	-68.130	37.460	20.613	-22.410	0.017	0.317
191.000	0.000	-69.810	41.600	19.873	-23.590	0.017	0.361
191.000	30.000	-69.760	40.500	20.013	-22.510	0.017	0.362
191.000	100.000	-67.740	33.840	19.867	-17.990	0.013	0.331
191.000	130.000	-65.910	37.790	20.033	-21.010	0.016	0.366
191.000	200.000	-63.370	33.650	19.517	-18.850	0.014	0.337
191.000	230.000	-61.010	31.150	19.547	-18.250	0.013	0.311
191.000	300.000	-59.530	31.220	19.143	-18.100	0.013	0.325
191.000	330.000	-58.510	28.220	18.640	-16.270	0.012	0.300
191.000	400.000	-58.460	25.710	18.570	-15.000	0.011	0.268
191.000	430.000	-60.230	21.850	19.443	-13.340	0.010	0.209
191.000	500.000	-61.450	25.550	20.800	-14.210	0.010	0.279
191.000	530.000	-63.190	36.510	19.940	-18.980	0.014	0.405
191.000	600.000	-63.290	34.150	19.143	-17.880	0.013	0.369
191.000	630.000	-61.920	34.910	19.343	-20.140	0.015	0.347
191.000	700.000	-46.510	31.740	17.810	-22.220	0.016	0.332
191.000	730.000	-0.613	24.520	13.593	-46.130	0.034	1.665
191.000	800.000	68.280	12.090	7.479	-48.110	0.036	0.475
191.000	830.000	140.200	5.641	1.989	-82.600	0.061	0.541
191.000	900.000	216.800	4.283	-2.946	-124.600	0.092	0.563
191.000	930.000	292.200	1.988	-9.284	-168.200	0.125	0.587
191.000	1000.000	360.100	-2.014	-23.653	-206.500	0.153	0.620
191.000	1030.000	424.000	-5.385	-26.037	-247.000	0.183	0.634
191.000	1100.000	478.500	-18.280	-39.750	-221.400	0.164	0.546

DAILY TOTAL ENERGY DENSITY

	(HR)	(MJ/M2)	(MJ/M2)	(MJ/M2)	(MJ/M2)	(MM)	
190.000	2400.000	15.504	1.634	-0.357	-11.144	4.604	0.628

MEAN HALF-HOURLY ENERGY FLUX DENSITY

DAY	TIME	RN	H	G	LE	ET	CLOSURE
	(HR)	(W/M2)	(W/M2)	(W/M2)	(W/M2)	(MM)	
195.000	1430.000	655.600	4.192	-72.483	-407.400	0.303	0.691
195.000	1500.000	640.200	-3.056	-66.683	-351.500	0.262	0.618
195.000	1530.000	619.800	13.400	-52.577	-338.900	0.252	0.574
195.000	1600.000	585.500	17.880	-50.567	-321.000	0.239	0.567
195.000	1630.000	527.200	42.460	-44.533	-373.800	0.278	0.686
195.000	1700.000	480.500	59.660	-33.983	-314.600	0.234	0.571
195.000	1730.000	420.400	76.400	-21.632	-346.900	0.258	0.678
195.000	1800.000	353.600	74.800	-15.918	-310.700	0.231	0.699
195.000	1830.000	275.800	82.400	-6.475	-249.300	0.186	0.620
195.000	1900.000	198.600	97.700	5.772	-185.700	0.138	0.431
195.000	1930.000	119.500	95.800	13.227	-138.500	0.103	0.322
195.000	2000.000	41.080	92.200	19.993	-139.300	0.104	0.771
195.000	2030.000	-24.770	57.070	23.570	-65.410	0.049	-6.950
195.000	2100.000	-64.440	60.620	28.643	-68.560	0.051	-0.222
195.000	2130.000	-71.100	51.390	30.297	-48.960	0.036	0.060
195.000	2200.000	-71.800	46.250	30.837	-47.910	0.035	-0.041
195.000	2230.000	-68.830	43.650	29.870	-41.780	0.031	0.048
195.000	2300.000	-68.320	47.460	29.237	-50.240	0.037	-0.071
195.000	2330.000	-68.260	52.280	28.400	-51.010	0.038	0.032
196.000	0.000	-67.790	51.360	27.383	-50.340	0.037	0.025
196.000	30.000	-66.990	45.450	26.073	-41.220	0.030	0.103
196.000	100.000	-65.760	47.840	25.000	-42.490	0.031	0.131
196.000	130.000	-65.180	39.230	24.337	-37.140	0.027	0.051
196.000	200.000	-65.030	47.210	23.473	-41.650	0.031	0.134
196.000	230.000	-64.610	42.340	23.143	-40.050	0.030	0.055
196.000	300.000	-63.530	37.890	22.507	-34.320	0.025	0.087
196.000	330.000	-63.440	26.370	22.450	-23.790	0.018	0.063
196.000	400.000	-62.680	20.490	22.597	-19.610	0.014	0.022
196.000	430.000	-62.430	27.770	22.253	-25.280	0.019	0.062
196.000	500.000	-64.020	34.470	21.670	-30.320	0.022	0.098
196.000	530.000	-65.600	32.660	21.630	-29.070	0.021	0.082
196.000	600.000	-66.040	21.930	21.833	-20.480	0.015	0.033
196.000	630.000	-65.510	22.470	22.020	-20.630	0.015	0.042
196.000	700.000	-50.130	22.280	21.103	-25.930	0.019	-0.126
196.000	730.000	-4.072	15.680	17.017	-33.070	0.024	1.343
196.000	800.000	66.860	10.190	9.518	-62.880	0.046	0.690
196.000	830.000	145.400	2.675	-5.569	-78.900	0.058	0.545
196.000	900.000	231.100	15.850	-22.210	-139.500	0.103	0.592
196.000	930.000	314.600	34.350	-32.403	-186.300	0.138	0.538
196.000	1000.000	390.200	36.440	-36.230	-219.700	0.163	0.518
196.000	1030.000	458.100	17.950	-47.837	-263.700	0.196	0.599
196.000	1100.000	518.400	6.525	-54.423	-250.400	0.186	0.526
196.000	1130.000	567.700	6.827	-55.300	-287.900	0.214	0.549
196.000	1200.000	607.900	-5.746	-58.140	-287.000	0.213	0.532
196.000	1230.000	645.300	-10.980	-66.923	-348.200	0.259	0.621
196.000	1300.000	644.700	3.749	-73.957	-334.400	0.249	0.579
196.000	1330.000	651.000	-6.742	-70.727	-293.700	0.219	0.518
196.000	1400.000	670.100	-3.928	-67.137	-399.900	0.298	0.670

DAILY TOTAL ENERGY DENSITY

	(HR)	(MJ/M2)	(MJ/M2)	(MJ/M2)	(MJ/M2)	(MM)	
195.000	2400.000	16.972	2.979	-0.615	-13.535	5.587	0.645

MEAN HALF-HOURLY ENERGY FLUX DENSITY

DAY	TIME	RN	H	G	LE	ET	CLOSURE
	(HR)	(W/M2)	(W/M2)	(W/M2)	(W/M2)	(MM)	
196.000	1430.000	691.400	3.963	-82.627	-365.200	0.272	0.593
196.000	1500.000	670.000	-0.096	-83.830	-388.400	0.289	0.663
196.000	1530.000	616.100	4.235	-62.157	-358.600	0.267	0.640
196.000	1600.000	623.500	23.150	-67.583	-339.400	0.253	0.569
196.000	1630.000	500.500	58.360	-58.977	-302.400	0.225	0.553
196.000	1700.000	498.200	61.500	-50.797	-358.200	0.267	0.663
196.000	1730.000	426.700	81.900	-39.667	-315.400	0.235	0.603
196.000	1800.000	355.000	105.200	-24.095	-315.300	0.235	0.635
196.000	1830.000	277.300	124.900	-7.422	-271.000	0.202	0.541
196.000	1900.000	195.600	125.100	5.149	-339.900	0.253	1.070
196.000	1930.000	114.900	111.100	11.669	-185.100	0.138	0.585
196.000	2000.000	37.050	114.800	16.503	-160.700	0.119	0.857
196.000	2030.000	-30.090	96.700	20.280	-111.100	0.083	-1.468
196.000	2100.000	-69.570	88.200	22.313	-86.200	0.064	0.042
196.000	2130.000	-76.000	69.250	22.953	-60.020	0.044	0.174
196.000	2200.000	-72.300	55.010	23.043	-48.620	0.036	0.130
196.000	2230.000	-70.000	55.240	23.000	-47.470	0.035	0.165
196.000	2300.000	-70.500	59.320	21.183	-51.260	0.038	0.163
196.000	2330.000	-70.800	61.480	19.837	-50.070	0.037	0.224
197.000	0.000	-69.580	53.940	19.913	-44.690	0.033	0.186
197.000	30.000	-68.640	53.930	19.827	-46.270	0.034	0.157
197.000	100.000	-68.150	48.640	19.507	-39.790	0.029	0.182
197.000	130.000	-67.890	47.000	18.587	-40.690	0.030	0.128
197.000	200.000	-67.860	46.920	18.120	-41.450	0.031	0.110
197.000	230.000	-66.880	43.370	17.813	-37.360	0.028	0.122
197.000	300.000	-66.540	38.350	17.997	-32.060	0.024	0.130
197.000	330.000	-66.670	29.130	18.477	-26.940	0.020	0.045
197.000	400.000	-66.480	27.120	18.457	-22.510	0.017	0.096
197.000	430.000	-66.170	29.990	18.173	-26.650	0.020	0.070
197.000	500.000	-65.320	28.640	18.243	-27.280	0.020	0.029
197.000	530.000	-64.900	29.690	18.327	-28.780	0.021	0.020
197.000	600.000	-63.900	26.890	18.537	-27.270	0.020	-0.008
197.000	630.000	-61.940	22.760	18.687	-24.440	0.018	-0.039
197.000	700.000	-46.650	25.840	17.907	-35.580	0.026	-0.339
197.000	730.000	1.274	15.770	14.657	-44.980	0.033	1.834
197.000	800.000	74.400	4.013	9.447	-67.770	0.050	0.760
197.000	830.000	154.800	-1.277	-0.317	-107.600	0.079	0.705
197.000	900.000	236.800	-10.240	-14.513	-154.300	0.114	0.740
197.000	930.000	317.500	-8.480	-30.950	-169.000	0.125	0.619
197.000	1000.000	392.000	-6.390	-43.540	-235.200	0.174	0.693
197.000	1030.000	459.800	-8.910	-53.977	-246.800	0.183	0.630
197.000	1100.000	519.100	-14.100	-61.777	-295.300	0.219	0.677
197.000	1130.000	570.400	-7.920	-58.393	-300.900	0.223	0.603
197.000	1200.000	611.000	-14.850	-58.300	-336.600	0.250	0.636
197.000	1230.000	642.800	-10.210	-65.173	-387.600	0.288	0.689
197.000	1300.000	663.000	-5.898	-76.617	-342.000	0.254	0.593
197.000	1330.000	676.900	3.865	-67.383	-352.300	0.262	0.572
197.000	1400.000	683.100	3.736	-69.127	-434.800	0.324	0.702

DAILY TOTAL ENERGY DENSITY

	(HR)	(MJ/M2)	(MJ/M2)	(MJ/M2)	(MJ/M2)	(MM)	
196.000	2400.000	17.230	3.223	-1.060	-14.636	6.043	0.706

MEAN HALF-HOURLY ENERGY FLUX DENSITY

DAY	TIME	RN	H	G	LE	ET	CLOSURE
	(HR)	(W/M2)	(W/M2)	(W/M2)	(W/M2)	(MM)	
197.000	1430.000	671.900	4.897	-82.253	-380.600	0.283	0.637
197.000	1500.000	652.400	20.480	-80.953	-390.000	0.291	0.647
197.000	1530.000	629.700	24.120	-60.537	-343.000	0.256	0.560
197.000	1600.000	590.900	38.000	-66.257	-364.500	0.272	0.622
197.000	1630.000	541.000	48.240	-65.980	-354.800	0.264	0.645
197.000	1700.000	486.200	70.100	-57.227	-342.700	0.255	0.635
197.000	1730.000	424.000	81.100	-41.554	-363.300	0.271	0.738
197.000	1800.000	356.400	103.600	-22.308	-331.000	0.247	0.681
197.000	1830.000	281.900	105.200	-9.688	-217.300	0.162	0.412
197.000	1900.000	204.600	127.300	-0.372	-307.700	0.229	0.883
197.000	1930.000	119.900	130.000	7.581	-223.400	0.166	0.733
197.000	2000.000	39.130	129.800	12.479	-197.300	0.147	1.308
197.000	2030.000	-33.390	117.700	16.513	-126.500	0.094	-0.521
197.000	2100.000	-75.100	87.500	20.013	-84.600	0.063	0.053
197.000	2130.000	-84.700	78.900	21.357	-66.880	0.050	0.190
197.000	2200.000	-84.400	84.600	21.060	-69.860	0.052	0.233
197.000	2230.000	-84.300	78.500	20.267	-64.520	0.048	0.218
197.000	2300.000	-82.500	80.400	19.677	-63.710	0.047	0.266
197.000	2330.000	-81.100	73.600	19.447	-60.110	0.044	0.219
198.000	0.000	-79.800	70.200	19.183	-53.100	0.039	0.282
198.000	30.000	-77.900	64.720	18.837	-49.110	0.036	0.264
198.000	100.000	-75.500	59.060	18.497	-43.060	0.032	0.281
198.000	130.000	-72.800	56.310	18.093	-42.040	0.031	0.261
198.000	200.000	-71.700	55.860	17.913	-41.410	0.031	0.269
198.000	230.000	-70.500	47.370	17.973	-34.590	0.026	0.243
198.000	300.000	-69.450	41.630	18.160	-33.630	0.025	0.156
198.000	330.000	-68.460	38.730	18.510	-30.130	0.022	0.172
198.000	400.000	-67.830	34.180	18.787	-28.030	0.021	0.125
198.000	430.000	-67.820	35.550	19.103	-30.010	0.022	0.114
198.000	500.000	-67.320	32.000	19.180	-27.510	0.020	0.093
198.000	530.000	-66.500	27.620	19.320	-25.840	0.019	0.038
198.000	600.000	-65.480	30.200	19.490	-27.400	0.020	0.061
198.000	630.000	-63.830	24.510	19.470	-25.730	0.019	-0.028
198.000	700.000	-48.940	27.200	18.600	-36.820	0.027	-0.317
198.000	730.000	-0.001	14.370	15.423	-34.870	0.026	1.329
198.000	800.000	72.000	12.630	10.527	-81.800	0.060	0.838
198.000	830.000	153.200	9.930	1.800	-133.100	0.098	0.795
198.000	900.000	233.600	-0.485	-12.318	-153.900	0.114	0.698
198.000	930.000	314.200	6.369	-27.057	-220.400	0.163	0.745
198.000	1000.000	389.300	-2.534	-38.957	-234.900	0.174	0.678
198.000	1030.000	456.000	-19.390	-52.653	-271.400	0.201	0.721
198.000	1100.000	516.800	-6.987	-61.533	-295.600	0.219	0.665
198.000	1130.000	568.900	9.800	-60.090	-324.800	0.241	0.619
198.000	1200.000	608.000	9.680	-59.487	-338.200	0.251	0.599
198.000	1230.000	637.000	8.830	-69.053	-361.800	0.269	0.621
198.000	1300.000	669.100	1.554	-82.427	-406.700	0.302	0.691
198.000	1330.000	660.400	16.590	-76.507	-416.000	0.310	0.684
198.000	1400.000	653.200	25.200	-78.043	-388.900	0.289	0.632

DAILY TOTAL ENERGY DENSITY

	(HR)	(MJ/M2)	(MJ/M2)	(MJ/M2)	(MJ/M2)	(MM)	
197.000	2400.000	16.867	3.987	-1.148	-15.377	6.348	0.725

MEAN HALF-HOURLY ENERGY FLUX DENSITY

DAY	TIME	RN	H	G	LE	ET	CLOSURE
	(HR)	(W/M2)	(W/M2)	(W/M2)	(W/M2)	(MM)	
198.000	1630.000	503.400	53.020	-32.300	-230.400	0.172	0.377
198.000	1700.000	470.300	57.110	-35.657	-326.100	0.243	0.619
198.000	1730.000	413.500	63.190	-27.127	-254.900	0.190	0.496
198.000	1800.000	346.600	63.370	-12.050	-299.600	0.223	0.706
198.000	1830.000	274.000	67.210	-4.669	-221.300	0.165	0.572
198.000	1900.000	196.100	64.510	-2.427	-208.900	0.156	0.746
198.000	1930.000	116.200	83.600	-0.265	-150.600	0.112	0.578
198.000	2000.000	35.150	84.300	2.143	-93.100	0.069	0.236
198.000	2030.000	-34.370	70.600	5.520	-83.000	0.062	-0.430
198.000	2100.000	-70.700	66.110	8.517	-45.390	0.034	0.333
198.000	2130.000	-74.300	61.160	10.997	-40.830	0.030	0.321
198.000	2200.000	-71.600	48.580	12.443	-31.940	0.024	0.281
198.000	2230.000	-69.490	51.130	14.100	-32.000	0.024	0.345
198.000	2300.000	-68.410	46.330	13.947	-29.670	0.022	0.306
198.000	2330.000	-67.240	43.840	14.030	-27.550	0.020	0.306
199.000	0.000	-66.230	41.990	14.250	-27.310	0.020	0.282
199.000	30.000	-66.470	50.590	14.613	-32.210	0.024	0.354
199.000	100.000	-67.520	46.810	14.497	-29.540	0.022	0.326
199.000	130.000	-68.020	46.970	15.280	-29.810	0.022	0.325
199.000	200.000	-68.540	48.950	16.157	-30.150	0.022	0.359
199.000	230.000	-67.250	36.800	16.360	-23.830	0.018	0.255
199.000	300.000	-65.760	31.840	17.423	-20.020	0.015	0.245
199.000	330.000	-64.260	30.400	17.870	-20.130	0.015	0.221
199.000	400.000	-62.780	29.260	17.503	-19.480	0.014	0.216
199.000	430.000	-61.890	25.520	17.937	-18.140	0.013	0.168
199.000	500.000	-62.170	24.560	18.387	-17.840	0.013	0.153
199.000	530.000	-61.980	22.880	19.327	-17.670	0.013	0.122
199.000	600.000	-60.300	16.140	20.370	-15.030	0.011	0.028
199.000	630.000	-59.960	17.150	21.327	-16.350	0.012	0.021
199.000	700.000	-48.550	12.530	20.703	-15.260	0.011	-0.098
199.000	730.000	-8.370	9.650	16.717	-28.060	0.021	2.206
199.000	800.000	50.180	0.567	10.790	-46.240	0.034	0.749
199.000	830.000	143.700	-10.120	3.362	-69.830	0.052	0.544
199.000	900.000	229.400	-18.170	-4.122	-97.800	0.072	0.515
199.000	930.000	303.100	18.750	-9.248	-207.100	0.153	0.641
199.000	1000.000	370.300	4.469	-23.020	-219.700	0.163	0.620
199.000	1030.000	434.900	11.720	-41.297	-249.400	0.185	0.604
199.000	1100.000	492.700	14.200	-48.140	-275.900	0.205	0.589
199.000	1130.000	542.800	17.110	-53.533	-306.400	0.228	0.591
199.000	1200.000	583.700	17.070	-60.697	-343.000	0.255	0.623
199.000	1230.000	616.100	0.521	-69.487	-368.800	0.274	0.674
199.000	1300.000	636.900	-3.081	-71.980	-330.300	0.246	0.590
199.000	1330.000	649.200	-2.991	-72.627	-394.000	0.294	0.689
199.000	1400.000	653.200	11.590	-72.133	-381.500	0.284	0.637
199.000	1430.000	645.400	6.017	-72.747	-402.800	0.300	0.693
199.000	1500.000	631.500	19.460	-70.010	-338.300	0.252	0.568
199.000	1530.000	605.000	15.730	-67.863	-336.300	0.251	0.597
199.000	1600.000	570.800	33.600	-62.557	-359.000	0.268	0.640

DAILY TOTAL ENERGY DENSITY

	(HR)	(MJ/M2)	(MJ/M2)	(MJ/M2)	(MJ/M2)	(MM)	
198.000	2400.000	16.376	2.795	-0.971	-12.892	5.327	0.655

MEAN HALF-HOURLY ENERGY FLUX DENSITY

DAY	TIME	RN	H	G	LE	ET	CLOSURE
	(HR)	(W/M2)	(W/M2)	(W/M2)	(W/M2)	(MM)	
209.000	1730.000	421.300	218.800	-4.473	-500.900	0.374	0.677
209.000	1800.000	344.000	152.900	3.321	-339.300	0.253	0.537
209.000	1830.000	272.700	140.100	9.263	-284.000	0.212	0.510
209.000	1900.000	195.700	166.400	16.108	-391.300	0.292	1.062
209.000	1930.000	108.400	191.700	26.190	-230.500	0.172	0.288
209.000	2000.000	13.550	148.500	26.960	-154.000	0.115	0.136
209.000	2030.000	-48.320	118.400	30.650	-98.700	0.074	1.115
209.000	2100.000	-77.600	97.600	34.507	-46.890	0.035	1.177
209.000	2130.000	-81.700	92.500	34.387	-59.830	0.044	0.691
209.000	2200.000	-80.700	81.400	34.993	-43.260	0.032	0.834
209.000	2230.000	-81.400	84.000	37.197	-91.100	0.068	-0.161
209.000	2300.000	-81.900	98.100	37.437	-73.700	0.055	0.549
209.000	2330.000	-83.100	92.400	38.187	-26.050	0.019	1.477
210.000	0.000	-82.500	92.600	36.793	-85.400	0.063	0.158
210.000	30.000	-80.100	93.900	34.743	-48.200	0.036	1.008
210.000	100.000	-74.900	73.500	31.560	-63.280	0.047	0.236
210.000	130.000	-74.700	70.700	31.377	-42.720	0.032	0.646
210.000	200.000	-74.000	78.200	30.807	-53.130	0.039	0.580
210.000	230.000	-72.900	69.390	29.773	-36.560	0.027	0.761
210.000	300.000	-73.700	66.570	29.977	-59.660	0.044	0.158
210.000	330.000	-73.700	63.540	29.340	-54.810	0.041	0.197
210.000	400.000	-67.050	40.290	27.960	-19.730	0.015	0.526
210.000	430.000	-67.800	43.800	28.360	-25.690	0.019	0.459
210.000	500.000	-63.080	41.510	28.003	-29.810	0.022	0.334
210.000	530.000	-64.200	28.530	28.410	-15.370	0.011	0.368
210.000	600.000	-53.880	10.080	28.030	-9.830	0.007	0.010
210.000	630.000	-51.010	23.220	29.113	-20.880	0.015	0.107
210.000	700.000	-38.770	5.689	29.177	1.327	0.000	0.731
210.000	730.000	-3.738	2.499	23.577	-8.620	0.006	0.309
210.000	800.000	48.960	11.220	13.240	-32.040	0.024	0.335
210.000	830.000	115.600	8.560	2.685	-32.460	0.024	0.202
210.000	900.000	195.200	17.150	-3.554	-106.100	0.079	0.464
210.000	930.000	273.600	36.630	-12.120	-189.000	0.140	0.583
210.000	1000.000	358.200	127.000	-11.870	-324.700	0.241	0.571
210.000	1030.000	430.500	136.000	-27.200	-328.500	0.244	0.477
210.000	1100.000	497.500	140.500	-34.810	-343.300	0.255	0.438
210.000	1130.000	559.500	175.900	-50.203	-418.300	0.311	0.476
210.000	1200.000	612.100	188.900	-68.700	-478.800	0.356	0.533
210.000	1230.000	654.900	182.600	-77.203	-491.300	0.366	0.534
210.000	1300.000	682.900	172.400	-85.663	-457.000	0.341	0.477
210.000	1330.000	701.000	168.500	-106.433	-481.600	0.359	0.527
210.000	1400.000	705.000	154.200	-112.530	-453.100	0.338	0.504
210.000	1430.000	697.600	159.500	-84.770	-407.500	0.304	0.405
210.000	1500.000	678.400	145.600	-61.360	-415.700	0.310	0.438
210.000	1530.000	648.400	174.300	-50.600	-424.000	0.317	0.418
210.000	1600.000	607.200	171.900	-45.720	-484.100	0.362	0.556
210.000	1630.000	553.200	157.500	-42.223	-465.600	0.348	0.603
210.000	1700.000	495.300	195.000	-21.927	-489.800	0.366	0.623

DAILY TOTAL ENERGY DENSITY

	(HR)	(MJ/M2)	(MJ/M2)	(MJ/M2)	(MJ/M2)	(MM)	
209.000	2400.000	16.776	9.018	-0.143	-17.523	7.254	0.511

MEAN HALF-HOURLY ENERGY FLUX DENSITY

DAY	TIME	RN	H	G	LE	ET	CLOSURE
	(HR)	(W/M2)	(W/M2)	(W/M2)	(W/M2)	(MM)	
210.000	1730.000	428.800	205.300	-2.241	-416.900	0.311	0.496
210.000	1800.000	352.200	171.600	7.779	-321.400	0.240	0.416
210.000	1830.000	275.700	152.800	9.448	-242.300	0.181	0.314
210.000	1900.000	196.000	151.600	17.583	-239.100	0.178	0.410
210.000	1930.000	112.200	158.800	23.373	-218.000	0.162	0.437
210.000	2000.000	23.320	79.400	21.010	-98.000	0.073	0.420
210.000	2030.000	-32.670	61.540	25.000	-46.750	0.035	1.928
210.000	2100.000	-51.330	27.260	27.570	-20.820	0.015	0.271
210.000	2130.000	-56.490	14.910	29.920	-7.780	0.006	0.268
210.000	2200.000	-62.220	30.720	30.240	-18.570	0.014	0.380
210.000	2230.000	-51.280	15.360	30.160	-15.970	0.012	-0.029
210.000	2300.000	-49.480	14.200	30.833	-11.060	0.008	0.168
210.000	2330.000	-62.560	32.500	30.367	-17.960	0.013	0.452
211.000	0.000	-60.320	42.890	30.643	-26.980	0.020	0.536
211.000	30.000	-72.900	90.600	34.370	-60.690	0.045	0.776
211.000	100.000	-76.200	93.300	33.703	-63.340	0.047	0.705
211.000	130.000	-75.800	89.800	31.363	-57.940	0.043	0.717
211.000	200.000	-79.100	97.700	32.007	-65.650	0.049	0.681
211.000	230.000	-77.300	92.800	30.150	-63.830	0.047	0.614
211.000	300.000	-77.100	100.700	29.600	-66.150	0.049	0.727
211.000	330.000	-72.400	71.000	27.310	-46.700	0.035	0.539
211.000	400.000	-70.800	67.310	27.063	-44.610	0.033	0.519
211.000	430.000	-66.380	48.160	26.883	-31.350	0.023	0.426
211.000	500.000	-67.500	59.920	27.190	-40.350	0.030	0.485
211.000	530.000	-69.040	65.010	27.900	-43.130	0.032	0.532
211.000	600.000	-59.480	30.710	26.207	-21.690	0.016	0.271
211.000	630.000	-55.210	37.950	26.807	-25.620	0.019	0.434
211.000	700.000	-48.260	36.660	25.693	-28.180	0.021	0.376
211.000	730.000	-4.499	54.610	21.900	-61.320	0.045	0.386
211.000	800.000	56.450	28.740	14.620	-44.520	0.033	0.222
211.000	830.000	122.400	7.560	2.996	-53.390	0.040	0.365
211.000	900.000	206.500	56.000	-1.445	-171.700	0.127	0.564
211.000	930.000	291.600	120.600	-2.265	-279.500	0.207	0.549
211.000	1000.000	368.300	195.000	-5.716	-420.900	0.312	0.623
211.000	1030.000	443.700	241.500	-16.797	-442.900	0.329	0.472
211.000	1100.000	512.400	263.300	-24.820	-526.000	0.391	0.539
211.000	1130.000	573.000	260.900	-40.557	-530.200	0.395	0.506
211.000	1200.000	621.900	262.900	-62.067	-588.700	0.439	0.582
211.000	1230.000	660.500	228.500	-69.997	-506.700	0.378	0.471
211.000	1300.000	688.900	237.000	-74.167	-535.100	0.399	0.485
211.000	1330.000	706.000	245.500	-87.153	-552.600	0.412	0.496
211.000	1400.000	709.000	220.700	-91.307	-561.000	0.419	0.551
211.000	1430.000	699.400	248.400	-66.450	-539.500	0.403	0.460
211.000	1500.000	676.900	248.100	-43.413	-540.600	0.404	0.462
211.000	1530.000	643.000	267.800	-32.440	-591.500	0.442	0.530
211.000	1600.000	598.300	276.800	-33.047	-523.200	0.391	0.436
211.000	1630.000	544.900	283.100	-28.797	-537.400	0.402	0.493
211.000	1700.000	484.000	280.000	-10.188	-534.800	0.400	0.538

DAILY TOTAL ENERGY DENSITY

	(HR)	(MJ/M2)	(MJ/M2)	(MJ/M2)	(MJ/M2)	(MM)	
210.000	2400.000	17.275	11.102	0.120	-19.624	8.123	0.490

MEAN HALF-HOURLY ENERGY FLUX DENSITY

DAY	TIME	RN	H	G	LE	ET	CLOSURE
	(HR)	(W/M2)	(W/M2)	(W/M2)	(W/M2)	(MM)	
211.000	1730.000	424.100	289.900	4.783	-558.000	0.417	0.625
211.000	1800.000	359.500	290.500	16.169	-528.400	0.395	0.633
211.000	1830.000	275.200	243.800	19.168	-356.000	0.266	0.381
211.000	1900.000	187.800	248.700	22.670	-304.000	0.227	0.263
211.000	1930.000	98.700	203.800	23.843	-227.700	0.170	0.195
211.000	2000.000	-1.645	155.200	24.783	-205.400	0.153	2.170
211.000	2030.000	-51.350	83.900	24.563	-87.100	0.065	-0.119
211.000	2100.000	-62.550	49.150	25.903	-38.860	0.029	0.281
211.000	2130.000	-66.250	31.210	26.883	-23.000	0.017	0.209
211.000	2200.000	-70.300	44.620	26.713	-24.860	0.018	0.453
211.000	2230.000	-73.300	55.410	28.527	-29.250	0.022	0.584
211.000	2300.000	-69.960	51.130	28.970	-29.500	0.022	0.528
211.000	2330.000	-74.000	60.760	29.243	-36.060	0.027	0.552
212.000	0.000	-80.800	89.800	31.757	-53.950	0.040	0.731
212.000	30.000	-86.400	97.000	33.323	-61.490	0.046	0.669
212.000	100.000	-80.200	77.000	30.317	-47.890	0.035	0.584
212.000	130.000	-71.300	59.810	28.437	-37.210	0.028	0.527
212.000	200.000	-72.400	70.600	27.533	-42.490	0.031	0.627
212.000	230.000	-72.100	65.620	25.543	-39.140	0.029	0.569
212.000	300.000	-72.300	61.250	24.860	-39.110	0.029	0.467
212.000	330.000	-57.820	22.780	23.790	-16.750	0.012	0.177
212.000	400.000	-53.640	24.390	24.823	-16.950	0.013	0.258
212.000	430.000	-62.530	44.990	25.483	-30.720	0.023	0.385
212.000	500.000	-50.250	5.594	25.860	-4.292	0.003	0.053
212.000	530.000	-47.620	5.928	25.860	-8.250	0.006	-0.107
212.000	600.000	-45.910	13.270	26.630	-18.090	0.013	-0.250
212.000	630.000	-46.220	11.750	27.527	-15.380	0.011	-0.194
212.000	700.000	-35.440	0.597	25.520	-1.516	0.001	-0.093
212.000	730.000	-3.971	-0.850	21.530	-2.604	0.002	0.197
212.000	800.000	55.870	13.220	12.340	-31.600	0.023	0.269
212.000	830.000	139.400	44.020	7.369	-98.400	0.073	0.371
212.000	900.000	225.300	109.900	7.220	-220.400	0.163	0.475
212.000	930.000	305.800	128.800	2.263	-272.000	0.201	0.465
212.000	1000.000	382.700	131.900	-6.567	-290.800	0.216	0.422
212.000	1030.000	441.900	136.500	-18.693	-308.700	0.229	0.407
212.000	1100.000	560.000	108.000	-38.467	-409.900	0.305	0.579
212.000	1130.000	530.500	69.700	-48.600	-364.600	0.271	0.612
212.000	1200.000	616.700	54.530	-80.367	-397.900	0.296	0.640
212.000	1230.000	647.400	61.000	-95.857	-367.200	0.273	0.555
212.000	1300.000	680.000	74.700	-100.117	-376.400	0.280	0.520
212.000	1330.000	701.000	67.040	-109.717	-383.500	0.286	0.535
212.000	1400.000	706.000	56.560	-115.453	-347.700	0.260	0.493
212.000	1430.000	708.000	56.450	-80.617	-347.200	0.259	0.463
212.000	1500.000	595.200	68.740	-55.250	-314.100	0.235	0.454
212.000	1530.000	431.400	88.700	-27.920	-249.600	0.186	0.399
212.000	1600.000	570.300	122.000	-24.580	-374.400	0.279	0.463
212.000	1630.000	285.300	37.600	-22.850	-153.400	0.114	0.441
212.000	1700.000	106.500	63.260	1.385	-106.600	0.079	0.402

DAILY TOTAL ENERGY DENSITY

	(HR)	(MJ/M2)	(MJ/M2)	(MJ/M2)	(MJ/M2)	(MM)	
211.000	2400.000	15.527	7.110	-0.114	-14.937	6.178	0.508

MEAN HALF-HOURLY ENERGY FLUX DENSITY

DAY	TIME	RN	H	G	LE	ET	CLOSURE
	(HR)	(W/M2)	(W/M2)	(W/M2)	(W/M2)	(MM)	
223.000	1630.000	528.700	6.030	-16.143	-304.000	0.226	0.581
223.000	1700.000	445.600	25.490	-12.853	-265.800	0.197	0.555
223.000	1730.000	391.300	33.240	-7.787	-278.200	0.206	0.639
223.000	1800.000	315.200	28.970	-5.207	-210.700	0.156	0.586
223.000	1830.000	223.800	33.500	-3.069	-159.300	0.118	0.570
223.000	1900.000	146.000	45.060	0.513	-114.200	0.085	0.472
223.000	1930.000	51.980	45.500	3.051	-102.400	0.076	1.034
223.000	2000.000	-15.220	25.010	3.951	-34.870	0.026	-0.875
223.000	2030.000	-47.990	27.150	5.613	-15.750	0.012	0.269
223.000	2100.000	-57.270	17.070	7.722	-8.280	0.006	0.177
223.000	2130.000	-59.320	18.180	9.297	-9.760	0.007	0.168
223.000	2200.000	-57.550	11.330	9.996	-1.254	0.001	0.212
223.000	2230.000	-58.880	18.040	11.033	-6.109	0.004	0.249
223.000	2300.000	-58.680	24.260	11.423	-10.970	0.008	0.281
223.000	2330.000	-58.160	22.310	11.733	-9.400	0.007	0.278
224.000	0.000	-56.220	28.230	11.770	-11.320	0.008	0.380
224.000	30.000	-55.300	30.260	11.437	-14.870	0.011	0.351
224.000	100.000	-54.130	22.320	10.960	-9.360	0.007	0.300
224.000	130.000	-52.060	29.700	10.843	-9.170	0.007	0.498
224.000	200.000	-53.770	18.690	11.007	-5.236	0.004	0.315
224.000	230.000	-54.220	19.040	10.943	-3.139	0.002	0.367
224.000	300.000	-54.490	17.520	11.060	-2.924	0.002	0.336
224.000	330.000	-56.510	17.510	11.557	-2.513	0.002	0.334
224.000	400.000	-56.240	16.020	11.700	-0.036	0.000	0.359
224.000	430.000	-57.030	13.360	12.060	0.160	0.000	0.301
224.000	500.000	-57.150	14.630	12.733	-1.807	0.001	0.289
224.000	530.000	-55.300	14.040	13.047	5.291	0.000	0.458
224.000	600.000	-54.780	13.630	12.950	2.207	0.000	0.379
224.000	630.000	-53.740	10.880	12.507	8.880	0.000	0.479
224.000	700.000	-51.260	12.000	11.900	11.720	0.000	0.603
224.000	730.000	-29.310	7.510	9.537	6.203	0.000	0.694
224.000	800.000	27.460	8.350	5.687	-16.130	0.012	0.235
224.000	830.000	95.800	-11.130	1.622	-39.220	0.029	0.517
224.000	900.000	170.100	-14.780	-2.591	-79.900	0.059	0.565
224.000	930.000	244.100	-17.880	-7.890	-83.200	0.061	0.428
224.000	1000.000	321.300	-36.600	-13.210	-152.300	0.113	0.613
224.000	1030.000	387.900	-43.000	-16.177	-203.500	0.151	0.663
224.000	1100.000	452.600	-33.530	-17.613	-229.900	0.170	0.606
224.000	1130.000	508.100	-25.190	-18.207	-268.900	0.199	0.600
224.000	1200.000	555.900	-26.130	-19.977	-352.400	0.261	0.706
224.000	1230.000	573.000	-17.990	-20.597	-346.200	0.257	0.659
224.000	1300.000	597.600	-9.040	-20.650	-354.300	0.263	0.630
224.000	1330.000	633.500	-4.852	-23.737	-378.200	0.281	0.628
224.000	1400.000	645.100	4.103	-22.987	-536.500	0.398	0.856
224.000	1430.000	640.600	10.460	-22.493	-470.600	0.349	0.744
224.000	1500.000	628.400	22.230	-21.080	-354.200	0.263	0.547
224.000	1530.000	609.500	27.730	-24.930	-403.300	0.300	0.642
224.000	1600.000	577.200	39.350	-13.393	-336.700	0.250	0.527

DAILY TOTAL ENERGY DENSITY

	(HR)	(MJ/M2)	(MJ/M2)	(MJ/M2)	(MJ/M2)	(MM)	
223.000	2400.000	15.311	0.969	-0.077	-11.092	4.595	0.664

MEAN HALF-HOURLY ENERGY FLUX DENSITY

DAY	TIME	RN	H	G	LE	ET	CLOSURE
	(HR)	(W/M2)	(W/M2)	(W/M2)	(W/M2)	(MM)	
224.000	1630.000	518.100	48.220	-10.103	-372.600	0.277	0.639
224.000	1700.000	456.900	73.200	-5.386	-372.700	0.277	0.663
224.000	1730.000	383.500	92.900	-0.153	-337.200	0.250	0.637
224.000	1800.000	308.000	92.000	3.596	-241.900	0.180	0.481
224.000	1830.000	231.600	110.000	8.955	-283.500	0.211	0.721
224.000	1900.000	147.100	91.100	8.536	-216.400	0.161	0.805
224.000	1930.000	48.200	85.600	8.939	-145.400	0.108	1.047
224.000	2000.000	-17.690	87.200	9.672	-84.800	0.063	0.299
224.000	2030.000	-55.250	69.360	10.062	-46.470	0.034	0.507
224.000	2100.000	-65.110	65.190	11.778	-41.510	0.031	0.444
224.000	2130.000	-67.210	64.040	13.757	-47.250	0.035	0.314
224.000	2200.000	-66.960	73.700	15.557	-54.310	0.040	0.377
224.000	2230.000	-63.880	58.680	15.377	-40.500	0.030	0.375
224.000	2300.000	-62.040	68.360	15.197	-46.920	0.035	0.458
224.000	2330.000	-65.750	62.020	15.330	-41.280	0.030	0.411
225.000	0.000	-63.900	37.820	14.677	-23.370	0.017	0.294
225.000	30.000	-59.340	41.740	14.047	-25.840	0.019	0.351
225.000	100.000	-59.410	43.210	13.367	-24.030	0.018	0.417
225.000	130.000	-63.240	33.960	13.220	-18.880	0.014	0.301
225.000	200.000	-62.670	27.750	12.883	-14.680	0.011	0.263
225.000	230.000	-59.820	25.990	12.457	-15.510	0.011	0.221
225.000	300.000	-56.080	26.230	12.450	-16.070	0.012	0.233
225.000	330.000	-52.760	34.190	12.353	-23.680	0.017	0.260
225.000	400.000	-51.250	34.620	11.400	-23.370	0.017	0.282
225.000	430.000	-53.750	43.530	11.440	-27.240	0.020	0.385
225.000	500.000	-55.290	38.330	11.740	-25.460	0.019	0.296
225.000	530.000	-54.470	29.540	12.147	-21.580	0.016	0.188
225.000	600.000	-54.230	29.260	12.420	-23.230	0.017	0.144
225.000	630.000	-55.640	30.310	12.767	-26.490	0.019	0.089
225.000	700.000	-53.060	22.660	11.793	-20.800	0.015	0.045
225.000	730.000	-40.000	20.420	10.877	-23.280	0.017	-0.098
225.000	800.000	27.930	10.910	8.163	-33.190	0.024	0.617
225.000	830.000	79.100	4.663	4.848	-64.600	0.048	0.714
225.000	900.000	166.000	-15.820	1.739	-91.300	0.067	0.639
225.000	930.000	255.800	-27.750	-3.240	-137.400	0.101	0.654
225.000	1000.000	353.900	-33.040	-9.570	-179.200	0.132	0.616
225.000	1030.000	424.000	-5.344	-12.319	-272.700	0.202	0.675
225.000	1100.000	490.900	-13.750	-13.797	-321.100	0.238	0.702
225.000	1130.000	499.200	-9.060	-16.560	-289.500	0.214	0.619
225.000	1200.000	534.200	35.260	-16.343	-347.600	0.258	0.603
225.000	1230.000	412.500	58.590	-14.940	-267.100	0.198	0.524
225.000	1300.000	385.200	56.180	-11.220	-290.300	0.215	0.626
225.000	1330.000	456.500	58.600	-14.600	-297.200	0.220	0.540
225.000	1400.000	419.600	78.500	-12.400	-254.500	0.189	0.432
225.000	1430.000	597.900	57.070	-20.033	-376.100	0.279	0.552
225.000	1500.000	651.800	62.530	-21.223	-440.100	0.327	0.599
225.000	1530.000	500.900	89.400	-15.303	-365.000	0.271	0.568
225.000	1600.000	408.500	124.500	-10.317	-342.600	0.255	0.548

DAILY TOTAL ENERGY DENSITY

	(HR)	(MJ/M2)	(MJ/M2)	(MJ/M2)	(MJ/M2)	(MM)	
224.000	2400.000	13.317	3.947	0.259	-12.772	5.261	0.650

MEAN HALF-HOURLY ENERGY FLUX DENSITY

DAY	TIME	RN	H	G	LE	ET	CLOSURE
	(HR)	(W/M2)	(W/M2)	(W/M2)	(W/M2)	(MM)	
231.000	730.000	-18.000	10.260	8.367	-4.855	0.004	0.561
231.000	800.000	-1.583	11.700	6.739	-11.240	0.008	-0.089
231.000	830.000	42.690	7.130	4.583	-19.440	0.014	0.260
231.000	900.000	130.200	14.950	0.834	-81.900	0.060	0.511
231.000	930.000	122.700	33.020	-0.860	-64.880	0.048	0.261
231.000	1000.000	196.700	41.650	-4.617	-127.800	0.095	0.449
231.000	1030.000	179.400	34.700	-5.708	-138.500	0.103	0.598
231.000	1100.000	296.900	16.010	-10.463	-169.200	0.125	0.535
231.000	1130.000	372.900	19.100	-16.043	-212.900	0.158	0.543
231.000	1200.000	482.300	-1.799	-18.900	-258.000	0.192	0.561
231.000	1230.000	546.900	11.220	-23.363	-346.000	0.257	0.639
231.000	1300.000	581.400	16.210	-26.650	-404.700	0.301	0.700
231.000	1330.000	601.800	36.280	-29.123	-415.500	0.309	0.662
231.000	1400.000	612.300	49.040	-29.797	-389.300	0.290	0.584
231.000	1430.000	611.800	67.050	-34.440	-416.900	0.311	0.606
231.000	1500.000	606.100	69.280	-25.090	-438.300	0.327	0.635
231.000	1530.000	584.700	85.500	-20.027	-370.400	0.276	0.505
231.000	1600.000	562.100	90.400	-17.903	-406.100	0.303	0.580
231.000	1630.000	419.900	108.100	-13.113	-337.900	0.252	0.565
231.000	1700.000	208.700	139.600	-4.982	-227.100	0.169	0.430
231.000	1730.000	292.500	129.300	-5.025	-319.400	0.238	0.661
231.000	1800.000	218.900	121.700	-4.877	-230.400	0.172	0.508
231.000	1830.000	200.800	109.100	-4.234	-193.900	0.145	0.431
231.000	1900.000	110.600	117.200	-1.652	-247.900	0.185	1.200
231.000	1930.000	53.420	94.700	-0.365	-142.100	0.106	0.893
231.000	2000.000	-21.760	78.300	1.201	-81.500	0.061	-0.156
231.000	2030.000	-40.710	74.700	0.949	-67.770	0.050	0.174
231.000	2100.000	-45.020	59.250	1.887	-31.560	0.023	0.642
231.000	2130.000	-43.540	52.520	2.818	-35.110	0.026	0.428
231.000	2200.000	-45.850	58.850	4.212	-64.540	0.048	-0.137
231.000	2230.000	-46.810	52.970	5.217	-47.220	0.035	0.138
231.000	2300.000	-47.720	67.870	6.576	-44.860	0.033	0.559
231.000	2330.000	-47.480	52.370	7.420	-52.290	0.039	0.002
232.000	0.000	-47.000	38.880	7.341	-14.570	0.011	0.613
232.000	30.000	-44.390	28.080	7.065	-18.040	0.013	0.269
232.000	100.000	-40.360	18.450	7.054	-12.270	0.009	0.186
232.000	130.000	-43.470	24.000	7.760	-13.600	0.010	0.291
232.000	200.000	-46.470	44.220	8.465	-32.080	0.024	0.319
232.000	230.000	-45.860	19.900	8.755	-12.270	0.009	0.206
232.000	300.000	-45.600	13.370	9.040	-8.960	0.007	0.121
232.000	330.000	-45.150	15.470	9.480	-10.570	0.008	0.137
232.000	400.000	-43.650	8.400	9.947	-2.832	0.002	0.165
232.000	430.000	-43.640	5.066	10.407	-1.292	0.001	0.114
232.000	500.000	-45.190	8.150	10.660	-2.692	0.002	0.158
232.000	530.000	-44.320	9.850	11.390	-4.205	0.003	0.171
232.000	600.000	-46.810	13.250	11.107	-8.330	0.006	0.138
232.000	630.000	-49.160	14.650	11.423	-9.990	0.007	0.123
232.000	700.000	-41.480	12.060	10.940	-7.210	0.005	0.159

DAILY TOTAL ENERGY DENSITY

	(HR)	(MJ/M2)	(MJ/M2)	(MJ/M2)	(MJ/M2)	(MM)	
231.000	2400.000	12.608	3.964	-0.190	-11.805	4.879	0.631

MEAN HALF-HOURLY ENERGY FLUX DENSITY

DAY	TIME	RN	H	G	LE	ET	CLOSURE
	(HR)	(W/M2)	(W/M2)	(W/M2)	(W/M2)	(MM)	
232.000	730.000	-16.650	16.650	9.327	-20.820	0.015	-0.569
232.000	800.000	0.780	23.460	8.452	-32.830	0.024	1.015
232.000	830.000	85.200	10.390	5.306	-50.220	0.037	0.440
232.000	900.000	156.100	6.082	2.010	-95.300	0.070	0.564
232.000	930.000	228.300	6.548	-1.231	-163.900	0.121	0.693
232.000	1000.000	301.400	4.876	-5.359	-206.100	0.153	0.680
232.000	1030.000	375.100	2.010	-8.984	-234.900	0.174	0.636
232.000	1100.000	445.100	16.700	-11.477	-280.400	0.208	0.608
232.000	1130.000	507.000	29.560	-11.750	-378.800	0.281	0.705
232.000	1200.000	554.300	38.100	-13.357	-363.600	0.270	0.602
232.000	1230.000	592.400	49.340	-14.800	-392.700	0.292	0.594
232.000	1300.000	550.500	63.760	-13.980	-431.400	0.321	0.685
232.000	1330.000	644.800	52.940	-15.083	-456.200	0.339	0.640
232.000	1400.000	633.000	34.630	-19.257	-440.900	0.328	0.662
232.000	1430.000	629.400	48.850	-19.607	-441.700	0.329	0.644
232.000	1500.000	593.100	36.040	-18.927	-405.400	0.302	0.643
232.000	1530.000	469.400	50.970	-14.177	-357.800	0.267	0.674
232.000	1600.000	451.200	81.900	-11.137	-303.900	0.226	0.504
232.000	1630.000	461.900	57.640	-12.147	-288.000	0.215	0.512
232.000	1700.000	424.000	60.470	-12.323	-306.200	0.228	0.597
232.000	1730.000	338.000	86.400	-6.461	-289.300	0.215	0.612
232.000	1800.000	279.400	66.550	-4.982	-215.900	0.161	0.544
232.000	1830.000	195.400	106.300	-1.872	-197.000	0.147	0.469
232.000	1900.000	109.900	84.900	0.153	-193.300	0.144	0.985
232.000	1930.000	34.330	76.800	0.940	-98.700	0.073	0.621
232.000	2000.000	-26.380	58.510	1.401	-57.970	0.043	0.022
232.000	2030.000	-45.540	42.640	1.507	-32.090	0.024	0.240
232.000	2100.000	-46.200	39.100	3.170	-18.810	0.014	0.472
232.000	2130.000	-40.170	19.480	4.405	-11.350	0.008	0.227
232.000	2200.000	-37.520	22.570	5.534	-10.180	0.008	0.387
232.000	2230.000	-43.970	13.880	6.655	-5.293	0.004	0.230
232.000	2300.000	-46.090	33.430	6.270	-19.400	0.014	0.352
232.000	2330.000	-42.780	25.310	5.654	-10.070	0.007	0.410
233.000	0.000	-40.260	21.410	6.446	-12.420	0.009	0.266
233.000	30.000	-29.320	25.380	6.433	-14.230	0.011	0.487
233.000	100.000	-38.680	33.560	6.410	-24.520	0.018	0.280
233.000	130.000	-40.100	22.980	7.165	-17.550	0.013	0.165
233.000	200.000	-33.360	25.010	6.470	-20.040	0.015	0.185
233.000	230.000	-33.670	4.156	7.127	1.005	0.000	0.194
233.000	300.000	-36.220	4.358	9.723	2.014	0.000	0.240
233.000	330.000	-28.580	3.754	9.789	2.600	0.000	0.338
233.000	400.000	-21.040	-0.906	7.973	4.123	0.000	0.246
233.000	430.000	-20.050	-0.229	7.014	6.127	0.000	0.452
233.000	500.000	-16.950	0.355	6.433	0.000	0.000	0.034
233.000	530.000	-19.320	-0.174	5.987	1.577	0.000	0.105
233.000	600.000	-22.130	-0.319	6.407	7.050	0.000	0.428
233.000	630.000	-16.190	1.135	5.754	0.380	0.000	0.145
233.000	700.000	-12.150	3.280	5.890	-1.602	0.001	0.268

DAILY TOTAL ENERGY DENSITY

	(HR)	(MJ/M2)	(MJ/M2)	(MJ/M2)	(MJ/M2)	(MM)	
232.000	2400.000	14.952	2.719	-0.092	-12.377	5.132	0.650

MEAN HALF-HOURLY ENERGY FLUX DENSITY

DAY	TIME	RN	H	G	LE	ET	CLOSURE
	(HR)	(W/M2)	(W/M2)	(W/M2)	(W/M2)	(MM)	
237.000	1830.000	128.300	183.400	20.733	-158.600	0.118	-0.166
237.000	1900.000	122.700	174.500	19.913	-332.700	0.247	1.109
237.000	1930.000	57.080	150.000	17.557	-200.800	0.149	0.681
237.000	2000.000	-28.090	119.900	19.207	-83.600	0.062	4.086
237.000	2030.000	-56.810	84.300	18.833	-75.200	0.056	0.240
237.000	2100.000	-53.690	37.610	17.023	-35.290	0.026	0.063
237.000	2130.000	-54.200	31.520	17.103	0.084	0.000	0.852
237.000	2200.000	-45.070	17.700	18.337	-2.076	0.002	0.584
237.000	2230.000	-46.550	17.490	19.740	-6.785	0.005	0.399
237.000	2300.000	-44.720	6.458	21.707	2.098	0.000	0.372
237.000	2330.000	-47.850	17.330	20.207	-5.226	0.004	0.438
238.000	0.000	-48.990	16.680	20.270	-3.565	0.003	0.457
238.000	30.000	-47.890	21.970	20.170	-11.100	0.008	0.392
238.000	100.000	-42.190	15.250	18.380	-9.930	0.007	0.223
238.000	130.000	-34.930	6.240	18.920	-3.933	0.003	0.144
238.000	200.000	-33.970	5.064	18.240	-5.237	0.004	-0.011
238.000	230.000	-32.290	3.150	17.907	2.331	0.000	0.381
238.000	300.000	-32.590	3.647	17.727	-0.559	0.000	0.208
238.000	330.000	-26.900	10.840	16.483	-10.500	0.008	0.033
238.000	400.000	-39.050	20.670	16.560	-18.870	0.014	0.080
238.000	430.000	-33.470	9.430	17.370	-11.970	0.009	-0.158
238.000	500.000	-39.780	47.120	16.747	-43.680	0.032	0.149
238.000	530.000	-27.930	52.310	15.017	-22.970	0.017	2.272
238.000	600.000	-24.300	44.150	13.713	-32.310	0.024	1.118
238.000	630.000	-18.020	24.230	11.683	-23.650	0.017	0.092
238.000	700.000	-17.500	19.650	10.393	-29.070	0.021	-1.326
238.000	730.000	-8.570	43.380	8.733	-45.530	0.034	13.163
238.000	800.000	12.070	46.030	6.476	-49.510	0.037	0.188
238.000	830.000	19.270	62.860	7.726	-84.200	0.062	0.790
238.000	900.000	64.630	40.910	6.373	-74.000	0.055	0.466
238.000	930.000	113.600	40.570	2.018	-109.500	0.081	0.596
238.000	1000.000	170.100	48.650	-2.569	-142.600	0.105	0.561
238.000	1030.000	233.500	47.100	-4.882	-189.000	0.140	0.621
238.000	1100.000	305.900	17.790	-13.378	-219.700	0.162	0.690
238.000	1130.000	227.700	37.720	-6.999	-187.000	0.138	0.676
238.000	1200.000	278.400	9.370	-11.176	-151.400	0.112	0.532
238.000	1230.000	362.800	11.640	-18.657	-271.000	0.200	0.754
238.000	1300.000	368.700	10.130	-21.080	-232.000	0.172	0.638
238.000	1330.000	606.700	-1.137	-38.583	-310.700	0.230	0.549
238.000	1400.000	636.700	-0.331	-45.927	-349.800	0.259	0.593
238.000	1430.000	567.700	41.120	-40.087	-330.900	0.245	0.549
238.000	1500.000	608.800	28.060	-46.090	-428.900	0.318	0.712
238.000	1530.000	552.700	36.050	-33.150	-344.800	0.256	0.594
238.000	1600.000	533.200	26.250	-26.950	-419.500	0.311	0.777
238.000	1630.000	495.700	23.910	-21.103	-321.300	0.238	0.627
238.000	1700.000	433.100	37.810	-10.013	-292.200	0.217	0.601
238.000	1730.000	350.000	55.260	-3.315	-271.200	0.201	0.623
238.000	1800.000	286.400	146.000	9.650	-338.500	0.251	0.650

DAILY TOTAL ENERGY DENSITY

	(HR)	(MJ/M2)	(MJ/M2)	(MJ/M2)	(MJ/M2)	(MM)	
237.000	2400.000	11.971	3.510	0.283	-11.315	4.658	0.637

MEAN HALF-HOURLY ENERGY FLUX DENSITY

DAY	TIME	RN	H	G	LE	ET	CLOSURE
	(HR)	(W/M2)	(W/M2)	(W/M2)	(W/M2)	(MM)	
240.000	1730.000	339.700	-10.570	3.456	-217.200	0.160	0.664
240.000	1800.000	261.300	25.530	7.495	-186.900	0.138	0.600
240.000	1830.000	175.500	28.950	8.312	-126.600	0.093	0.531
240.000	1900.000	86.400	31.020	8.718	-75.500	0.056	0.468
240.000	1930.000	11.260	47.900	10.090	-81.500	0.060	1.574
240.000	2000.000	-45.520	22.410	11.139	-13.640	0.010	0.255
240.000	2030.000	-60.340	15.840	15.127	-9.400	0.007	0.142
240.000	2100.000	-64.390	20.690	15.357	-14.030	0.010	0.136
240.000	2130.000	-64.620	32.180	15.853	-24.480	0.018	0.158
240.000	2200.000	-67.360	32.170	16.203	-27.610	0.020	0.089
240.000	2230.000	-66.830	34.890	17.337	-32.000	0.023	0.058
240.000	2300.000	-63.380	29.830	17.407	-32.560	0.024	-0.059
240.000	2330.000	-60.970	33.900	19.037	-31.550	0.023	0.056
241.000	0.000	-64.060	37.550	21.070	-28.740	0.021	0.205
241.000	30.000	-62.760	39.760	22.367	-29.750	0.022	0.248
241.000	100.000	-64.010	38.570	22.173	-27.400	0.020	0.267
241.000	130.000	-72.600	55.910	24.227	-39.820	0.029	0.333
241.000	200.000	-74.200	55.410	25.673	-42.240	0.031	0.271
241.000	230.000	-66.300	44.570	24.327	-33.630	0.025	0.261
241.000	300.000	-65.050	35.430	23.127	-24.040	0.018	0.272
241.000	330.000	-61.940	26.000	22.950	-17.140	0.013	0.227
241.000	400.000	-57.890	27.400	23.783	-21.700	0.016	0.167
241.000	430.000	-56.840	24.240	23.657	-18.270	0.013	0.180
241.000	500.000	-51.890	13.750	23.430	-10.030	0.007	0.131
241.000	530.000	-56.480	12.990	22.267	-7.470	0.005	0.161
241.000	600.000	-58.260	14.720	21.953	-8.700	0.006	0.166
241.000	630.000	-56.690	10.280	22.360	-4.161	0.003	0.178
241.000	700.000	-57.890	13.770	22.167	-6.249	0.005	0.211
241.000	730.000	-46.180	7.680	21.867	-2.950	0.002	0.195
241.000	800.000	-0.859	8.270	19.683	-14.670	0.011	0.340
241.000	830.000	71.500	-1.037	16.063	-45.950	0.034	0.537
241.000	900.000	143.500	-14.400	13.900	-88.600	0.065	0.654
241.000	930.000	230.100	-32.610	11.845	-133.400	0.098	0.686
241.000	1000.000	302.200	-51.350	7.254	-163.500	0.120	0.694
241.000	1030.000	369.000	-81.600	2.767	-207.900	0.153	0.779
241.000	1100.000	419.800	-106.200	-2.351	-223.200	0.164	0.789
241.000	1130.000	469.800	-121.200	-6.267	-266.100	0.196	0.836
241.000	1200.000	508.000	-123.700	-10.760	-264.600	0.195	0.781
241.000	1230.000	542.300	-118.600	-13.850	-302.700	0.223	0.797
241.000	1300.000	568.700	-96.800	-15.800	-294.900	0.218	0.708
241.000	1330.000	592.100	-117.300	-18.980	-401.900	0.297	0.906
241.000	1400.000	592.500	-92.200	-19.690	-334.500	0.247	0.745
241.000	1430.000	505.000	-67.810	-15.213	-267.800	0.198	0.685
241.000	1500.000	420.300	-31.530	-13.320	-262.200	0.194	0.722
241.000	1530.000	458.300	-18.610	-10.423	-315.200	0.233	0.745
241.000	1600.000	503.800	-24.050	-12.163	-333.600	0.247	0.727
241.000	1630.000	475.400	-21.630	-13.583	-351.400	0.260	0.808
241.000	1700.000	342.200	29.210	-4.385	-298.800	0.221	0.798

DAILY TOTAL ENERGY DENSITY

	(HR)	(MJ/M2)	(MJ/M2)	(MJ/M2)	(MJ/M2)	(MM)	
240.000	2400.000	12.458	-0.505	0.806	-10.379	4.252	0.821

MEAN HALF-HOURLY ENERGY FLUX DENSITY

DAY	TIME	RN	H	G	LE	ET	CLOSURE
	(HR)	(W/M2)	(W/M2)	(W/M2)	(W/M2)	(MM)	
251.000	1030.000	136.800	-28.050	3.239	-78.300	0.057	0.759
251.000	1100.000	227.700	-47.720	-5.249	-87.200	0.064	0.607
251.000	1130.000	291.400	-64.620	-12.435	-117.500	0.086	0.653
251.000	1200.000	345.100	-84.100	-17.410	-156.200	0.115	0.733
251.000	1230.000	391.900	-89.000	-24.990	-172.400	0.127	0.712
251.000	1300.000	601.700	-136.000	-46.063	-268.200	0.197	0.727
251.000	1330.000	559.000	-104.200	-51.613	-227.800	0.168	0.654
251.000	1400.000	588.400	-100.400	-51.107	-250.700	0.185	0.653
251.000	1430.000	642.000	-103.000	-53.937	-195.700	0.144	0.508
251.000	1500.000	611.200	-90.600	-50.160	-200.800	0.148	0.519
251.000	1530.000	574.300	-83.400	-49.730	-252.700	0.187	0.641
251.000	1600.000	516.200	-55.740	-38.650	-308.500	0.228	0.763
251.000	1630.000	453.600	-36.300	-28.060	-231.300	0.171	0.629
251.000	1700.000	388.700	-19.720	-18.817	-330.200	0.244	0.946
251.000	1730.000	258.200	23.020	-7.985	-281.200	0.208	1.032
251.000	1800.000	245.600	22.280	-6.793	-134.200	0.099	0.469
251.000	1830.000	146.500	30.840	-2.802	-112.600	0.083	0.569
251.000	1900.000	55.320	39.870	1.467	-47.550	0.035	0.135
251.000	1930.000	-12.400	58.470	4.731	-96.700	0.071	-4.985
251.000	2000.000	-52.490	43.280	7.287	-32.510	0.024	0.238
251.000	2030.000	-55.110	16.620	9.720	-2.410	0.002	0.313
251.000	2100.000	-51.590	2.527	13.993	-2.061	0.002	0.012
251.000	2130.000	-55.460	17.770	11.123	-18.590	0.014	-0.018
251.000	2200.000	-57.590	13.060	10.267	-4.980	0.004	0.171
251.000	2230.000	-57.960	15.600	9.873	0.937	0.000	0.344
251.000	2300.000	-54.410	12.990	9.737	1.101	0.000	0.315
251.000	2330.000	-53.010	20.200	9.503	-7.420	0.005	0.294
252.000	0.000	-56.790	19.280	9.343	-11.710	0.009	0.160
252.000	30.000	-57.830	15.040	9.626	7.900	0.000	0.476
252.000	100.000	-57.230	13.560	9.970	-9.800	0.007	0.080
252.000	130.000	-57.580	13.620	10.513	-4.549	0.003	0.193
252.000	200.000	-21.760	6.980	9.240	-15.020	0.011	-0.642
252.000	230.000	-9.800	9.340	6.048	-20.210	0.015	-2.897
252.000	300.000	-34.690	9.490	7.027	-18.100	0.013	-0.311
252.000	330.000	-58.750	14.420	10.410	11.890	0.000	0.544
252.000	400.000	-56.070	8.820	11.223	9.980	0.000	0.419
252.000	430.000	-52.460	6.672	11.940	16.750	0.000	0.578
252.000	500.000	-48.440	7.940	11.017	10.350	0.000	0.489
252.000	530.000	-42.820	7.890	9.970	17.570	0.000	0.775
252.000	600.000	-47.280	8.920	10.537	21.560	0.000	0.830
252.000	630.000	-44.010	9.890	10.377	24.750	0.000	1.030
252.000	700.000	-33.840	5.167	9.287	29.440	0.000	1.409
252.000	730.000	-32.220	8.400	8.386	11.100	0.000	0.818
252.000	800.000	25.410	-4.259	3.866	-18.180	0.013	0.766
252.000	830.000	18.690	-3.341	1.680	-21.150	0.016	1.202
252.000	900.000	32.610	-5.854	0.917	-24.270	0.018	0.898
252.000	930.000	69.110	-10.930	-1.941	-51.790	0.038	0.934
252.000	1000.000	135.000	-21.680	-6.837	-58.900	0.043	0.629

DAILY TOTAL ENERGY DENSITY

	(HR)	(MJ/M2)	(MJ/M2)	(MJ/M2)	(MJ/M2)	(MM)	
251.000	2400.000	11.075	-1.093	-0.400	-6.675	2.852	0.728

MEAN HALF-HOURLY ENERGY FLUX DENSITY

DAY	TIME	RN	H	G	LE	ET	CLOSURE
	(HR)	(W/M2)	(W/M2)	(W/M2)	(W/M2)	(MM)	
252.000	1030.000	242.400	-38.930	-14.160	-54.520	0.040	0.409
252.000	1100.000	366.400	-61.580	-22.707	-114.100	0.084	0.511
252.000	1130.000	357.100	-39.350	-24.733	-148.100	0.109	0.564
252.000	1200.000	420.200	-32.460	-30.353	-218.400	0.161	0.643
252.000	1230.000	477.000	-13.610	-36.530	-187.500	0.139	0.457
252.000	1300.000	503.300	-0.633	-38.767	-260.700	0.193	0.563
252.000	1330.000	613.600	-6.761	-42.637	-328.200	0.243	0.587
252.000	1400.000	453.600	50.150	-35.610	-359.100	0.266	0.739
252.000	1430.000	526.700	35.480	-33.007	-273.300	0.202	0.482
252.000	1500.000	550.100	31.600	-35.040	-266.600	0.198	0.456
252.000	1530.000	499.600	65.880	-32.370	-281.100	0.208	0.461
252.000	1600.000	495.000	42.060	-29.377	-270.500	0.200	0.491
252.000	1630.000	493.400	52.680	-29.250	-336.700	0.250	0.612
252.000	1700.000	429.800	63.580	-21.317	-234.600	0.174	0.419
252.000	1730.000	334.600	85.100	-15.790	-276.300	0.205	0.600
252.000	1800.000	212.800	85.600	-8.083	-266.000	0.197	0.881
252.000	1830.000	155.000	76.100	-7.122	-78.900	0.058	0.019
252.000	1900.000	61.200	91.500	-4.038	-111.400	0.082	0.348
252.000	1930.000	-8.970	79.400	0.030	-74.900	0.055	0.503
252.000	2000.000	-52.820	72.000	2.952	-46.250	0.034	0.516
252.000	2030.000	-60.040	59.780	3.746	12.640	0.000	1.286
252.000	2100.000	-59.150	56.700	3.726	-41.130	0.030	0.281
252.000	2130.000	-49.520	43.040	3.560	-60.550	0.045	-0.381
252.000	2200.000	-39.550	35.750	2.818	-5.160	0.004	0.833
252.000	2230.000	-34.340	35.430	2.034	21.180	0.000	1.752
252.000	2300.000	-54.540	38.680	2.761	-7.390	0.005	0.604
252.000	2330.000	-55.130	32.080	3.484	-41.860	0.031	-0.189
253.000	0.000	-54.420	28.740	4.070	18.940	0.000	0.947
253.000	30.000	-46.140	26.110	3.953	-16.880	0.012	0.219
253.000	100.000	-51.240	24.680	4.081	-1.230	0.001	0.497
253.000	130.000	-52.980	24.400	4.312	-10.990	0.008	0.276
253.000	200.000	-50.540	26.310	4.607	-27.470	0.020	-0.025
253.000	230.000	-48.640	23.530	4.335	5.428	0.000	0.654
253.000	300.000	-23.260	18.810	2.692	-25.230	0.019	-0.312
253.000	330.000	-32.270	22.150	1.954	23.170	0.000	1.495
253.000	400.000	-26.600	17.640	1.917	15.600	0.000	1.347
253.000	430.000	-35.330	18.710	2.119	-17.760	0.013	0.029
253.000	500.000	-44.510	20.610	2.970	-52.610	0.039	-0.770
253.000	530.000	-49.100	19.260	3.518	-10.300	0.008	0.197
253.000	600.000	-54.510	18.180	4.084	7.830	0.000	0.516
253.000	630.000	-49.460	19.040	4.023	-1.391	0.001	0.388
253.000	700.000	-44.970	14.950	3.279	11.950	0.000	0.645
253.000	730.000	-42.830	17.190	2.493	12.170	0.000	0.728
253.000	800.000	-11.940	14.410	0.497	4.162	0.000	1.623
253.000	830.000	44.120	5.545	-2.637	-67.780	0.050	1.500
253.000	900.000	77.200	2.813	-7.491	-67.550	0.050	0.929
253.000	930.000	88.300	6.002	-7.943	-57.390	0.042	0.639
253.000	1000.000	187.800	-0.837	-12.917	-92.900	0.069	0.536

DAILY TOTAL ENERGY DENSITY

	(HR)	(MJ/M2)	(MJ/M2)	(MJ/M2)	(MJ/M2)	(MM)	
252.000	2400.000	11.622	2.354	-0.741	-8.387	3.546	0.555

MEAN HALF-HOURLY ENERGY FLUX DENSITY

DAY	TIME	RN	H	G	LE	ET	CLOSURE
	(HR)	(W/M2)	(W/M2)	(W/M2)	(W/M2)	(MM)	
256.000	1530.000	557.600	-53.310	-27.407	-221.900	0.165	0.519
256.000	1600.000	515.600	-51.860	-27.007	-317.900	0.236	0.757
256.000	1630.000	471.500	-23.310	-25.743	-287.200	0.213	0.697
256.000	1700.000	407.200	-18.070	-24.003	-212.900	0.158	0.603
256.000	1730.000	341.800	-1.086	-21.223	-263.700	0.195	0.826
256.000	1800.000	226.400	23.660	-13.646	-71.000	0.053	0.223
256.000	1830.000	127.700	41.060	-8.614	-87.300	0.065	0.388
256.000	1900.000	17.480	64.550	-4.222	-37.270	0.028	-2.058
256.000	1930.000	-29.570	55.080	-2.378	-26.120	0.019	0.906
256.000	2000.000	-64.180	46.440	0.319	-34.450	0.025	0.188
256.000	2030.000	-65.940	48.500	2.652	-23.150	0.017	0.401
256.000	2100.000	-62.650	41.080	3.949	-40.570	0.030	0.009
256.000	2130.000	-58.610	47.180	4.789	-10.840	0.008	0.675
256.000	2200.000	-50.670	47.820	5.199	-35.010	0.026	0.282
256.000	2230.000	-45.620	29.270	5.705	-21.710	0.016	0.189
256.000	2300.000	-47.450	53.020	5.932	-24.190	0.018	0.694
256.000	2330.000	-57.830	48.860	5.719	-3.306	0.002	0.874
257.000	0.000	-59.530	38.370	6.405	-25.620	0.019	0.240
257.000	30.000	-57.570	29.500	7.021	-8.320	0.006	0.419
257.000	100.000	-49.840	21.390	7.857	-12.280	0.009	0.217
257.000	130.000	-51.700	16.560	8.200	-8.570	0.006	0.184
257.000	200.000	-48.240	13.740	8.777	-3.518	0.003	0.259
257.000	230.000	-43.580	13.630	8.810	-1.454	0.001	0.350
257.000	300.000	-51.460	15.090	8.960	-6.020	0.004	0.213
257.000	330.000	-48.610	22.750	8.720	-5.389	0.004	0.435
257.000	400.000	-39.440	19.550	8.757	-6.552	0.005	0.424
257.000	430.000	-32.840	22.100	8.477	-8.240	0.006	0.569
257.000	500.000	-31.310	24.760	8.035	-28.060	0.021	-0.142
257.000	530.000	-31.260	19.630	7.641	-17.280	0.013	0.099
257.000	600.000	-21.190	20.690	7.302	-24.100	0.018	-0.246
257.000	630.000	-6.974	13.250	6.310	-16.540	0.012	-4.952
257.000	700.000	-0.098	12.850	5.532	-24.070	0.018	2.065
257.000	730.000	-6.665	18.610	4.776	-22.040	0.016	-1.816
257.000	800.000	-17.000	20.000	4.914	-14.710	0.011	0.438
257.000	830.000	11.860	17.410	3.811	-25.710	0.019	0.530
257.000	900.000	120.400	-19.010	0.761	-58.640	0.043	0.641
257.000	930.000	115.600	-25.460	-2.189	-43.370	0.032	0.607
257.000	1000.000	71.800	-7.290	-3.996	-49.530	0.036	0.838
257.000	1030.000	86.700	-6.961	-6.446	-34.120	0.025	0.512
257.000	1100.000	109.600	-11.120	-8.153	-30.560	0.023	0.411
257.000	1130.000	223.600	-19.530	-12.040	-129.400	0.096	0.704
257.000	1200.000	314.000	-43.920	-17.063	-167.200	0.124	0.711
257.000	1230.000	309.000	-21.090	-18.570	-156.900	0.116	0.613
257.000	1300.000	334.500	-5.051	-20.843	-196.200	0.145	0.642
257.000	1330.000	420.300	-9.030	-20.673	-154.200	0.114	0.408
257.000	1400.000	597.600	-50.650	-28.000	-332.600	0.247	0.673
257.000	1430.000	655.700	-66.790	-35.107	-264.600	0.196	0.534
257.000	1500.000	636.500	-61.780	-32.980	-159.300	0.118	0.366

DAILY TOTAL ENERGY DENSITY

	(HR)	(MJ/M2)	(MJ/M2)	(MJ/M2)	(MJ/M2)	(MM)	
256.000	2400.000	10.067	0.740	-0.351	-6.756	2.778	0.619

MEAN HALF-HOURLY ENERGY FLUX DENSITY

DAY	TIME	RN	H	G	LE	ET	CLOSURE
	(HR)	(W/M2)	(W/M2)	(W/M2)	(W/M2)	(MM)	
304.000	30.000	-76.500	41.750	10.883	-16.640	0.012	0.383
304.000	100.000	-76.700	49.480	11.180	-22.020	0.016	0.419
304.000	130.000	-76.900	48.670	10.717	-21.810	0.016	0.406
304.000	200.000	-77.500	43.330	11.113	-18.450	0.013	0.375
304.000	230.000	-78.600	44.290	11.377	-18.370	0.013	0.386
304.000	300.000	-77.600	38.360	12.003	-13.330	0.010	0.382
304.000	330.000	-78.800	37.060	12.593	-13.090	0.010	0.362
304.000	400.000	-78.900	29.700	13.267	-9.990	0.007	0.300
304.000	430.000	-79.600	29.090	14.107	-8.150	0.006	0.320
304.000	500.000	-81.100	26.990	14.470	-5.454	0.004	0.323
304.000	530.000	-80.200	22.370	14.930	-4.068	0.003	0.280
304.000	600.000	-78.400	22.160	14.973	-2.171	0.002	0.315
304.000	630.000	-78.000	23.390	14.713	-3.050	0.002	0.321
304.000	700.000	-79.300	26.700	13.893	-10.160	0.007	0.253
304.000	730.000	-77.800	27.160	13.117	-10.130	0.007	0.263
304.000	800.000	-73.100	23.720	12.680	-9.450	0.007	0.236
304.000	830.000	-43.970	21.770	10.200	-14.510	0.011	0.215
304.000	900.000	19.210	15.000	4.624	-27.690	0.020	0.532
304.000	930.000	73.400	-2.422	-1.889	-43.100	0.032	0.637
304.000	1000.000	152.100	-11.420	-8.493	-74.600	0.055	0.599
304.000	1030.000	226.400	-15.590	-15.880	-116.300	0.085	0.626
304.000	1100.000	308.600	-23.660	-24.533	-153.400	0.113	0.623
304.000	1130.000	361.700	-21.600	-29.340	-210.400	0.155	0.698
304.000	1200.000	355.000	-10.740	-31.003	-216.300	0.159	0.701
304.000	1230.000	441.500	-27.150	-40.100	-254.200	0.187	0.701
304.000	1300.000	459.400	-19.260	-39.937	-232.100	0.171	0.599
304.000	1330.000	464.300	-23.170	-40.127	-289.400	0.213	0.737
304.000	1400.000	446.000	-23.030	-37.280	-274.400	0.202	0.728
304.000	1430.000	415.900	-6.915	-33.083	-277.000	0.204	0.742
304.000	1500.000	375.700	15.540	-28.023	-237.100	0.175	0.637
304.000	1530.000	349.900	17.490	-24.990	-244.200	0.180	0.698
304.000	1600.000	291.800	33.040	-20.137	-240.600	0.177	0.764
304.000	1630.000	232.400	45.330	-14.860	-188.600	0.139	0.659
304.000	1700.000	145.300	83.700	-8.433	-189.400	0.140	0.772
304.000	1730.000	65.530	82.600	-3.208	-125.700	0.093	0.692
304.000	1800.000	13.200	73.500	-0.635	-92.500	0.068	1.512
304.000	1830.000	-51.120	62.640	4.441	-46.540	0.034	0.345
304.000	1900.000	-70.500	45.350	8.567	-24.650	0.018	0.334
304.000	1930.000	-66.270	21.080	12.963	-8.410	0.006	0.238
304.000	2000.000	-68.820	27.650	13.800	-15.150	0.011	0.227
304.000	2030.000	-71.600	49.070	14.490	-25.560	0.019	0.412
304.000	2100.000	-72.300	33.240	14.280	-17.030	0.012	0.279
304.000	2130.000	-71.400	31.920	15.033	-14.500	0.011	0.309
304.000	2200.000	-66.600	21.020	16.253	-7.720	0.006	0.264
304.000	2230.000	-69.850	30.140	15.257	-13.270	0.010	0.309
304.000	2300.000	-61.710	-11.090	18.503	5.248	0.000	-0.135
304.000	2330.000	-57.320	-2.034	21.920	2.394	0.000	0.010
305.000	0.000	-59.560	-0.771	23.777	4.496	0.000	0.104

DAILY TOTAL ENERGY DENSITY

	(HR)	(MJ/M2)	(MJ/M2)	(MJ/M2)	(MJ/M2)	(MM)	
304.000	2400.000	5.611	1.882	-0.003	-6.927	2.840	0.900

APPENDIX B

SELECTED HALF-HOURLY ENERGY BALANCE PLOTS

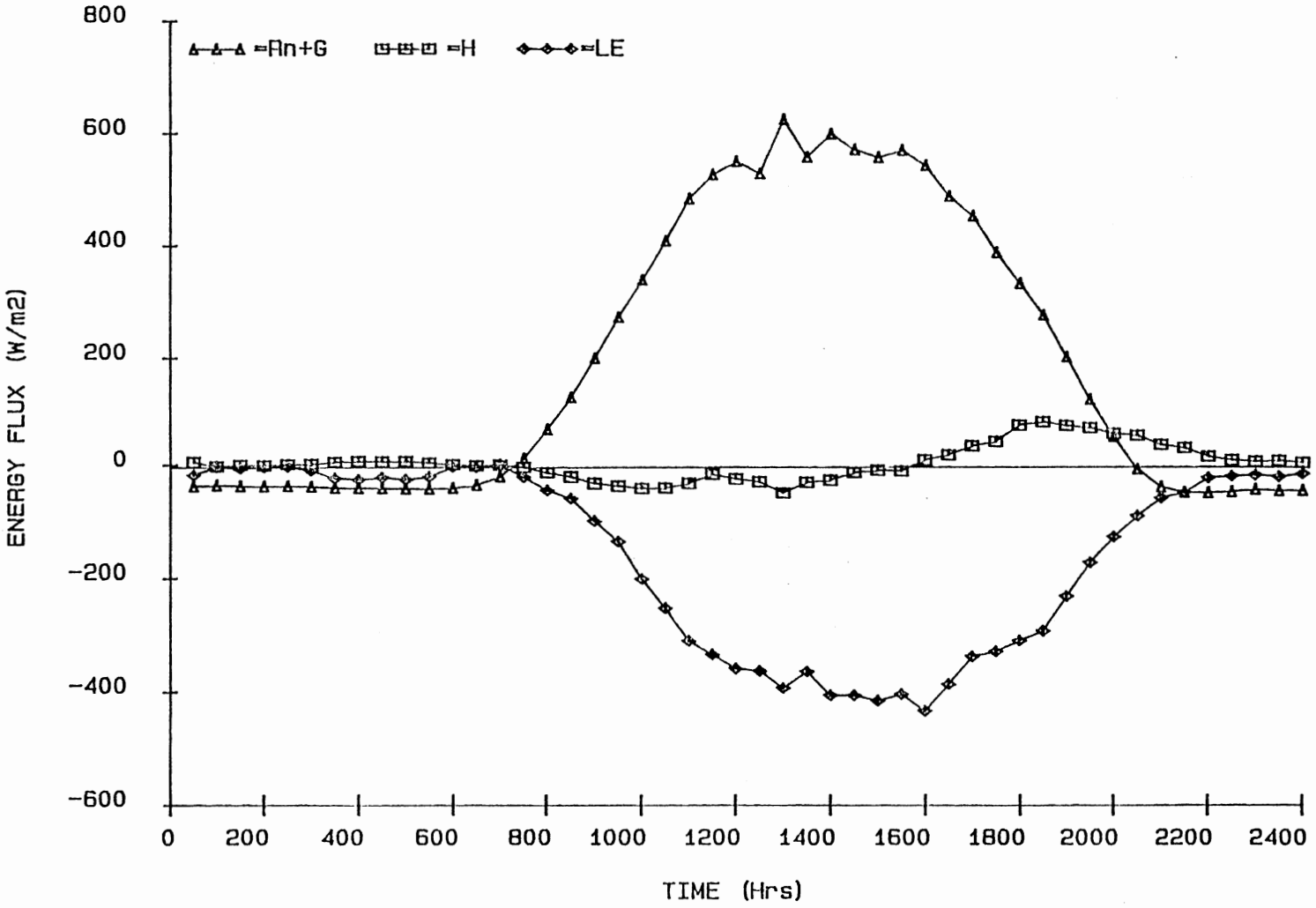

Figure 29. Energy Balance Fluxes for Day 177

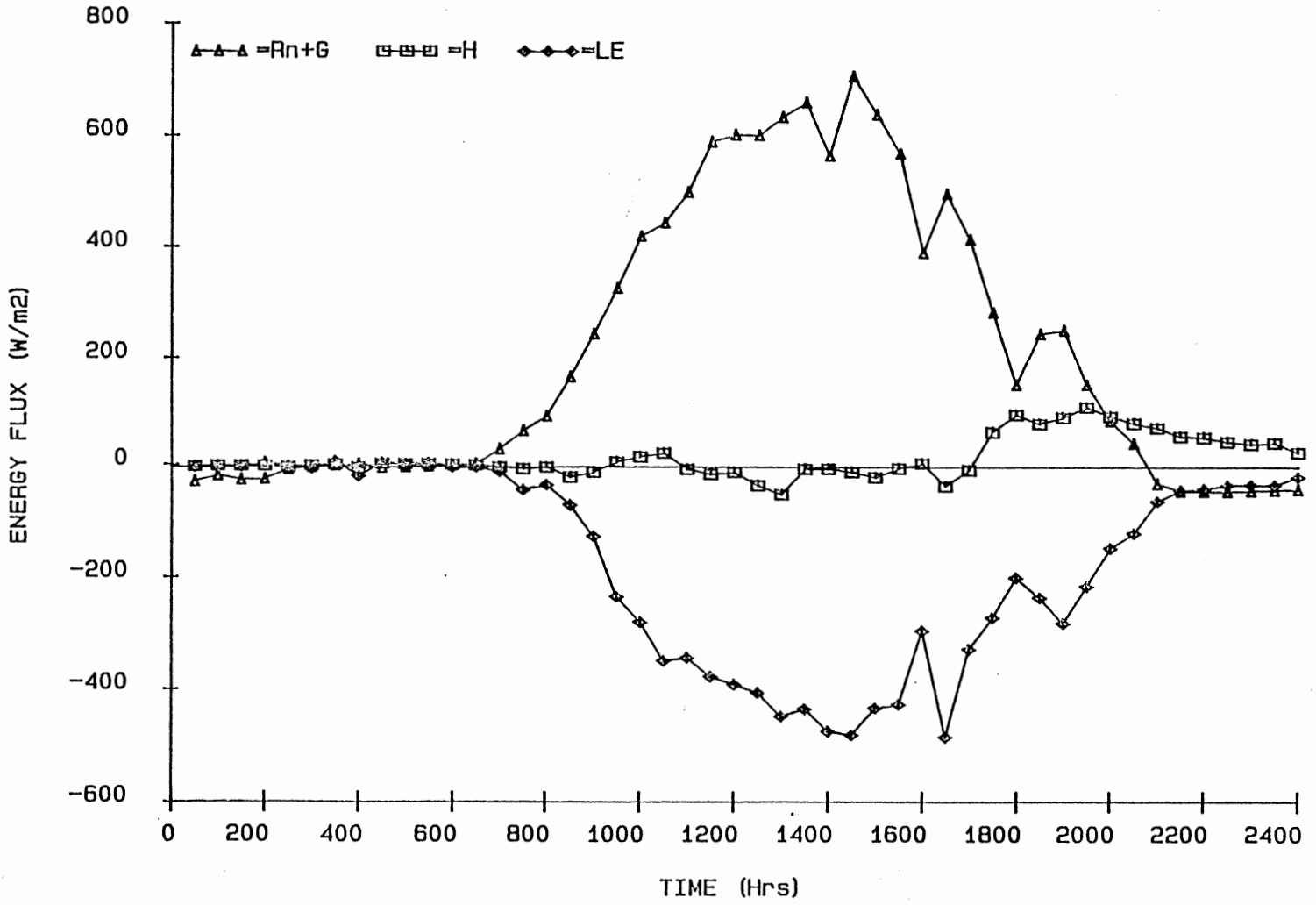

Figure 30. Energy Balance Fluxes for Day 184

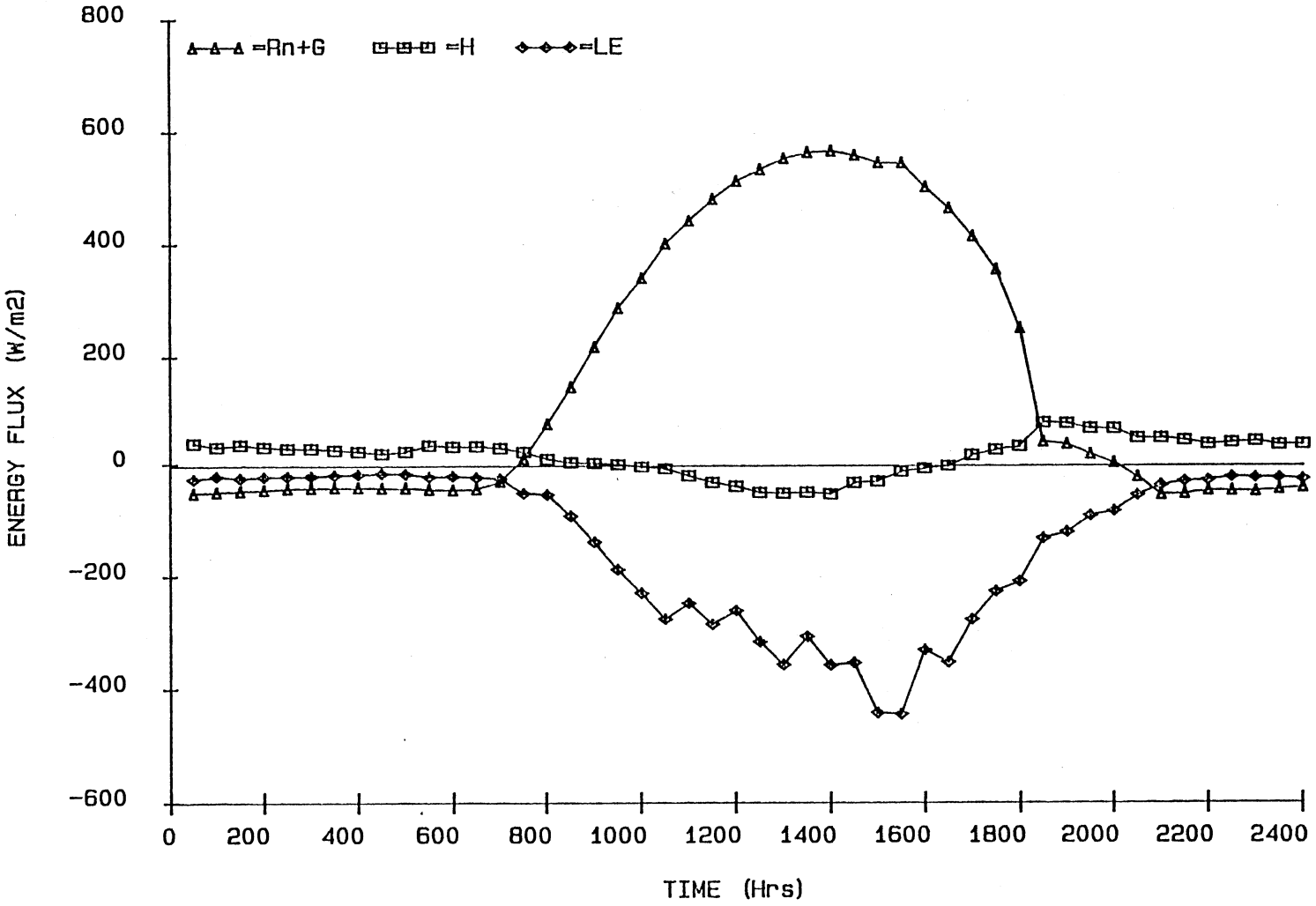

Figure 31. Energy Balance Fluxes for Day 191

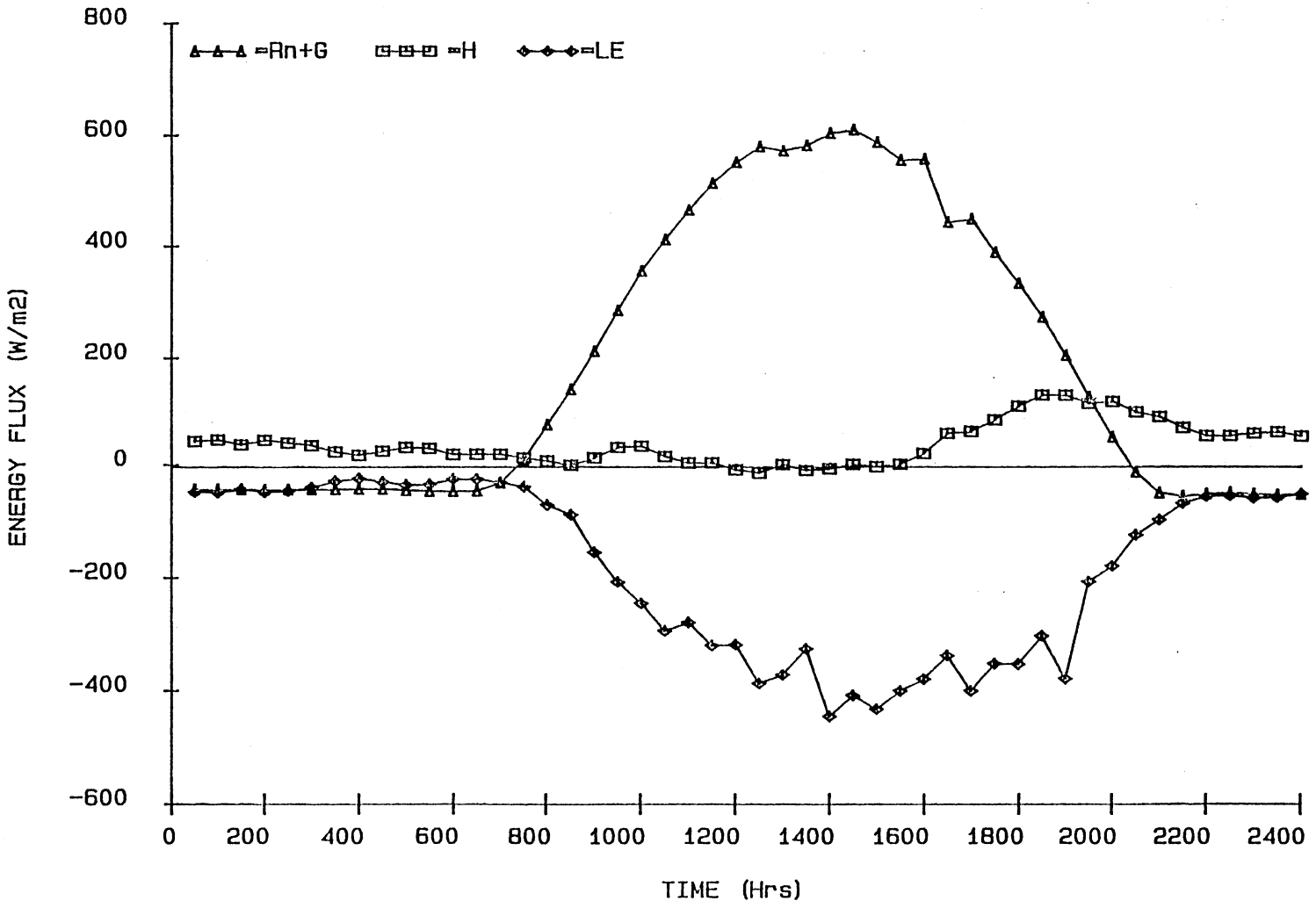

Figure 32. Energy Balance Fluxes for Day 196

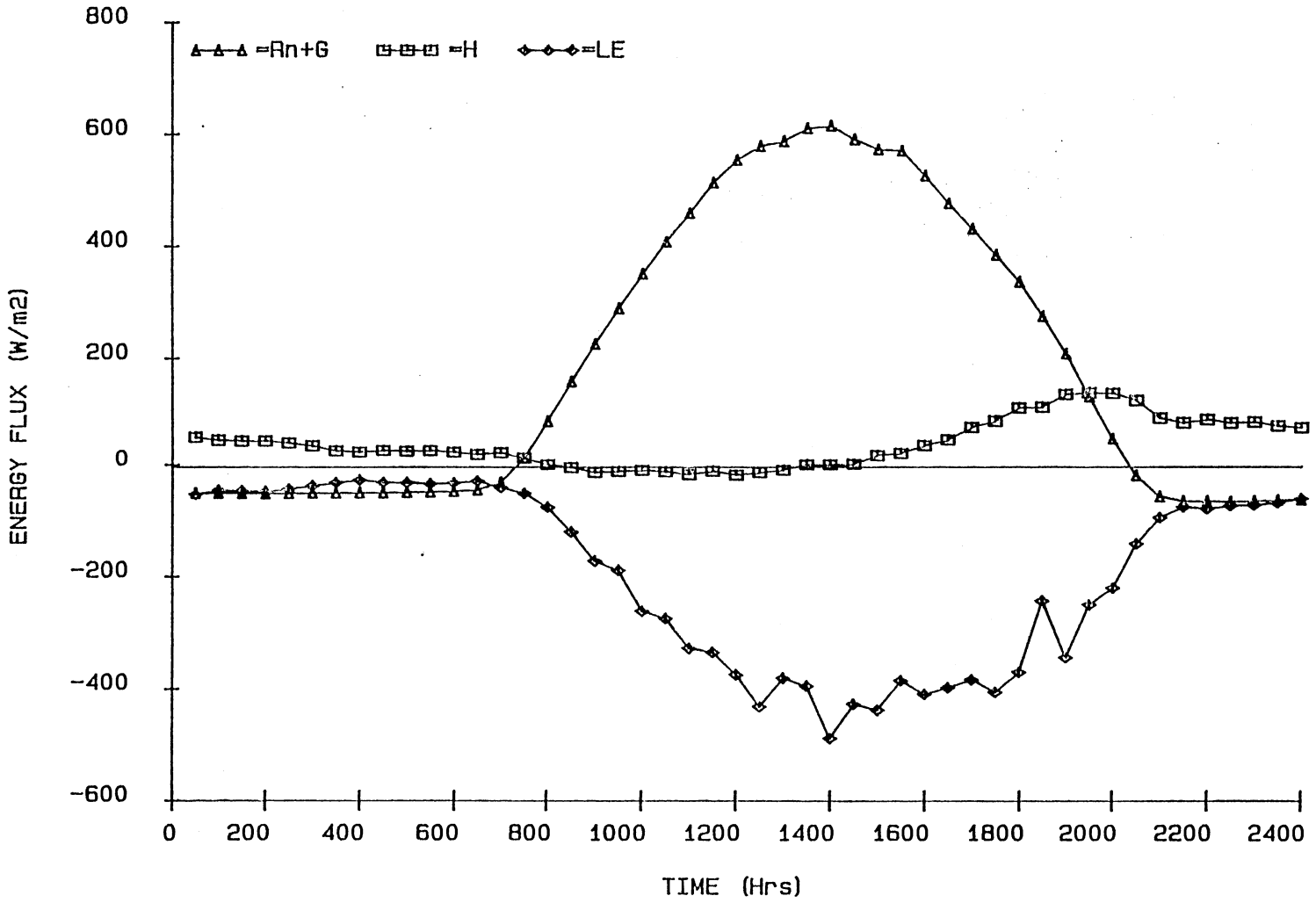

Figure 33. Energy Balance Fluxes for Day 197

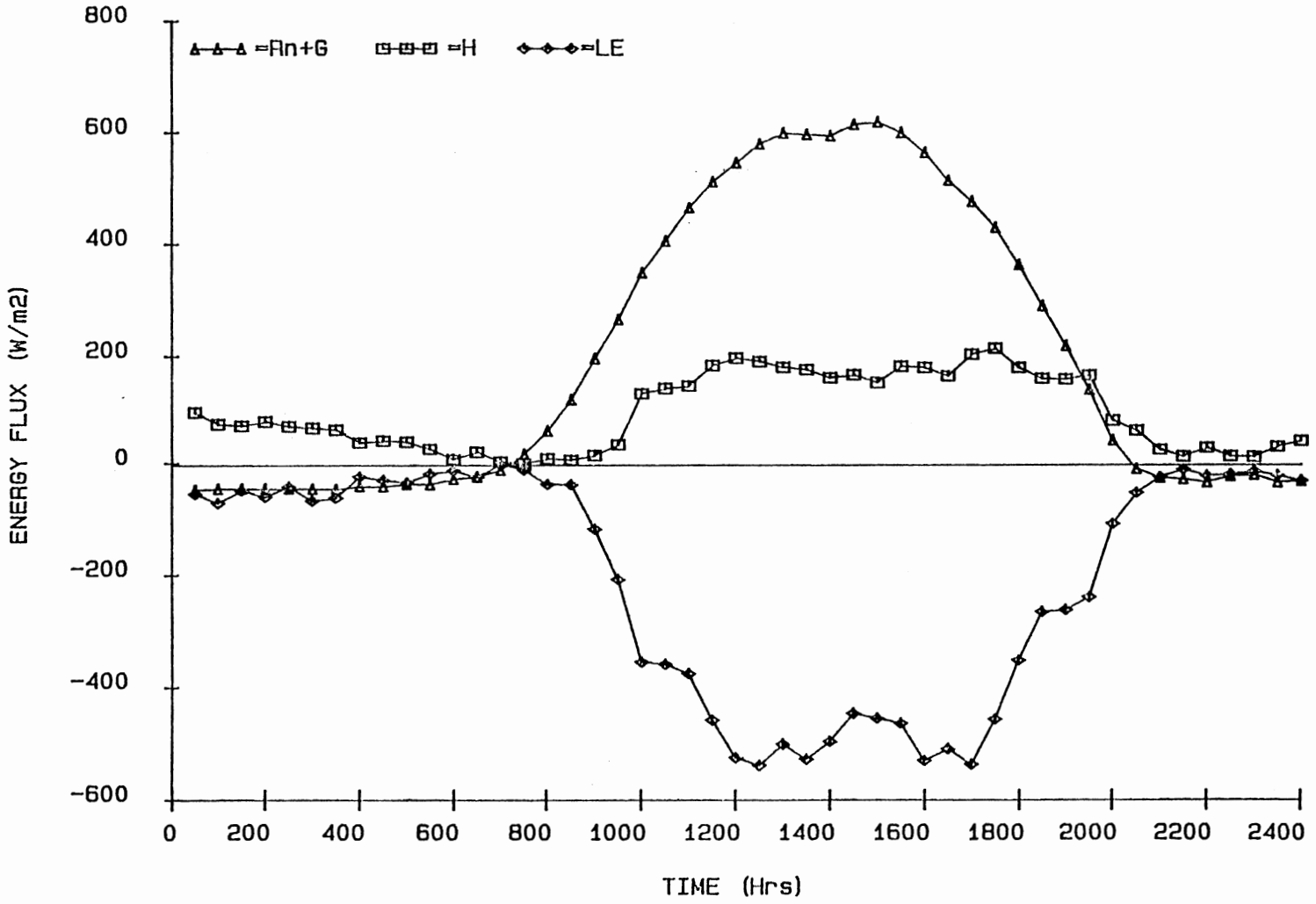

Figure 34. Energy Balance Fluxes for Day 210

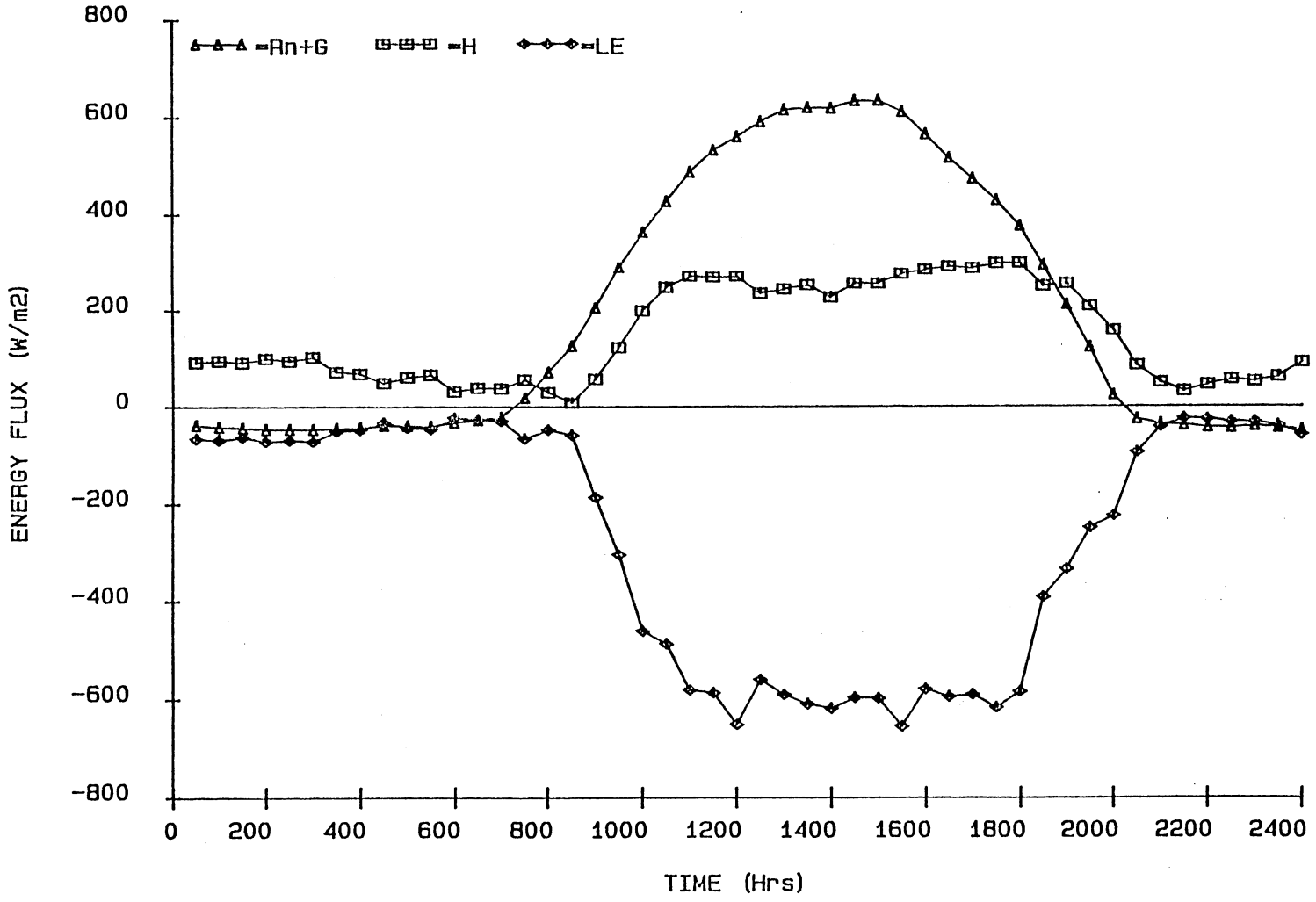

Figure 35. Energy Balance Fluxes for Day 211

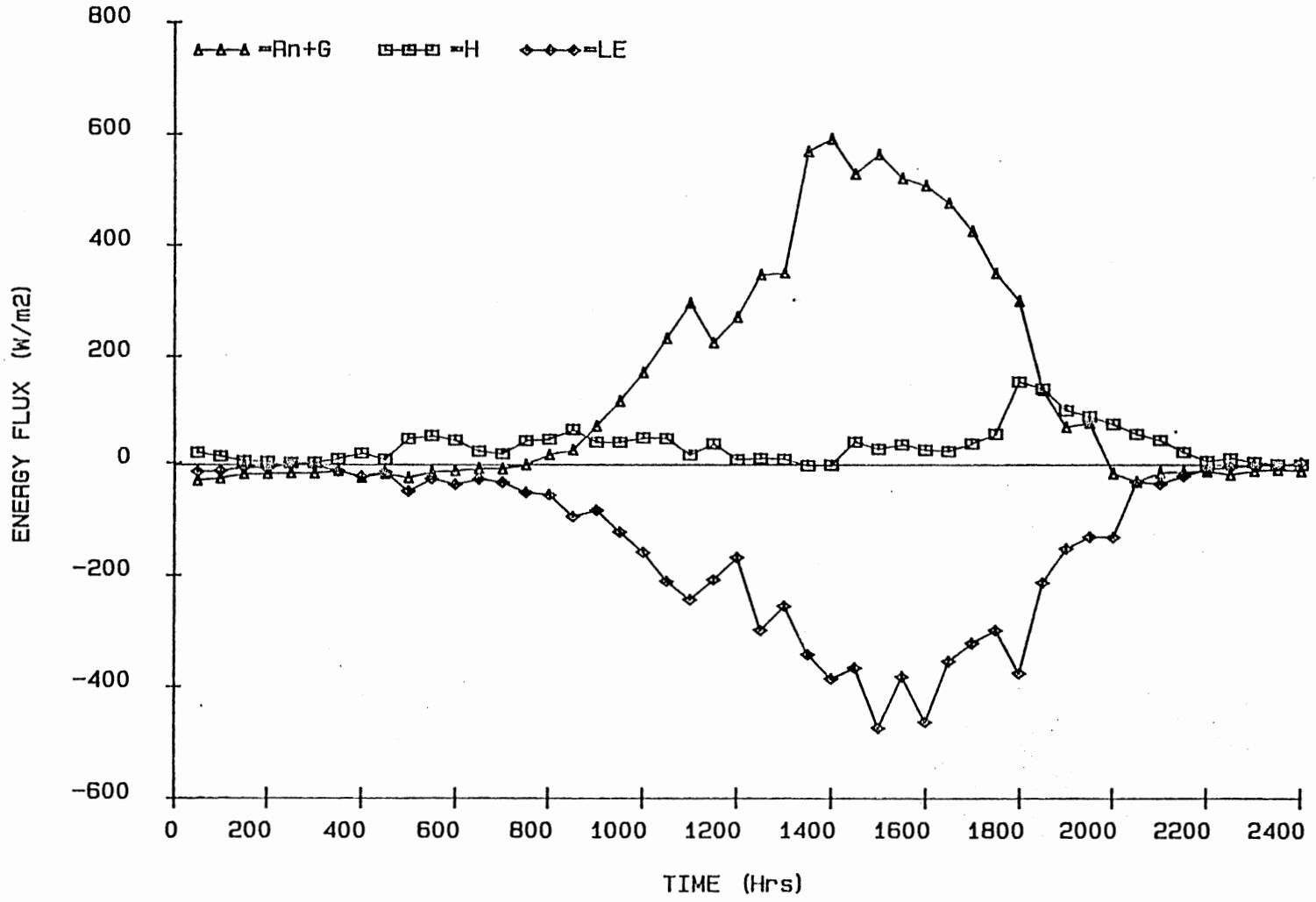

Figure 36. Energy Balance Fluxes for Day 238

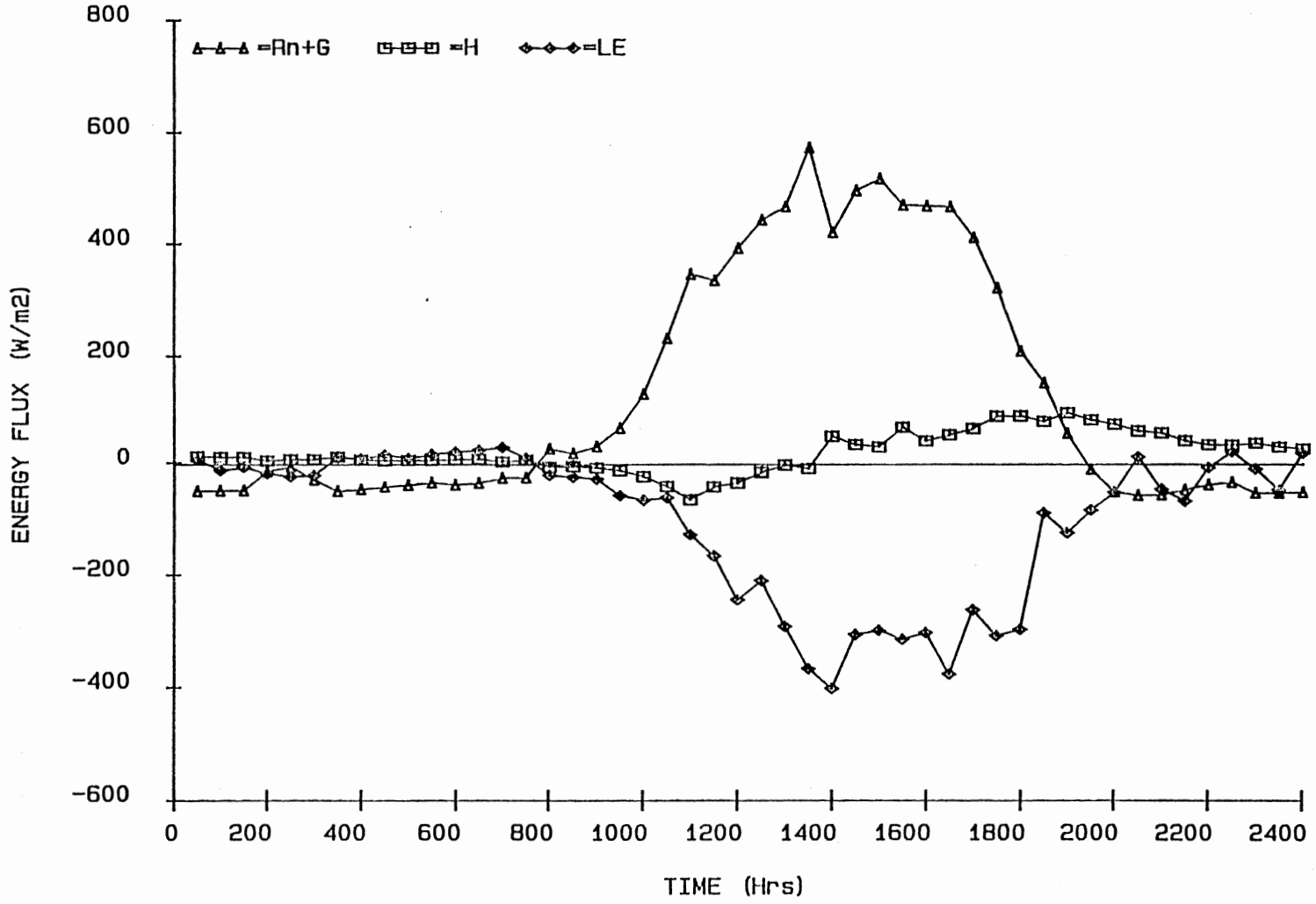

Figure 37. Energy Balance Fluxes for Day 252

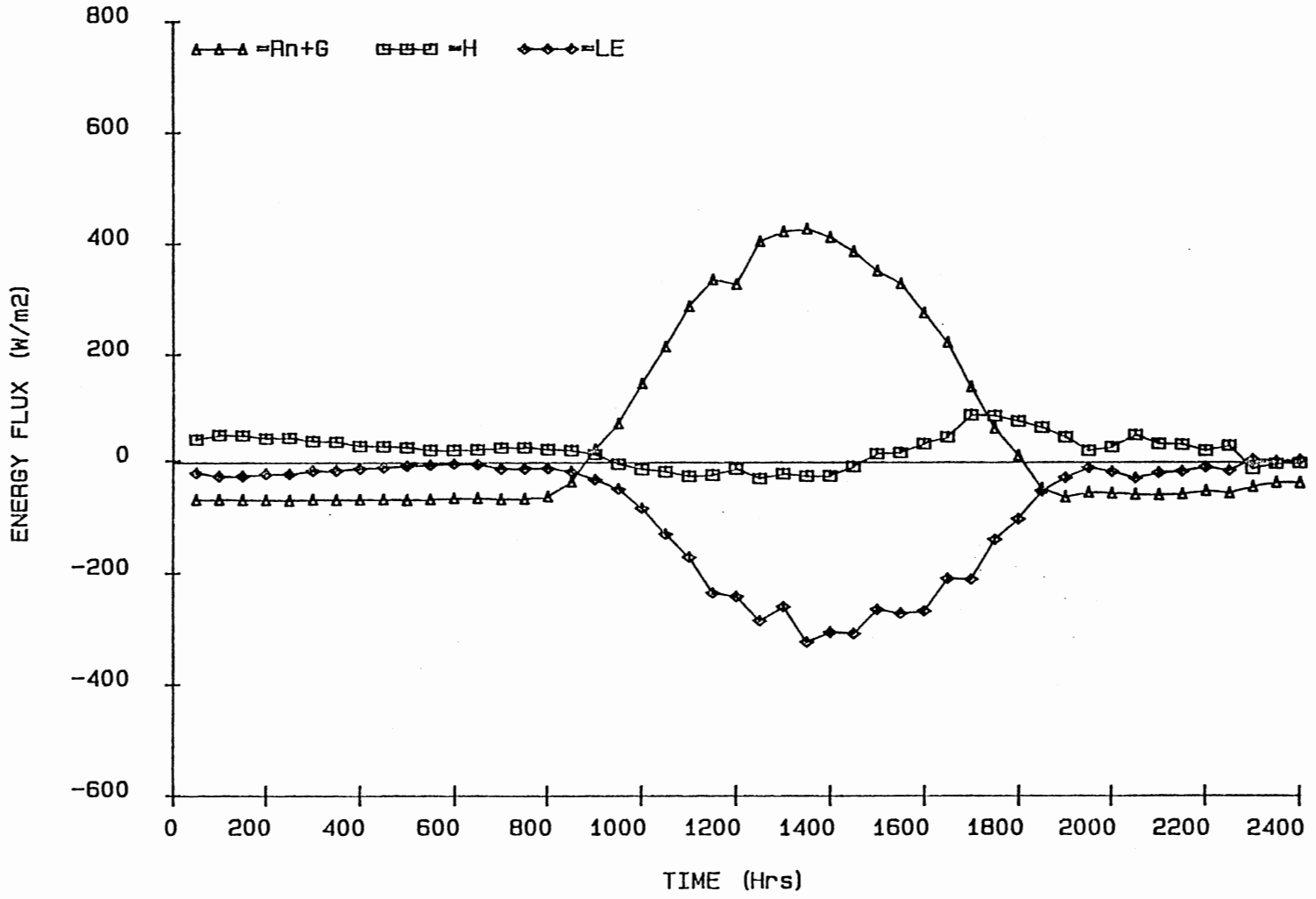

Figure 38. Energy Balance Fluxes for Day 304

VITA

Michael Andrew Kizer

Candidate for the Degree of

Doctor of Philosophy

Thesis: CALIBRATION OF A CLIMATOLOGICAL EVAPOTRANSPIRATION PREDICTION EQUATION USING EDDY CORRELATION METHODS

Major Field: Agricultural Engineering

Biographical:

Personal Data: Born in Eugene, Oregon, April 16, 1949, the son of Wilbur L. and Nicky Kizer. Married to Sheryl L. Meyer on April 10, 1976. Father of sons Matthew D. and Eric A. Kizer.

Education: Graduated from Harrisburg Union High School in Harrisburg, Oregon, in June, 1967; received Bachelor of Science Degree in Agricultural Engineering from Oregon State University in June, 1971; received Master of Science Degree from Oregon State University in June, 1976; completed requirements for the Doctor of Philosophy degree at Oklahoma State University in May, 1987.

Professional Experience: Peace Corps Volunteer, West Malaysia, July, 1971, to August, 1973; Graduate Research Assistant, Department of Agricultural Engineering, Oregon State University, July, 1974, to April, 1976; Adjunct Assistant Professor of Agricultural Engineering, North Carolina A & T State University, April, 1976, to August, 1983; Graduate Research Assistant, Department of Agricultural Engineering, Oklahoma State University, January, 1984, to present.

Organizations: American Society of Agricultural Engineers; Alpha Epsilon; Tau Beta Pi.